## *Re-os isotope constraints on the age of the Lithospheric mantle beneath western Greenland.*

Michelle Webb

University of Durham

Thermo ELECTRON CORPORATION

Department of Earth Sciences



**Master's Thesis**

# Re-Os Isotope Constraints on the age of the Lithospheric Mantle beneath Western Greenland.

Sukkertoppen Ice Cap, South West Greenland

**Michelle Webb**



**Submitted: September 2007**

Supervisors: Prof Graham Pearson & Dr Sven Monrad Jensen

# Abstract

Alkaline magmatic activity across Western Greenland (W.G.) provides a record of lithosphere evolution over the last 600 Ma. Ultra Mafic Lamprophyre (UML) magmatism in particular has erupted an exceptional inventory of mantle xenoliths allowing a detailed look at the lithospheric root beneath both the exposed craton and the re-worked Archean terrane (RAT) of the Kangerlussuaq region, SW Greenland. Samples from within the re-worked Archean terrane more commonly have diopside plus garnet, i.e. they are more lherzolitic whereas highly depleted harzburgites and dunitic lithologies are prevalent amongst xenoliths erupted through the undisturbed Archean craton.

W. Greenland peridotite xenoliths show a large range in bulk composition. The peridotites are MgO – rich (44-51 wt%), with most samples overlapping the range for cratonic peridotites and being generally more MgO-rich than non-cratonic or massif peridotites. In contrast $SiO_2$ contents are relatively low (36-43 wt%), being at the lower end of the range for both cratonic and non-cratonic/massif peridotites, indicating that the W.G. mantle has not experienced significant $SiO_2$ enrichment. The low $SiO_2$ of most residual, minimally metasomatised harzburgites indicate particularly othopyroxene poor protoliths. This contributes to growing evidence that the Kaapvaal cratonic lithosphere is the exception rather than the rule in terms of craton lithosphere bulk compositions and evolution.

A selection of dunitic, harzburgitic and lherzolitic lithologies have been analysed for Re-Os isotopes and PGE abundances. Os ranges from 0.86 to 5.02 ppb, scattering around the typical average for cratonic residues. Re contents range from 0.009 to 0.290 ppb, and are all less than primitive mantle. However, in extended PGE patterns Re can be seen to be anomalously high in numerous samples and has obviously experienced secondary enrichment, possibly by UML infiltration. Pt and particularly Pd demonstrate their incompatible behaviour during high degrees of melting, with Pt as low as 0.035 and Pd depleted to 0.007 ppb, comparable to highly depleted residues from other cratons (Pearson *et al*, 2004). The effects of metasomatism are also seen on Pd in some samples but this element is less disturbed than Re and, for some samples, (Pd/Ir)*n* correlates well with indices of melt depletion such as $Al_2O_3$ consistent with high degrees of melting. Some disturbance relates to metasomatic introduction of clinopyroxene in certain rocks.

Re-depletion ages for the most residual W.G. peridotites, corrected to the 600 My eruption age for the host UML, range from 1.8 to 3.0 Ga, with Archean depletion ages clearly evident in the lithosphere beneath the RAT of the Nagssugtoqidian. Archean (>2.5 Ga) ages are found in even the deepest derived (>200 km) samples indicating that the basal lithosphere is of this age.

The ages for W.G. peridotites together with pressure and temperature investigations by Sand (2007) indicate clearly that an Archean keel existed beneath the region that extended well into the diamond stability field at 600 Ma, both on the recognised craton and beneath the region of re-worked Archean crust suggesting that further exploration in this area can be targeted right across the region where UML's occur. The validity of these findings is emphasised by the recent new finds of macro-diamonds in the Kangerlussuaq region (Hudson Resources Website).

# Table of Contents

*Title*
*Abstract* ..... 2
*Table of Contents* ..... 3
*Appendices* ..... 4
*List of Figures* ..... 5
*List of Tables* ..... 6
*Acknowledgements* ..... 7

**CHAPTER 1: INTRODUCTION**
1.1. *Overview* ..... 8
*1.2. Aims* ..... 9
1.3. *Geological Background* ..... 10
1.4. *Regional Geology* ..... 11
*1.5. The Geology at depth* ..... 14
1.5.1 *Alkaline dyke classification* ..... 15
1.6 *Tectonic History* ..... 15
1.7 *Field Observations* ..... 16
1.7.1 *Safartoq Area – In the Archean Block* ..... 17
1.7.2 *Kangerlussuaq Area – In the Reworked Archean Terrane* ..... 18

**CHAPTER 2: W. GREENLAND SAMPLES**
2.1 *Collection of samples* ..... 19
2.2 *Size and distribution* ..... 19
2.3 *Off vs. on-craton xenoliths* ..... 22
2.4 *The UML host Rock* ..... 22

**CHAPTER 3: ANALYTICAL METHODS**
3.1 *Preparation of samples* ..... 23
3.2 *Rock powder weighing and digestion* ..... 23
3.2.1 *Carius Tube Digestion* ..... 24
3.2.2 *Asher Digestion* ..... 25
3.3 *Os Chemistry*
3.3.1 *Os Extraction* ..... 26
3.3.2 *The Os Cut* ..... 26
3.3.3 *Os Back Extraction* ..... 27
3.3.4 *Os Micro-distillation* ..... 27
3.4 *PGE Chemistry*
3.4.1 *The PGE Cut* ..... 28
3.4.2 *PGE Column Chemistry* ..... 29
3.5 *Triton analysis of Os*
3.5.1 *Preparation of Samples for Triton Analysis* ..... 30
3.5.2 *Triton Mass Spectrometry* ..... 30
3.5.3 *Triton Analysis of Osmium Isotopes* ..... 31
3.6 *Element analysis of Re* ..... 31
3.7 *Whole rock /XRF analysis* ..... 31

**CHAPTER 4: DESCRIPTION OF MAJOR ELEMENT GEOCHEMICAL DATA**
4.1 *Introduction* ..... 32
4.2 *Major Element Compositions: Xenoliths* ..... 32
4.2.1 *MgO vs. $TiO_2$, $Al_2O_3$ & CaO* ..... 33
4.2.2 *$SiO_2$ vs. $TiO_2$, CaO & MgO* ..... 35
4.2.3 *$Al_2O_3$ vs. CaO & $SiO_2$* ..... 38
4.2.4 *$K_2O$ vs. $P_2O_5$ &$TiO_2$* ..... 39
4.2.5 *$A_2O_3$ vs. V (ppm) and Cr (ppm)* ..... 40

**CHAPTER 5: DESCRIPTION OF PGE & Re GEOCHEMICAL DATA**
5.1 *Introduction* ..... 42

5.1.1 *I-PGE & P-PGE Groups* ..... 42
5.1.2 *$^{187}Os/^{188}Os$ Ratios* ..... 43
5.2 *Description of PGE and Re concentrations*
5.2.1 *PGE Concentrations* ..... 45
5.2.2 *Os & Re Concentrations* ..... 47
5.3 *W.G. PGE patterns – general characteristics* ..... 48
5.4 *(Pd/Ir)n vs. $Al_2O_3$* ..... 49
5.5 *W.G. PGE patterns – Group characteristics* ..... 50
5.5.1 *Group 1 PGE Fractionation Pattern* ..... 50
5.5.2 *Group 2 PGE Fractionation Pattern* ..... 51
5.5.3 *Group 3 PGE Fractionation Pattern* ..... 52
5.5.4 *Grouping characteristics* ..... 53
5.6 *Positive platinum anomaly in sample 474568* ..... 54
5.7 *Os Isotope characteristics of W.G. peridotites* ..... 55
5.8 *Age Determinations*
5.8.1 *Model Ages: $T_{RD}$, $T_{MA}$ & $T_{RD\ erup...}$* ..... 56
5.8.2 *W.G. Ages* ..... 57

**CHAPTER 6: SYNTHESIS**
6.1 *Mantle Signatures – Major Elements*
6.1.1 *Bulk Composition* ..... 60
6.1.2 *Typical Cratonic Mantle* ..... 61
6.1.3 *The degree of partial melting in W.G. peridotites* ..... 63
6.1.4 *Fe and Ti metasomatism* ..... 65
6.2 *PGE systematics of the W.G. cratonic lithospheric mantle* ..... 66
6.3 *Investigation of a positive Pt anomaly in sample 474568* ..... 69
6.4 Timing & *Stabilisation of the craton in S.W. Greenland* ..... 71
6.5 *Diamond potential in W.G* ..... 73

**CHAPTER 7: CONCLUSION**
7.1 *Conclusions* ..... 75
7.2 *Diamond Potential* ..... 76
7.3 *Future work* ..... 77

*References* ..... 78-86

# Appendices

**WESTREN GREENLAND DATA**

Appendix A – Rock samples
A (I) *Western Greenland Rock sample list* ..... 87
Appendix B – Major Element Data
(I) *Western Greenland Peridotite suite* ..... 88
(II) *Western Greenland Peridotite ratios* ..... 89
B (III) *Western Greenland Peridotite Trace Elements* ..... 90
(IV) *Western Greenland UML suite* ..... 91
(V) *Western Greenland UML Trace Elements* ..... 92
Appendix C – Platinum Group Element Data
(I) *Western Greenland PGE ppb data* ..... 93
C (II) *Western Greenland PGE ratios & Ages* ..... 94

**CRATONIC DATA-OTHER PERIDOTITE SUITES**

Appendix D – Major Element Data
(I) *Kaapvaal Peridotite suite* ..... 95
(II) *Canadian Peridotite suite* ..... 99
(III) *Tanzanian Peridotite suite* ..... 101
D

(IV) *Siberian Peridotite suite*..... 103
(V) *East Greenland Peridotite suite*..... 105
(VI) *West Australian Peridotite suite*..... 107

**NON-CRATONIC DATA – NON EUROPEAN**
Appendix E – Major Element Data
(I) *African Peridotite suite*..... 108
(II) *Australian Peridotite suite*..... 110
E (III) *Mongolian Peridotite suite*..... 112
(IV) *Chinese Peridotite suite*..... 113
(V) *Beni Bousera Peridotite suite*..... 114
(VI) *Vitim*..... 115

**NON-CRATONIC DATA- EUROPEAN**
Appendix F – Major Element Data
(I) *Hungarian Peridotite suite*..... 116
(II) *Romanian Peridotite suite*..... 117
F (III) *Italian Peridotite suite*..... 118
(IV) *British Peridotite suite*..... 119

**PGE DATA- OTHER PERIDOTITE SUITES**
Appendix G – Platinum Group Element Data
(I) *Kaapvaal PGE ppb data*..... 120
(II) *Beni Bousera ppb data*..... 121
(III) *Vitim ppb data*..... 122
G (IV) *Slave & Namibia ppb data*..... 123
(V) *Lesotho ppb data*..... 124
(VI) *Somerset Island ppb data*..... 125

# List of Figures

Cover picture. Sukkertoppen Ice Cap, GEUS, Minex website
**CHAPTER 1- Introduction**
Fig.1.1 Satellite image of Greenland and surrounding countries..... 10
Fig 1.2 Map of Greenland showing the North Atlantic Craton..... 11
Fig 1.3 Drawing by Escher *et al*, 1976 & Paradise Valley Photo..... 12
Fig 1.4 Regional geology of the research area..... 13
Fig 1.5 Four scenarios of lithospheric mantle..... 14
Fig 1.6 Field Locations..... 16
Fig 1.7 Field photograph, UML sill at camp2..... 17
Fig 1.8 Field photograph Francois Dyke..... 18

**CHAPTER 2 – W.G. peridotite samples**
Fig 2.1 GEUS Geological map..... 19
Fig 2.2 Various field photographs of xenoliths..... 20
Fig 2.3 Photograph of xenolith peridotite sample 474538..... 21
Fig 2.4 Photograph of xenolith peridotite sample 474527..... 22
Fig 2.5 Photograph of the UML with xenoliths..... 22

**CHAPTER 3 – Geochemistry and Analytical methods**
Fig 3.1 Carius Tubes..... 24
Fig 3.2 The Anton Paar-Perkin-Elmer high pressure asher (HPA-S)..... 25
Fig 3.3 Quartz asher vessels..... 25
Fig 3.4 Centrifuge tubes on the shaker plate..... 26
Fig 3.5 Micro-distillation- addition of $Cr_2O_3$..... 27
Fig 3.6 Micro-distillation Sealed rocket vial..... 27
Fig 3.7 Rocket vials on the hotplate..... 28
Fig 3.8 PGE columns..... 29

Fig 3.9 Triton filament welding..... 30
Fig 3.10 Pt ribbon on the filaments..... 30
Fig 3.11 Triton Mass Spectrometer..... 31

**CHAPTER 4 – Major element geochemical data**
Fig 4.1 Major elements – MgO vs. $TiO_2$, $Al_2O_3$ & CaO..... 34
Fig 4.2 Major elements – $SiO_2$ vs. $TiO_2$, CaO & MgO..... 35
Fig 4.3 Major elements – $Al_2O_3$ vs. CaO & $SiO_2$..... 38
Fig 4.4 Major elements – $K_2O$ vs. $P_2O_5$ & $TiO_2$..... 39
Fig 4.5 Major & Minor trace elements – $Al_2O_3$ wt% vs. V & Cr (ppm)..... 40

**CHAPTER 5 – PGE geochemical data**
Fig 5.1 Typical PGE fractionation patterns..... 42
Fig 5.2 Re & Os concentrations & $^{187}Re/^{188}Os$ for various rocks..... 43
Fig 5.3 Group IIIA Mantle evolution line..... 44
Fig 5.4 W.G. & various PGE concentrations..... 45
Fig 5.5 Os (ppb) & Ir (ppb) histograms..... 46
Fig 5.6 Os (ppb) vs. Re (ppb) for W.G. & others..... 47
Fig 5.7 W.G. PGE fractionation pattern, all samples..... 48
Fig 5.8 a). Pd (ppb) vs. Ir (ppb). b). (Pd/Ir)*n* vs. $Al_2O_3$..... 49
Fig 5.9 W.G. Group 1 PGE fractionation pattern..... 50
Fig 5.10 W.G. Group 2 PGE fractionation pattern..... 51
Fig 5.11 W.G. Group 3 PGE fractionation pattern..... 52
Fig 5.12 Photomicrographs of sample 474568..... 54
Fig 5.13 Gamma Os various rock types..... 55
Fig 5.14 W.G. gamma Os histogram..... 55
Fig 5.15 Os Isotope evolution diagram..... 56
Fig 5.16 W.G. Model age histograms..... 57
Fig 5.17 W.G. Model age – Os evolution..... 59

**CHAPTER 6 – Interpretation**
Fig 6.1 Major element bulk Earth Mg/Si vs. Al/Si..... 60
Fig 6.2 $MgO/SiO_2$ vs. $SiO_2$..... 61
Fig 6.3 A) percentage of melting vs. Ol Mg# B) Age vs. Ol Mg#..... 63
Fig 6.4 (Pd/Ir)*n* vs. $Al_2O_3$..... 64
Fig 6.5 A) FeO* vs. $Al_2O_3$, B) $TiO_2$ vs. $Al_2O_3$, C & D, W.G. groups..... 65
Fig 6.6 PGE fractionation patterns for W.G. & various peridotites..... 68
Fig 6.7 Pd vs. Pt with close up inset..... 69
Fig 6.8 $T_{RD\ erup}$ vs. Re (ppb)..... 71
Fig 6.9 W.G. age range and map..... 72
Fig 6.10 W.G. Age range against distance..... 72
Fig 6.11 Four scenarios..... 73
Fig 6.12 A) Temperature vs. Pressure. B) Pressure (GPa) vs. Age (Ga)..... 74

**CHAPTER 7 – Conclusion**
Fig 7.1 Illustration of W.G. mantle lithosphere..... 76
Fig. 7.2 Diamonds Hudson resources..... 77

# List of Tables

Table 1.1 A timeline of tectonic events for S.W. Greenland..... 16
Table 4.1 SiO2 contents of all peridotite xenolith suites..... 36
Table 4.2 Data sources for major element peridotite xenolith suites..... 37
Table 5.1 $^{187}Os/^{188}Os$ various reservoirs..... 44
Table 5.2 W.G. (Pd/Ir)*n* group summary..... 49
Table 5.3 W.G. Group characteristics..... 53
Table 5.4 W.G. Groups and model ages..... 58
Table 6.1 W.G. Groups interpretations..... 67

# Acknowledgements


- A big thank you to Prof Graham Pearson for his support, knowledge, understanding, patience and above all else humour. You have the ability to make people feel at ease, you're easy to talk to and very approachable, a great teacher and an even better friend. Thank you.
- I would like to especially thank Thermo Electron for sponsoring me to do a Masters by Research, a rare thing these days, I am eternally grateful.
- I gratefully acknowledge Dr Geoff Nowell for his advice and support in the labs.
- I would like to sincerely thank Dr Ambre Luguet your chemistry knowledge is unsurpassed, thank you for teaching me all that you know about Re-Os geochemistry, and of course French swear words too.
- I also gratefully thank Dave Sales for always accommodating any rock sample work that came your way.
- Many thanks to Dr Chris Ottley for your assistance with the Element 2.
- I wish to thank Karina Sand and Dr Sven Monrad Jensen for my very inspirational trip to the GEUS Diamond workshop in Denmark, their hospitality was wonderful, and the workshop was amazing for me. Special thanks to Karina for putting me up for 4 days, and your wonderful breakfasts too. "Your big and your good"!
- A special thanks to Prof Bob Thompson for inspiring me so much in my last year of undergraduate study to chose mantle geochemistry as a career.
- I also wish to thank Dr Scott Dreher & Dr Chris Dale for teaching me many procedures, and especially Chris for PGE data corrections.
- To Dr Akira Ishikawa for his great advice, thanks a million.
- Merci beaucoup, to Dr Jean-Pierre Lorand (Natural History Museum, Paris), for your investigation into the sulphide anomalies in sample 474568. Your kindness and generosity was very much appreciated.
- A huge thank you goes to Eddie and Helen for your understanding and patience. And making me loads of coffees!
- Lastly, I would like to thank the whole of the Geochemistry Group at Durham, I have made some wonderful friends that I will never forget.

# CHAPTER 1

# INTRODUCTION

# Chapter 1:

# Introduction

## 1.1 Overview

The development of the Archean lithospheric mantle is important for understanding when the continental crust began to stabilise in the young Earth. By 3.5 billion years ago (Ga) five significant areas of crust had formed in what is now known today as Archean cratons in North America, Siberia, Africa, Australia and Eastern Europe (Baltica) (Windley, 1977). The term craton is used for stable areas of crust and mantle which have not experienced any significant deformation for more than 500 million years (Ma). They are commonly found in the central areas of continents and are protected from deformations by their surrounding mobile zones. Evidence from diamond inclusions shows that these cratons were already thicker than 60km, even ~1Ga after the formation of the Earth (Boyd, 1985; Westerlund *et al.*, 2006). Almost all our knowledge of the formation of lithospheric mantle keels in the early Earth comes from fragments of mantle entrained in deeply-derived magmatic rocks, termed xenoliths. This study follows this line of investigation by using peridotite xenoliths sampled by alkaline rocks in W. Greenland to understand the timing of formation of the lithospheric mantle beneath this area of the North Atlantic Craton (NAC).

Lithospheric (solid crust & upper mantle) mantle xenoliths brought to the Earth's surface, through or around the edges of cratons, via magmatic activity can be geochemically and petrologically investigated to determine their composition, depth and age of formation. The significance of these investigations has implications for the mantle environment in which the xenoliths came from. Currently there is much debate focussed on whether modern day plate tectonics operated at 3.5 Ga and considerable uncertainty surrounding the melting environments in the Archean mantle, i.e., whether cratonic lithospheric mantle was generated in subduction zone settings or via plume activity (e.g., Davies, 1995; Griffin *et al.*, 2003; Leitch, 2004; Ernst, 2007; Simon *et al.*, 2007).

In this study over 160 lithospheric mantle xenoliths have been collected from c.600 Ma old alkaline dykes and sills (Larsen & Rønsbo, 1993; Mitchell *et al.*, 1999; Jensen *et al.*, 2003) which have intruded across a region of reworked Archean crust and undeformed Archean crust in S.W. Greenland. The xenoliths comprise lherzolitic, harzburgitic and dunitic lithologies and are thought to represent the lithospheric mantle root beneath this region of ancient crust.

The investigations to be carried out in this study involve using the platinum group elements (osmium, iridium, ruthenium, platinum, and palladium) and rhenium, together with the Re-Os isotope system. The Re-Os system has been shown to be singularly successful at dating mantle depletion events in peridotites (e.g., Meisel *et al.*, 2001; Pearson *et al.*, 1995a & b; Pearson *et al.*, 2004). The addition of PGEs to the analytical suite allows more stringent assessment of the effects of mantle metasomatism on the Re-Os system and so provides some indication of which samples are likely to be more disturbed than others (Pearson *et al.*, 2002; Pearson *et al.*, 2004). In addition, examination of inter-element PGE fractionations offer an insight into the variety of processes that may have affected cratonic lithosphere during and subsequent to its formation. Along with the PGE geochemistry, major elements have been analysed to further understand how their compositional variations reflect the possible melting environment and metasomatism. Using the PGEs and the major element compositions, comparisons can be made with other cratonic and circum-cratonic mantle xenolith suites, with an aim to characterise typical Archean cratonic mantle lithosphere and the processes that generate and modify it. Pressure and temperature investigations on the xenoliths from this area have also been carried out by GEUS (Geological Survey of Denmark & Greenland) in a separate Masters Research project by Sand (2007).

This study is currently a small part of a larger more comprehensive investigation into the lithospheric mantle beneath western Greenland, and the diamond potential of the area.

## 1.2 Aims

The aim of this project is to analyse a sub-set of mantle xenoliths for Re-Os isotopes and PGEs in order to provide the first age constraints for mantle lithosphere beneath the Kangalaussaq area of S.W. Greenland. Of particular interest was the potential age difference of lithosphere beneath the Archean and reworked Archean crustal terranes. Whole rock major element data will also be used to characterise the major element composition of the xenoliths in comparison with other cratonic peridotites. Alkaline rocks containing diamonds have recently been found in both crustal terranes and there is considerable exploration interest in determining whether or not these diamonds originate from typical cratonic mantle (GEUS, 2004).

## 1.3 Geological background

The exposed Archean rocks of SW Greenland have similar stratigraphy and metamorphic grade to Archean rocks found in the Labrador Province of NE Canada, East Greenland and the Lewisian complex of NW Scotland, and are collectively termed as the North Atlantic Cratonic region (Windley, 1977). The opening of the North Atlantic in the Tertiary separated the craton into the several fragments revealed today (Fig. 1.1).

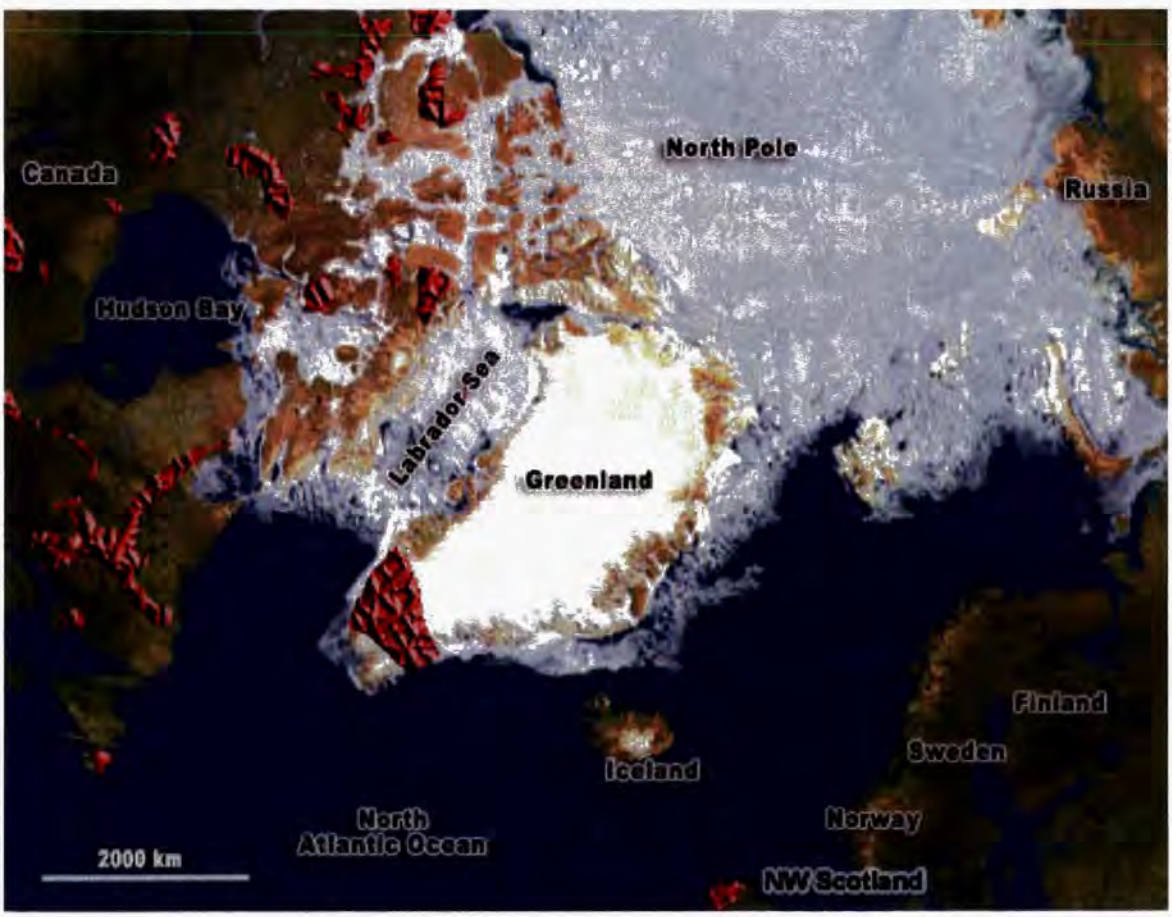


**Fig. 1.1** Satellite image of Greenland and the surrounding countries. Red areas are the North Atlantic cratonic regions.

## 1.4 Regional geology

The North Atlantic Craton (NAC) in southern Greenland lies between two areas of reworked Archean mobile belts. To the North is the Nagssugtoqidian Mobile Belt, refereed to here as the Reworked Archean Terrane (RAT: later discussed in more detail in section **1.6** Tectonic History), and to the South is the Ketilidian Mobile Belt (Bridgewater *et al.*, 1973) (Fig 1.2). This study is focussed on the north-western boundary of the NAC, where two generations of mafic dykes have intruded into the southern margin of the Nagssugtoqidian mobile belt and the northern margin of the Archean craton. The Kangâmiut Dyke Swarm emplaced doleritic dykes c.2040 Ma ago, trending NE-SW (Cadman *et al*, 2001), and alkaline dykes emplaced c.600 Ma ago showing no specific orientation (Larsen & Rønsbo, 1993). Different levels of exposed deformation in the Kangâmiut dykes mark the boundary between the RAT and the Archean craton (Fig. 1.3). The c.600 Ma alkaline dykes do not show any deformation in either the RAT or the craton. This research concentrates on the xenoliths that have been entrained by the c.600 Ma alkaline dykes, between the Kangerlussuaq and the Safartoq area of S.W. Greenland (Fig, 1.4).


**Fig. 1.2** Map of Greenland, showing the North Atlantic Craton between two Proterozoic mobile belts. The red oval indicates this research area. The Nagssugtoqidian is referred to here as the reworked Archean Terrane (RAT). To the North of the Nagssugtoqidian is the lesser known Disko Craton. (modified from Tappe *et al.*, 2004).

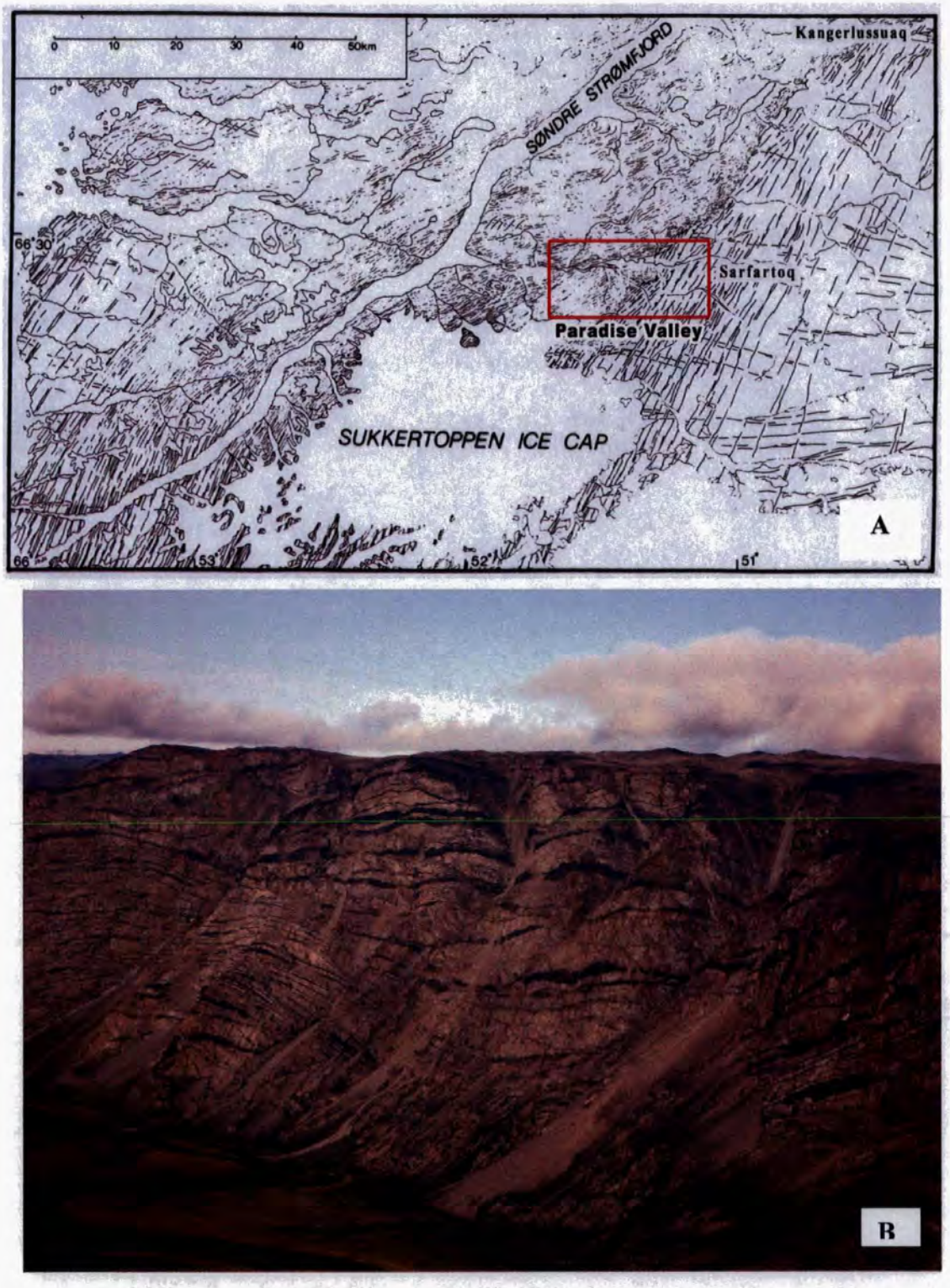


**Fig. 1.3. A.** The boundary between the Archean and the mobile belt can be seen very clearly by this drawing by Escher *et al.*, 1976. The Kangâmiut dykes are undeformed in the Archean NE of the Sukkertoppen Ice Cap, but NW of here the dykes are clearly disturbed. Red square shows where the photograph (**B**) was taken, looking down Paradise Valley, photo courtesy of Graham Pearson.

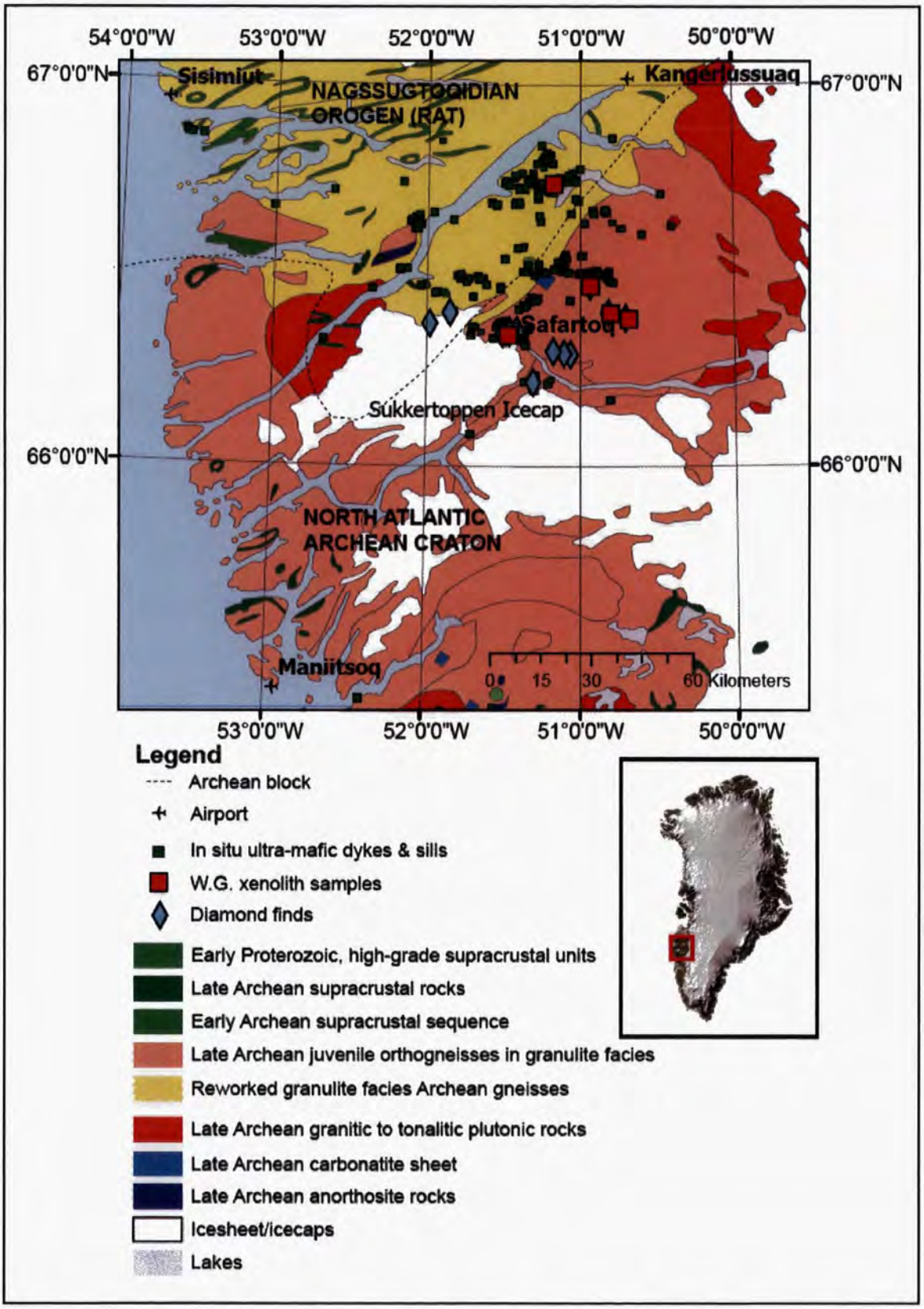


**Fig. 1.4**.Regional geology map of the research area. The dotted line indicates the aeromagnetic boundary between the RAT (Reworked granulite facies, Archean Gneisses) and the Archean craton. The red squares indicate where mantle derived peridotite xenoliths have been sampled for this study. The small green squares indicate where the alkaline dykes and sills have been reported. Blue diamonds denote reported diamond occurrences.

## 1.5 The geology at depth

One question that has arisen as a result of the recent diamond exploration activity, is whether the xenoliths in both crustal terranes have travelled through Archean lithospheric mantle or reworked Archean lithospheric mantle or even new Proterozoic lithospheric mantle? Previous work by the Geological Survey of Denmark (GEUS) and Hudson Resources Inc (2005) on this area have discovered micro-diamonds in some of the alkaline host rocks. There are several possibilities for the deep lithospheric structure beneath this area, illustrated in Fig. 1.5. Some possibilities involve diamonds being sampled in both terranes from typical cratonic mantle and other scenarios involve diamonds being sampled from mantle that is significantly younger than Archean, for instance, 2.0 Ga mantle produced during the Nagssugtoqidian orogeny.

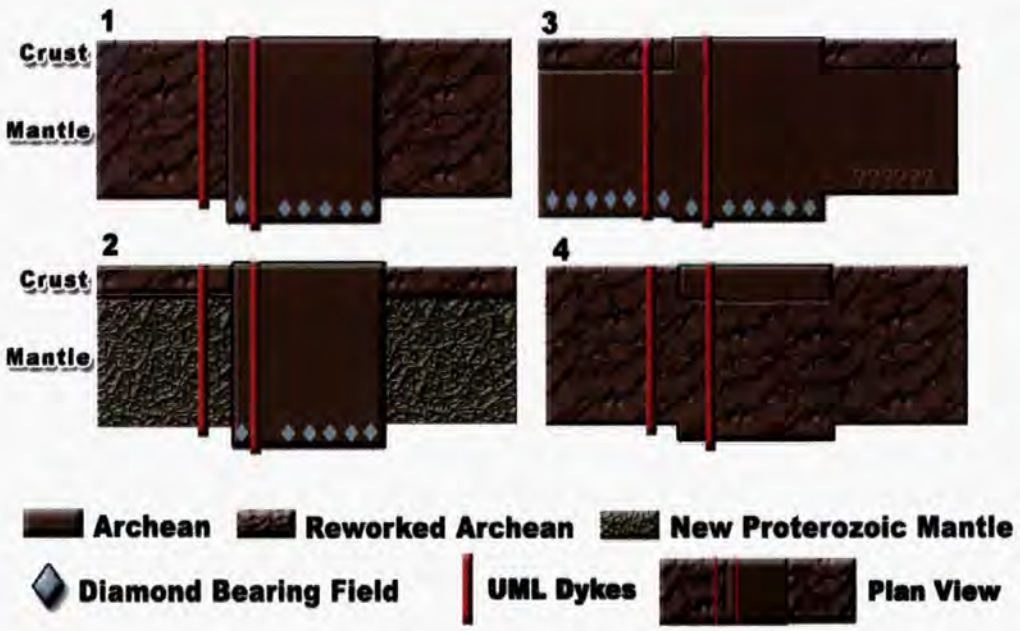


**Fig. 1.5.** In each of these four diagrams the crust on the surface appears the same, but the lithospheric mantle and diamond potential is different in each case.
**1.** The Archean and the reworked Archean in the crust continues into the mantle.
**2.** The reworked Archean mantle has been replaced by new Proterozoic mantle.
**3.** Only the Archean in the crust has been reworked.
**4.** Only the Archean in the crust has been preserved, entire mantle has been reworked.

### 1.5.1 Alkaline dyke classification

Currently there is significant debate concerning the classification of the alkaline dykes. Larsen & Rex (1992) have described these dykes as kimberlitic where as Mitchell *et al* (1999) uses mineralogical criteria to argue that most of the 600 Ma intrusions belong to the ultra-mafic lamprophyre (UML) clan of rocks. Most of the recent GEUS literature (e.g., Jensen *et al.*, 2003; Sand, 2007) use the term kimberlite for the dykes in this region and Neilsen (2006) makes a convincing case, based on detailed mineralogical criteria, for the name kimberlite being used for at least some of these rocks. It is not the purpose of this study to investigate this problem further and the term ultra-mafic lamprophyre (UML) will be used throughout to denote the host rocks. The use of this term does not endorse one classification over the other and resolution of this issue awaits a thorough petrological and mineral chemical investigation of many individual occurrences.

## 1.6 Tectonic History

This study area is situated on the north-western boundary of a large Archean craton, the North Atlantic Craton (NAC) in southern West Greenland (Fig.1.2). The Nagssugtoqidian to the North of the main craton exposure is a reworked Archean 'mobile belt'. The Kangâmiut Dykes mark the onset of a short term continental break-up event at c.2040 Ma ago. Thermal thinning in the Nagssugtoqidian resulted in the formation of a sedimentary basin at c.1950-1920 Ma, followed by convergence and consumption of the basin floor between c.1920-1870 Ma. This event produced a crustal thickening of the mobile belt and led to the Nagssugtoqidian Orogeny at c.1775 Ma (Cadman *et al.*, 2001). This syn-tectonic and thermal event aided the emplacement of the Kangâmiut dykes. A summary of the tectonic events which led to the Nagssugtoqidian orogeny and subsequent events are summarised in Table 1.

**Table 1**. A timeline of tectonic events which have effected the Safartoq area of S.W. Greenland.

| Million Years ago | Event | Ref |
|---|---|---|
| ~3870-2820 | Amphibolite & Granulite metamorphic facies | McGregor *et al.*, 1986 |
| ~2800 | TTG gneisses, Ilivertalik granite intrusion | Myers, 1984 |
| ~2750 | North Atlantic Craton formation | Windley, 1977 |
| ~2040 | Emplacement of the Kangamiut Dyke Swarm | Cadman *et al.*, 2001 |
| ~1950-1920 | Formation of a sedimentary basin | van Gool *et al.*, 2002 |
| ~1920-1870 | Convergence-consumption of the oceanic plate | Connelly *et al.*, 2000 |
| ~1860-1840 | Suture & peak metamorphism, crustal thickening | Marker *et al.*, 1995 |
| ~1825 | Large scale upright folding trending W-E | van Gool *et al.*, 2002 |
| ~1775 | Nagssugtoqidian Orogeny | van Gool *et al.*, 2002 |
| ~600 | Emplacement of the UML dykes & sills | Nielsen *et al.*, 2006 |
| ~70 | Continental break up, opening of the Labrador Sea | van Gool *et al.*, 2002 |
| ~55 | Opening of the North Atlantic | Saunders *et al.*, 1997 |

## 1.7 Field Observations

Fieldwork and rock sampling was carried out by the Geological Survey of Denmark and Greenland (GEUS) and the University of Durham in the summer of 2004. UML and xenolith samples were collected from Kangerlussuup Nunna (off-craton), Kissavissat Qooruate, Atanaligaarsiut and Safartoq (on-craton) (Fig. 1.6). The Kangerlussuaq region is referred to as the off-craton area and the Safartoq region is referred to as the on-craton area.


**Fig. 1.6** Map of the study area showing the locations where xenoliths and host rock samples were collected from. The grey dashed line denotes the aeromagnetic craton boundary (van Gool, 2002).

### 1.7.1 Safartoq area – In the Archean block

The c600 Myr old UML dykes occur in the form of shallowly dipping (around 15° N) dykes and sills (Fig. 1.7). The dykes are emplaced into red/pink banded Archean gneisses the UML dykes are trending E-W and ENE-WSW. A large carbonatite complex is situated on the boundary between the RAT and the Archean craton, north of Safartoq, and named the Safartoq carbonatite complex. The UML dykes have earlier been interpreted as cone-sheets related to the carbonatite complex (Secher & Jensen, 2004).


**Fig. 1.7** UML sill at Camp 2, on-craton in the Safartoq area

### 1.7.2 Kangerlussuaq area – In the Reworked Archean Terrane (RAT)

The RAT comprises of reworked Archean amphibolite facies gneisses (van Gool *et al.*, 2002). The c600 Ma UML dykes intruded into the RAT are undeformed, indicating that regional tectonic activity in this area had ceased by the time they were emplaced. Most UML dyke outcrops are weathered out, indicating a linear depression in the landscape (Fig. 1.8). The UML dykes are around ~1 to 1.5 m thick, and commonly occur as shallowly dipping sills, however, there are some vertical dykes present. With the action of freeze-thaw most sills/dykes are represented by large ultra-mafic boulder trails. These boulders can be traced E to W over a distance of 500 m.

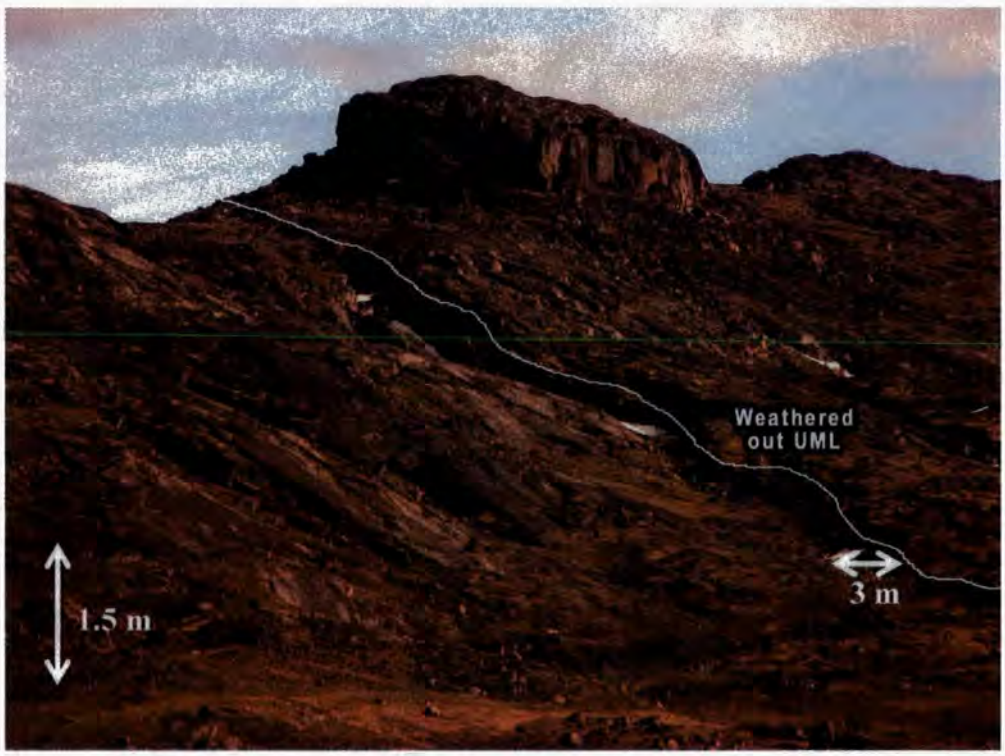


**Fig. 1.8** François Dyke, off-craton in the Kangerlussuaq area.
Notice the weathered out feature.

### 1.8 Previous Diamond Investigations

Previous investigations by GEUS into the diamond potential of the Safartoq area in 1998, returned 474 micro-diamonds and 5 macro-diamonds for the UML dykes (Jensen *et al.*, 2004). The diamonds do not have recognisable crystal faces and are graphite coated (Boucher, 2000).

# CHAPTER 2

# WESTERN GREENLAND XENOLITH SAMPLES

# Chapter 2:

# W.G. Samples

## 2.1 Collection of Samples

Xenoliths and their ultra-mafic host rocks were collected from a traverse covering 300 km on and off the North Atlantic Craton in S.W. Greenland. The study area is indicated by the blue oval on Figure 2.1.

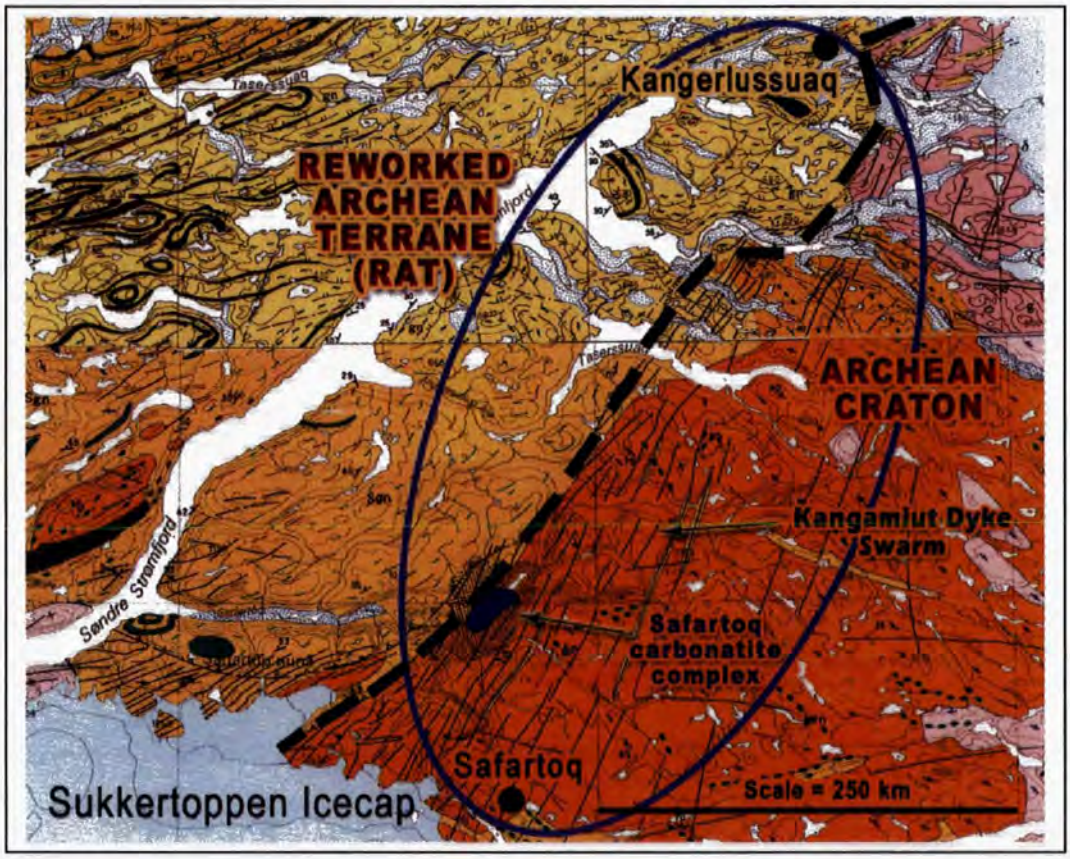


**Fig. 2.1** Map of the study area in S.W. Greenland. Host rocks and xenoliths were collected on and off the craton between Kangerlussuaq and Safartoq. Black dashed line denotes the boundary between the Archean and the RAT (aeromagnetic boundary distinction, van Gool, 2002). *Map adapted from section 2a & 3h from the GEUS online map database.*

## 2.2 W.G. Peridotite Xenoliths

### 2.2.1 Size & distribution

The size of the peridotite xenoliths ranges from approximately 6 to 50cm. The samples which were used for analyses were all larger than 10 x 10cm. Each sample weighed over

500g. The distribution of the peridotite xenoliths were in some places very concentrated in the UML dykes, almost to the point where there were more xenoliths than matrix (Fig. 2.2 A & B). In other cases some peridotite xenoliths were very large and were found alone in the UML dyke (Fig. 2.2 F).

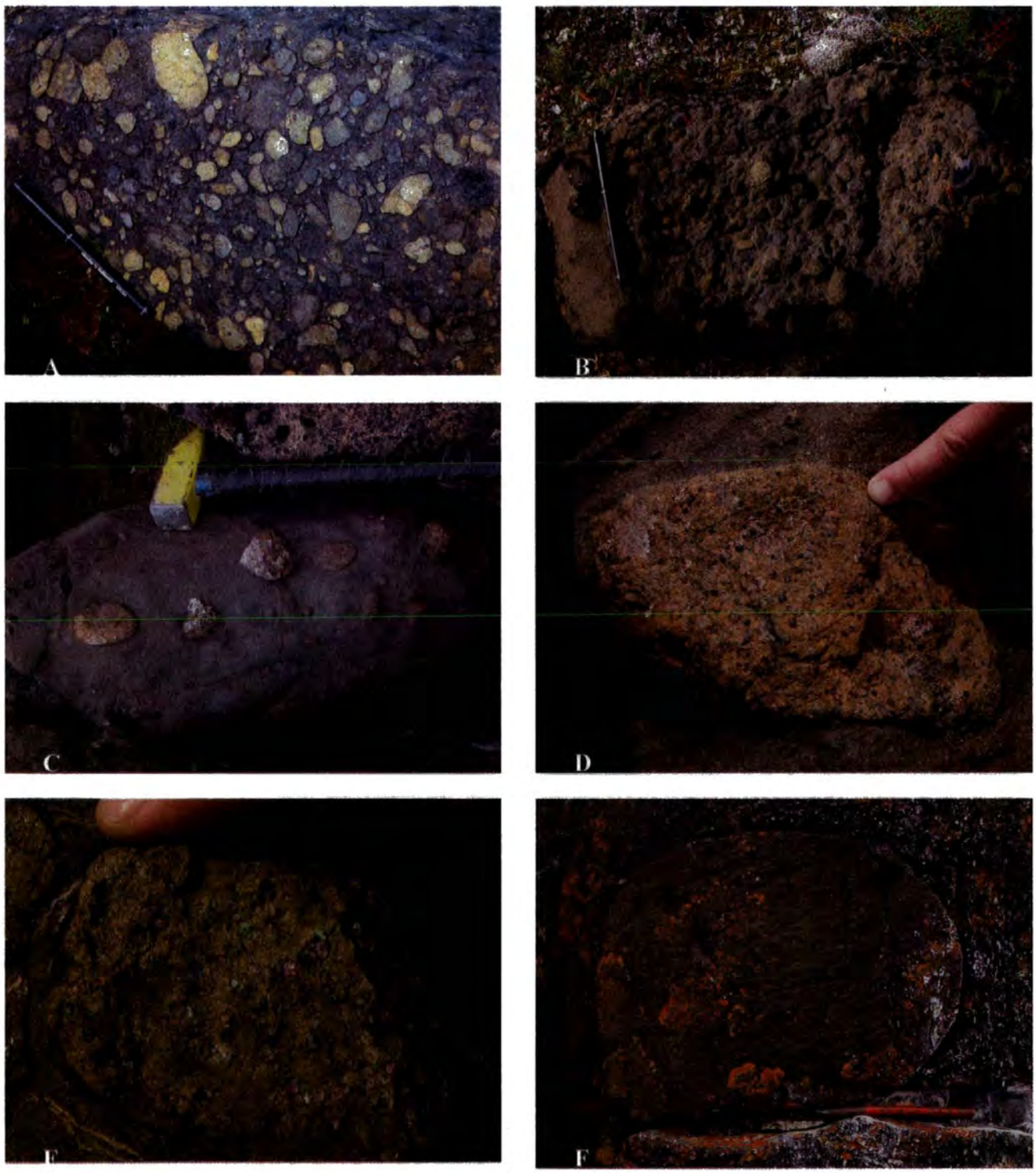


**Figure 2.2** **A**. A high concentration of xenoliths in an UML boulder, on-craton. Pen is 14cm long. **B**. An UML boulder with a high concentration of small xenoliths, on-craton. **C**. A large UML boulder ~1m wide, with 7 large peridotite xenoliths standing proud of the surface of the boulder. **D**. A 14 x 9cm peridotite xenolith, standing proud of a UML boulder, small garnets are seen standing proud of the xenolith, off-craton. **E**. Garnets and clinopyroxenes are clearly seen in this 10 x 7 cm harzburgite xenolith, on-craton. **F**. A football sized peridotite xenolith in an UML dyke.

The UML dykes and sills are more susceptible to weathering and as a result, the xenoliths are quite often standing proud of the surface. The xenoliths are weathered on the outside with an orange rust colour on the surface. This is from the high concentration of olivines in the samples. In samples which are split exposing the fresh sample inside, the colour is usually dark grey to black. Some of the samples are fine grained and identifying minerals to the naked eye is not possible. Other samples like 474538 seen here in Figure 2.3, the crystals are much larger and this xenolith clearly contains ~5mm sized garnets. This sample is found in the Archean craton.


**Fig. 2.3** Sample 474538 (on-craton) of the W.G. peridotite suite. This sample shows clearly the orange weathered surface and the grey-black fresh interior. Millimetre sized garnets are visible on the weathered and the freshly cut surface.

### 2.2.2 Off vs. On-craton xenolths

Sample 474538 (Fig.2.3) was found on-craton. Figure 2.4 shows sample 474527 a xenolith found in the reworked Archean terrane. Both xenoliths have similar characteristics. Both have a fine grained grey-black matrix and ~1-5mm sized garnets. The garnets in the on-craton xenolith are less altered than the off-craton xenolith. Clinopyroxene is more common in the off-craton xenoliths.

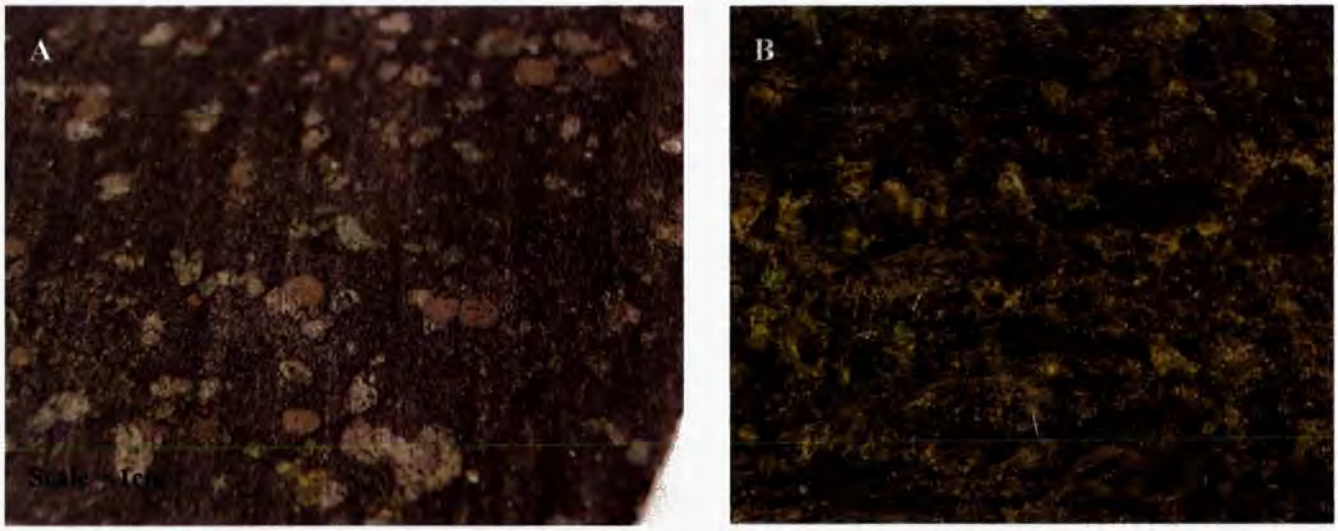


**Fig 2.4** Shows sample 474527 (off-craton) **A.** shows the cut sample of the xenolith, where the minerals clinopyroxene and garnet are easy to see. **B.** Shows the weathered rusty olivines on the surface of this xenolith.

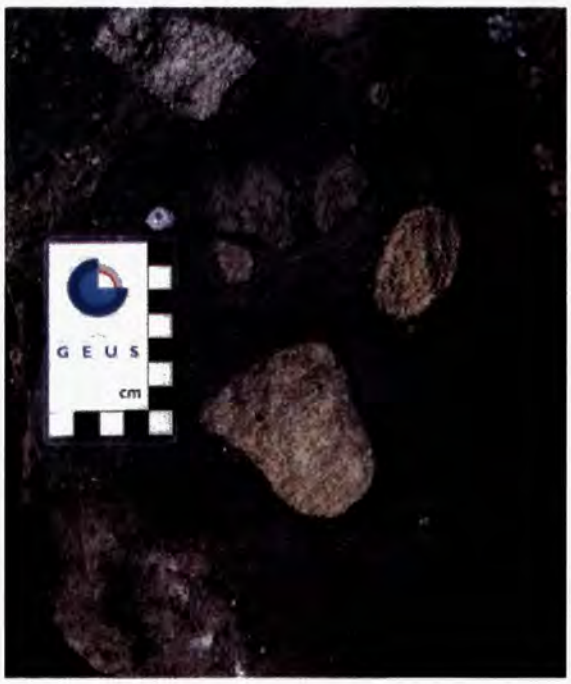


## 2.3 The UML host rock

The ultra-mafic lamprophyre rocks are fine grained, most are aphanitic and the mineralogy is too small to identify without a thin section. Where minerals are large enough to identify, the most common is olivine, followed by garnets and some ilmenites. Many of the samples of the host rock contain veins of carbonate infiltrating the rock. Some macrocrysts of olivine in the lamprophyre are highly serpentinized around the edges.

**Fig. 2.5** A lamprophyre boulder containing xenoliths from W.G. (GEUS, 2004).

# CHAPTER 3

# ANALYTICAL METHODS

# Chapter 3:

# Geochemistry and Analytical Methods

## 3.1 Preparation of Xenoliths

All the weathered edges and serpentinisation on the xenoliths were removed with a diamond lap saw, exposing the block of peridotite in the centre. In order to remove any contamination from the saw blade, all the edges of the blocks were rubbed with corundum paper. The blocks were then placed in an ultrasonic bath, where small particles of dust would be dislodged and removed. The clean blocks were then split into smaller sized pieces using a splitter, and further crushed in a jaw crusher to 1-3mm sized grains. The grains were then transferred to an agate ball mill to produce a rock powder fine enough for digestion. A minimum of 500g of powder was stored for each sample.

## 3.2 Rock powder weighing and digestion

1 gram of the powdered sample was weighed in a clean environment and carefully transferred to a Carius tube or quartz Asher reaction vessel for digestion (described in more detail below). The advantage of this method of digestion means that all the PGEs (Os, Ir, Ru, Pt, Pd) plus Re can be retrieved from the same dissolution. Each sample was spiked with 5 µL of 'peridotite' spike solution enriched in $^{194}Pt$, $^{191}Ir$, $^{190}Os$, $^{185}Re$, $^{106}Pd$ & $^{99}Ru$ and used to recalculate concentrations during data analysis. The amount of spike is also weighed. This spike weight can then be factored into the calculation process of the data. The accepted dissolution for Re-Os isotope determination is a high temperature "inverse" aqua regia digestion (Shirey and Walker, 1995; Pearson & Woodland, 2000; Meisel *et al.*, 2001). Although this does not dissolve the rock powder completely Shirey and Walker (1995) and Pearson and Woodland (2000) have recorded good results from this method. The aqua regia consists of 2.5 mLs of chilled ultra-pure concentrated (conc.) hydrochloric acid (HCl) and 5 mLs of chilled and sparged (heated to 80°C and then air is bubbled through to remove any volatile Os), ultra-pure conc. nitric acid ($HNO_3$). The aqua regia was added to each Carius tube or reaction vessel, containing the sample powder and the weighed quantity of 'peridotite' spike.

### 3.2.1 Carius Tube digestion

The Carius tube method has proved to be a very effective means of digestion of Re-Os isotope determination (Shirey & Walker, 1995; Pearson & Woodland, 2000). However, there are some safety issues in using this technique. The aqua regia must be chilled to slow down the reaction of the acids and minimise the pressure build up in the tube before sealing. The Carius tubes are made from Pyrex/borosilicate glass, they have a long thin open neck to allow for the sample to be introduced via Teflon funnels and long enough for the tube to be sealed, and then reopened. The tubes containing the aqua regia are stood in a freezing mixture of dry ice and ethanol, to maintain the retarded reaction, and to reduce the possible loss of volatile Os and Ru tetroxides. The tubes must be sealed as soon as possible. The neck of the tubes are sealed using an oxygen and propane torch. Whilst the other tubes are being sealed, the sealed tubes are placed back into the dry ice mixture. It is important to subdue the reaction as much as possible in the tube, to minimise the risk of the tube exploding. When all the tubes are sealed they are left in a rack behind a safety shield to warm up to room temperature. Leaving the tubes to acclimatise allows for the detection of weaknesses in any of the tubes. Also allowing the tubes to acclimatise lessens the risk of the tubes exploding when temperatures begin to rise in the oven. The Carius tubes are then placed in stainless steel jackets to contain any potential Carius tube explosion, and transferred to a cold oven. The oven is slowly increased to 240°C, for 24 hours. The oven is completely cooled before removing the tubes. Again the tubes were stood in dry ice and ethanol to reduce the internal pressure before opening. After opening the tubes would be transferred to the fume cupboard for the following osmium extraction procedure (**Section 3.3.1**).

The Carius tube digestion method is very effective for Re-Os isotope determination, but there is an issue with Pt blanks, due to the 'high' Pt contents in the borosilicate glass that is used to make the Carius Tube (Fig. 3.1).

**Fig. 3.1** Borosilicate Carius tubes.

### 3.2.2 Asher digestion

The high pressure Asher (Fig. 3.2) ((HPA-S) Anton Paar-Perkin-Elmer), digestion technique is described by Meisel *et al* (2001). This technique uses 90 mL quartz glass vessels with quartz glass lids (Fig 3.3). The advantage of using this digestion method is that the vessels can be cleaned and reused. However, because the technique is still in its infancy, it is uncertain if there are any problems with memory blanks. To avoid this


**Fig. 3.2** The Anton Paar-Perkin-Elmer high pressure asher (HPA-S).
**Fig. 3.3** 7 x 90 mL quartz vessels with glass lids.

problem there are 3 sets of 7 vessels used for peridotite, basalt, and lunar sample digestions respectively. The cleaning procedure requires that the vessels are leached with aqua regia under high pressure and temperature in the HPA as well, as being cleaned manually. Another advantage of the HPA digestion is that the samples are subjected to both high pressures (130 bar) and high temperatures (300°C) for 5 hours. This method is more effective in dissolving the silicates and refractory phases such as high temperature sulphides and alloys, which are likely to occur in mantle peridotites (Luguet *et al.,* 2003 & 2007; Lorand *et al.,* 1999 & 2007). However, there is still some residue in the bottom of the vessels after digestion. The Pt blanks are low and appear to be much favorable than the Carius tube Pt blanks.

The volume concentration of reverse aqua regia to put into the Asher vessels with the sample and the spike is the same for the Carius tube method. The HCl and the $HNO_3$ are still chilled, but the HCl is put in the vessels just before they are sealed with Teflon tape. The sealed vessels are placed in the HPA overnight. The vessels are then removed the following morning from the Asher and taken to the fume cupboard for opening immediately and the osmium extraction procedure (**Section 3.3.1**).

## 3.3 Os Chemistry

### 3.3.1 Os Extraction

Each tube/vessel containing the aqua regia and digested sample was opened in a prepared fume cupboard. 7.5 mL of MilliQ $H_2O$ (reverse osmosis purification of 18.2 MΩ cm of water in a MilliQ system), was gently added to each tube. Using a transfer pipette the MQ $H_2O$ and reverse aqua regia supernatant was gently agitated and transferred to a clean 50 mL centrifuge tube. 1 mL of chilled carbon tetrachloride ($CCl_4$) was then added to the carius tube/asher vessel and shaken gently (great care must be taken when using the $CCl_4$, as this is toxic and carcinogenic, nitrile gloves, goggles and lab coat must be worn). The $CCl_4$ was then pipetted off the sample and added to the 50ml centrifuge tube which contained the aqua regia and MQ $H_2O$ solution. Then an additional 2 mL of $CCl_4$ was added to the centrifuge tube and transferred to a shaker plate for 5 minutes (Fig. 3.4).

**Fig. 3.4** Shows the 50 mL centrifuge tubes containing the aqua regia, MQ $H_2O$ and the $CCl_4$, on the shaker.

After 5 minutes of shaking the centrifuge tube was removed from the shaker plate and the $CCl_4$ was pipetted off into a clean 20 mL Savillex Teflon beaker, containing 4 mL of chilled conc. ultra-pure hydrobromic acid (HBr). Then a further 2 mL of $CCl_4$ was added to the aqua regia and MQ $H_2O$ solution and placed back on the shaker plate for 5 minutes. After 5 minutes the centrifuge tube was removed from the shaker plate and the $CCl_4$ was transferred to the 20 mL Teflon beakers containing the 4 mL HBr together with the previous 3 mL of $CCl_4$. This step was repeated once more, until there was 7 mL of $CCl_4$ and 4 mL of HBr in the 20 mL Teflon beakers.

### 3.3.2 The Os cut

The 20 mL Teflon beakers containing the hydrobromic acid and the carbon tetrachloride were then left to agitate on the shaker plate overnight.

### 3.3.3 Os Back Extraction

After the Os cut samples ($CCl_4$ & HBr) have been on the shaker plate overnight, the beakers were removed and the solution was allowed to settle. After a few minutes the HBr and the $CCl_4$ would separate and the HBr would be sitting on top of the $CCl_4$. The HBr was then pipetted off the $CCl_4$ into clean 20 mL Teflon beakers, taking care not to incorporate any of the $CCl_4$. The $CCl_4$, can be discarded and the HBr samples were then placed on the hotplate to dry down, ready for the micro-distillation procedure (**Section 3.3.4**).

### 3.3.4 Os Micro-distillation

40 µL of 12N sulphuric acid ($H_2SO_4$) was added to the dried HBr sample (the Os cut), in order to re-hydrate the sample and prepare it for chromic acid addition. Teflon tape was applied around the thread of a clean 7 mL Teflon "rocket" vial, to ensure a tight seal for the micro-distillation process. 20 µL of conc. HBr was pipetted into the apex of the rocket vial. The shape of the rocket vial allows the droplet to be retained here even when the vial is turned upside down. The lid of the rocket vial was placed facing upwards and 20 µL of the $H_2SO_4$ sample solution was pipetted into the centre of the lid. Then 20 µL of chromic acid ($CrO_3$) was carefully incorporated into the 12N $H_2SO_4$ droplet on the lid (Fig. 3.5). The chromic acid oxidises the Os to $OsO_4$.

**Fig 3.5** Shows the chromium oxide ($Cr_2O_3$) being added to the 12N sulphuric acid ($H_2SO_4$) droplet in the rocket vial lid. **Fig. 3.6** Shows the rocket vial upside down and sealed with the hydrobromic acid (HBr) droplet in the bottom of the cone, and the chromium oxide and sulphuric acid in the lid.

The rocket vial now containing the HBr was turned upside down and screwed carefully back on the lid (Fig. 3.6). Keeping the rocket vial upside down and very steady, aluminium foil was wrapped around the rocket vial with only the point of the conical base protruding out of the top. This encourages the volatile $OsO_4$ vapour to condense

where there is no foil, i.e. in and around the HBr droplet in the apex of the cone. The rocket vial is then placed upside down on the hotplate at 90°C for 2 hours (Fig. 3.7).

**Fig. 3.7** Rocket vials on the hotplate, with aluminium foil wrapped around the base and the sides. The foil directs the heat up towards the cooler exposed tips of the cone.

After 2 hours the rocket vials were removed from the hotplate and the foil was carefully removed. Still with the vials upside down, the lid were removed and the vial was moved away from the lid. The vial base was then carefully turned the right way up, and placed back on the hotplate to dry down. The lids were then cleaned with MQ $H_2O$ to be placed back on the vials when the sample was dry.

## 3.4 PGE Column Chemistry

### 3.4.1 The PGE cut

The remaining aqua regia and MQ $H_2O$ solution (which now contains the highly siderophile elements minus the Os) in the 50 mL centrifuge tubes was transferred into clean 30 mL Teflon beakers and dried down on a hotplate. After the aqua regia had dried to a residue, 1 mL of SPA conc. HCl was added to the beaker, the cap was replaced, and the beaker was returned to the hotplate for 1 hour. After 1 hour the cap was removed and the sample was allowed to dry down to a residue again. After the sample had dried again, 10 mL of 0.5N HCl was added to the beaker, the cap was replaced, and the beaker was returned to the hotplate for one hour. The beakers were then taken off the hotplate and allowed to cool. At this point the samples were ready for their PGE column chemistry (**Section 3.4.2**).

### 3.4.2 PGE column Chemistry

The aqua regia and MQ $H_2O$ from the extraction procedure were in the 30 mL Teflon beakers which had been dried down, and then re-hydrated with 10 mL of 0.5N UPA HCl and left to cool. They were now ready for the PGE column chemistry. 1$cm^3$ of clean Bio-Rad AGI-X8 100-200# resin was pipetted into each column. The columns were then preconditioned with 6 mL of 6N SPA HCl, then 10 mL of MilliQ $H_2O$ and then 5 mL of 0.5N UPA HCl (Fig 3.8). The 10 mL of sample in the beakers was then pipetted onto

**Fig. 3.8** Photo taken in the clean lab, of the PGE column chemistry. The orange colour in the columns is the resin. Acid is dripping through the columns into the waste beakers below.

each column. Then 10 mL of 1N HCl/1N HF (hydrofluoric acid) was added to each column, this removes the hafnium, zirconium and yttrium (Hf, Zr, and Y oxides can interfere with several Pt, Ir and Pd isotopes) from the columns into waste beakers below. The leaching of the Hf, Zr and Y were initiated by Luguet & Pearson (unpublished) to reduce oxide interferences during analyses. Then 10 mL of 0.8N $HNO_3$ was added to each column, to convert it to nitrate. Then 12 mL of 13.5N $HNO_3$ was added to the columns and the Ir, Ru, Pt, & Re cut was collected in clean 20 mL Teflon beakers. The resin in the columns was then rinsed by adding 5 mL of MQ $H_2O$. 40 mL of 1N HCl/1N HF was then added to the columns in 10 mL batches and then 5 mL of MQ $H_2O$ was added to the columns, to remove any remaining Zr and Y. 20 mL of 9N HCL was added to each column and the Pd cut was collected in separate clean 20 mL Teflon beakers. Both sets of beakers were placed on a hotplate at 90°C to dry down. Once the samples were dry, they each needed re-hydrating with 1 mL of 0.5N HCl and transferred to clean 2 mL centrifuge tubes, for analysis on the Thermo Finigan Element 2 HR-ICP-MS.

## 3.5 Triton Analysis of Os

### 3.5.1 Preparation of samples for Triton analysis

Platinum ribbon (0.02 x 0.001 inch, obtained from Electronic Space Products Inc.) was welded onto clean filament posts ready for osmium loading (Fig. 3.9 & Fig. 3.10). The

**Fig. 3.9** Shows the Pt ribbon being welded onto the filament
**Fig. 3.10** Shows the filaments with their welded Pt ribbons, ready for the Os loading procedure.

dried down osmium sample in the rocket vial was loaded onto the filament. The dried sample was re-hydrated with 0.5 μL of 9N HBr, this droplet was pipetted onto the centre of the platinum ribbon and dried with a heating lamp. 0.5 μL of mixed barium oxide $Ba(OH)_2$/NaOH activator was dried on top of the sample on the platinum ribbon. The filaments were then loaded onto a magazine which was inserted into the negative ion source of the Triton mass spectrometer (Fig. 3.11).

### 3.5.2 Triton Mass spectrometry

The mass spectrometer is used to measure the isotope ratio of the sample. The barium activator, in combination with a slow oxygen bleed into the source, produces a $OsO_3^-$ ion beam. The ions are sent into a magnetized acceleration chamber where lighter ions are deflected more than the heavier ions onto a secondary electron multicollector.


**Fig. 3.11** Thermo Finnigan. Triton Mass Spectrometer (N-TIMS). The image shows the –ve ion source, used for Os analyses only.

### 3.5.3 Triton analysis of osmium isotopes

The Os isotopes were analysed on the Triton operating in negative ion mode. All Os signals are measured by peak-hopping on the SEM. The raw Os data results are corrected for spike and blank concentrations. The rest of the PGE's and Re were analysed on the Element 2.

## 3.6 Element 2 analysis of PGE's and Re.

The sample is nebulized and delivered through a glass tube by an argon carrier gas. The sample is then exposed to radio frequency which converts the gas into a plasma. PGEs (Ir, Pt, Ru, Pd) and Re were analysed on a Thermo Finnigan Element 2 ICP-MS, following Dale *et al.*, (2007 in review).

## 3.7 Whole rock analysis

Major elements were obtained by X-ray fluorescence spectrometry (XRF); analyses were carried out by the Geological Survey of Denmark (GEUS).

# CHAPTER 4

# DESCRIPTION OF MAJOR ELEMENT GEOCHEMICAL DATA

# Chapter 4:

# Description of Major Element Geochemical Data

## 4.1 Introduction

Lithophile elements are Na, K, Si, Al, Ti, Mg and Ca, they are rock forming minerals of the crust and mantle. Siderophile elements are Fe, Co, Ni, Pt, Re and Os and have an affinity for iron and concentrate in the core. These elements can be further divided into their preference to be in the melt, and described as fusible elements or incompatible elements. Or they prefer to be in the residue left after melting and are described as refractory elements or compatible elements. Fusible elements which prefer to be in the melt are Na, K, Al, Ca, Si, and Ti, they often have low amounts in the mantle. Refractory elements such as Mg, Fe and Cr often have high amounts in the mantle, forming solid residues. Fluids are driven off oceanic slabs as they subduct into the mantle, and result in some elements being more mobile in fluids. Fluids that flux through the mantle can alter the composition of the residue. Na, K, Ca, and Fe, can often be transported in these fluids, their interaction with the solid residues in the mantle, is referred to as mantle metasomatism. The effect of mantle metasomatism can disturb their compositional signatures, especially when plotting their major element compositions.

## 4.2 Whole rock compositions

32 peridotite xenolith samples taken from the c600 Ma alkaline dykes in the Kangalussuaq and Safartoq area of South West Greenland have been analysed for major element compositions. The incompatible elements CaO, $Al_2O_3$ and $TiO_2$ should show negative correlations with MgO. Figure 4.1 shows the incompatible elements plotted against MgO for Western Greenland (W.G.) peridotites, non-cratonic peridotites, Kaapvaal peridotites, East Greenland peridotites and a primitive mantle sample for comparison. Western Greenland on-craton samples are denoted by the red squares, the off craton samples are denoted by the black diamond in the centre of the red squares. There are also 3 samples which have their sample names indicated.

These have been highlighted specifically to track their behaviour and are discussed later in Chapter 6.

### 4.2.1 MgO vs. $TiO_2$, $Al_2O_3$ & CaO

W.G. peridotite xenolith samples have high contents of MgO between 41-51 wt.% as shown in Fig. 4.1, and showing similar contents to East Greenland (E.G.) which have 42-51 wt.% MgO. Cratonic Kaapvaal peridotite xenoliths have slightly lower MgO contents between 40-49 wt.%. The non-cratonic peridotite xenolith suite have a wide range in MgO contents between 32-48 wt.%. The off-craton peridotite xenoliths for W.G. (red squares with black diamonds) do not appear to be showing any similar characteristics in $TiO_2$/MgO or CaO/MgO, but they do appear to be slightly grouped in the $Al_2O_3$/MgO plot. Overall $TiO_2$, $Al_2O_3$, and CaO for W.G. samples do show negative correlations with MgO. However, sample 474566 has a very high content of $TiO_2$ (1.7 wt.%) and CaO (5.9 wt.%), and shows a very positive correlation to MgO. This sample also has the lowest concentration of MgO at 41.6 wt.%. Sample 488858 is also very high in $TiO_2$ (0.4 wt.%) with a given MgO, but has a very low ratio of CaO/MgO (0.3/44.8 wt.%). Generally the $TiO_2$ contents of the W.G. xenoliths (0.03-1.7 wt.%) is higher than those for other cratonic xenoliths, i.e. Kaapvaal and E.G. The $Al_2O_3$ contents of the W.G. xenoliths range from 0.06-1.8 wt.% and plot in a similar field to the other cratonic peridotite suites, but they do extend to a more depleted composition.

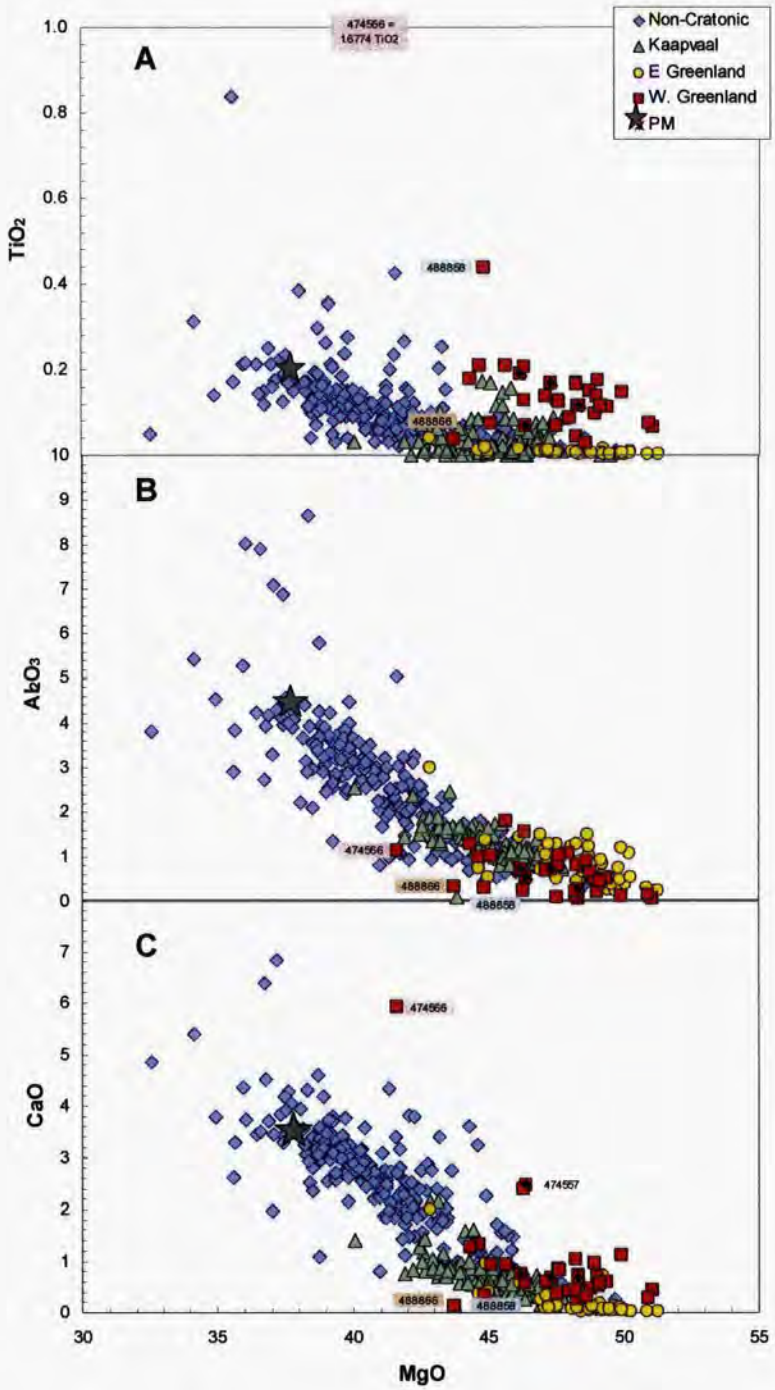


**Figure 4.1**.Whole rock MgO relations, **A**. MgO vs $TiO_2$. **B**. MgO vs $Al_2O_3$. **C** MgO vs CaO. **Red squares** =western Greenland on-craton peridotite xenolith suite (this study), **red squares with black diamonds** =western Greenland off-craton (this study). **Blue diamonds** = non-cratonic peridotite xenolith suite (Hungary (Embey-Isztin *et al.*, 1989), Romania (Vaselli *et al.*, 1995), Italy (Morton, 1987 & Dupuy *et al.*, 1987), British Isles (Hunter & Upton, 1987), Australia (Frey & Green, 1974; McDonough, unpublished; Yaxley *et al.*, 1991; Stoltz & Davies, 1988; Griffin *et al.*, 1987), Mexico (Luhr & Aranada-Gomez, 1997), Mongolia (Press *et al.*, 1986), China (Qi *et al.*, 1995; Song & Frey, 1999), Africa (Bedini *et al.*, 1997; Dautria & Girod, 1987; , Dupuy *et al.*, 1986)). **Green triangles** = cratonic peridotite xenolith suite, Kaapvaal, South Africa (Pearson *et al.*, 1995; Boyd *et al.*, 1993; Boyd *et al.*, 1999; Boyd & Mertzman, 1987). **Yellow circles** = cratonic peridotite xenolith suite, E. Greenland (Bernstein *et al.*, 1998). **Grey star** = Primitive mantle (McDonough & Sun, 1995). All oxides normalised to 100% water-free. Actual data is given for all in Appendix A, B, C, D, E & F.

### 4.3.2 $SiO_2$ vs. $TiO_2$, CaO and MgO

$SiO_2$ contents of the W.G. peridotite xenolith suite range from between 36-45 wt.%, with an average of 42 wt.% (Fig. 4.2). Figure 4.2 shows W.G. samples compared to other peridotite suites and the primitive mantle (sources are given in Figure 4.1 and Table 4.2) The E.G. suite show a similar range of $SiO_2$ between 39-46 wt.%, with an average of 43 wt.%. The non-cratonic data points show a wide range in $SiO_2$ from 39-52 wt.%, with an average of 45 wt.%. The Kaapvaal peridotite xenolith suite show a much higher average of $SiO_2$ at 46 wt.%, and range from 43-49 wt.%. An interesting point to make here is based on the average of $SiO_2$ in all the peridotite suites, and that the cratonic Kaapvaal suite has the highest average as seen in Table 4.1. Not expected for depleted cratonic peridotites.

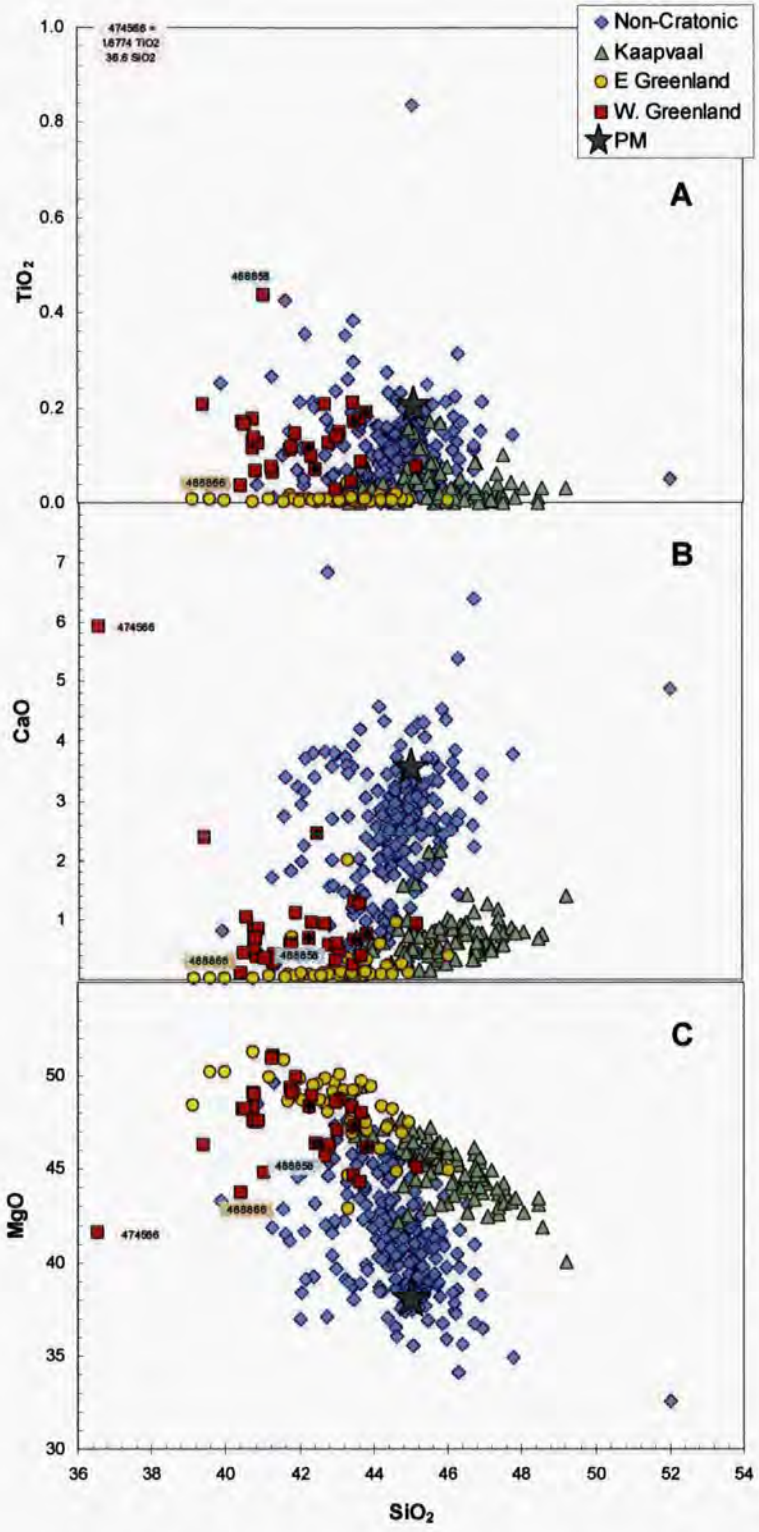


There is no correlation observed with the off-craton samples for W.G.

**Fig. 4.2** Whole rock $SiO_2$ relations, **A**. $TiO_2$ vs $SiO_2$, **B**. CaO vs $SiO_2$, **C**. MgO vs $SiO_2$. For sources see Fig. 1.

**Table. 4.1** $SiO_2$ contents of all the peridotite xenolith suites

| Location | Range | Average |
|---|---|---|
| Kaapvaal | 43-49 wt.% | 46 wt.% |
| Non-cratonic | 39-52 wt.% | 45 wt.% |
| E.G. | 39-46 wt.% | 43 wt.% |
| W.G. | 37-45 wt.% | 42 wt.% |

The W.G. peridotite sample 474566 has the lowest $SiO_2$ at 36 wt.%. Samples 488858 and 488866 have similar $SiO_2$ contents to the majority of the W.G. samples, and do not display any unusual anomalies.

**Table 4.2** Data sources for major element compositions of peridotite xenolith suites.

| Location | Authors | Year |
|---|---|---|
| ***Non-cratonic*** | | |
| Europe | | |
| Hungary, TVR | Embey-Isztin *et al* | 1989 |
| Romania, Perjani Mtns | Vaselli *et al* | 1995 |
| Italy | Morton | 1987 |
| Sardinia | Dupuy *et al* | 1987 |
| British Isles | Hunter & Upton | 1987 |
| Rest of the world | | |
| USA | Menzies & Hawkesworth | 1987 |
| Various | Jagoutz *et al* | 1979 |
| S.E. Australia | Frey & Green | 1974 |
| S.E. Australia | McDonough | unpublished |
| S.E. Australia, Victoria | Yaxley *et al* | 1991 |
| E. Australia | Stolz & Davies | 1988 |
| Australia, Queensland | Griffin *et al* | 1987 |
| Mexico | Luhr & Aranada-Gomez | 1997 |
| Mongolia | Press *et al* | 1986 |
| S.E. China | Qi *et al* | 1995 |
| China, Hannuoba | Song & Frey | 1989 |
| East African Rift, Ethiopia | Bedini *et al* | 1997 |
| N. Africa | Dautria & Girod | 1987 |
| Algeria, Hoggar | Dupuy *et al* | 1986 |
| ***Cratonic*** | | |
| S. Africa, Kaapvaal | Pearson *et al* | 1995 |
| S. Africa, Kaapvaal | Boyd *et al* | 1993 |
| S. Africa, Kaapvaal | Boyd *et al* | 1999 |
| S. Africa, Kaapvaal | Boyd & Mertzman | 1987 |
| Tanzania, Labait | Lee & Rudnick | 1999 |
| N. Tanzania, Olmani | Rudnick *et al* | 1993 |
| Tanzania, | Rudnick *et al* | 1994 |
| Siberia | Boyd *et al* | 1997 |
| Canada, Slave, Jericho K | Kopylova & Russell | 2000 |
| Canada, Somerset Island | Irvine *et al* | 2003 |
| Canada, Somerset Island | Schmidberger & Francis | 1999 |
| W. Australia | Jaques *et al* | 1990 |
| E. Greenland | Bernstein *et al* | 1998 |
| Beni Bousera, Morocco | Pearson *et al* | 2004 |
| Vitim, | Pearson *et al* | 2004 |
| Lesotho, | Pearson *et al* | 2004 |
| Namibia, | Pearson *et al* | 2004 |

### 4.3.3 $Al_2O_3$ vs. CaO & $SiO_2$

$Al_2O_3$ is particularly useful in major element and PGE systematics as it is not effected by serpentinization or metasomatism. Therefore the $Al_2O_3$ content of the residual rock should be undisturbed, while other more mobile elements like Ca and Si may have been altered from their original composition. Figure 4.3 shows $Al_2O_3$ contents against the CaO and $SiO_2$ contents of various peridotite suites. The CaO for the W.G. xenoliths ranges from 0.2-5.9 wt.% with an average of 0.9 wt.%. The W.G peridotites have higher contents of CaO than E. Greenland. The E. Greenland peridotite suite ranges from 0.05-2.0 wt.% with an average of 0.2 wt.%. W.G. sample 474566 has a very elevated content of CaO, as seen in other plots. Samples 488890 and 474557 show elevated contents of CaO. Exploring the K, Ti, and P, will help to investigate the possibility of these samples being contaminated by the host magma (Fig 4.4).

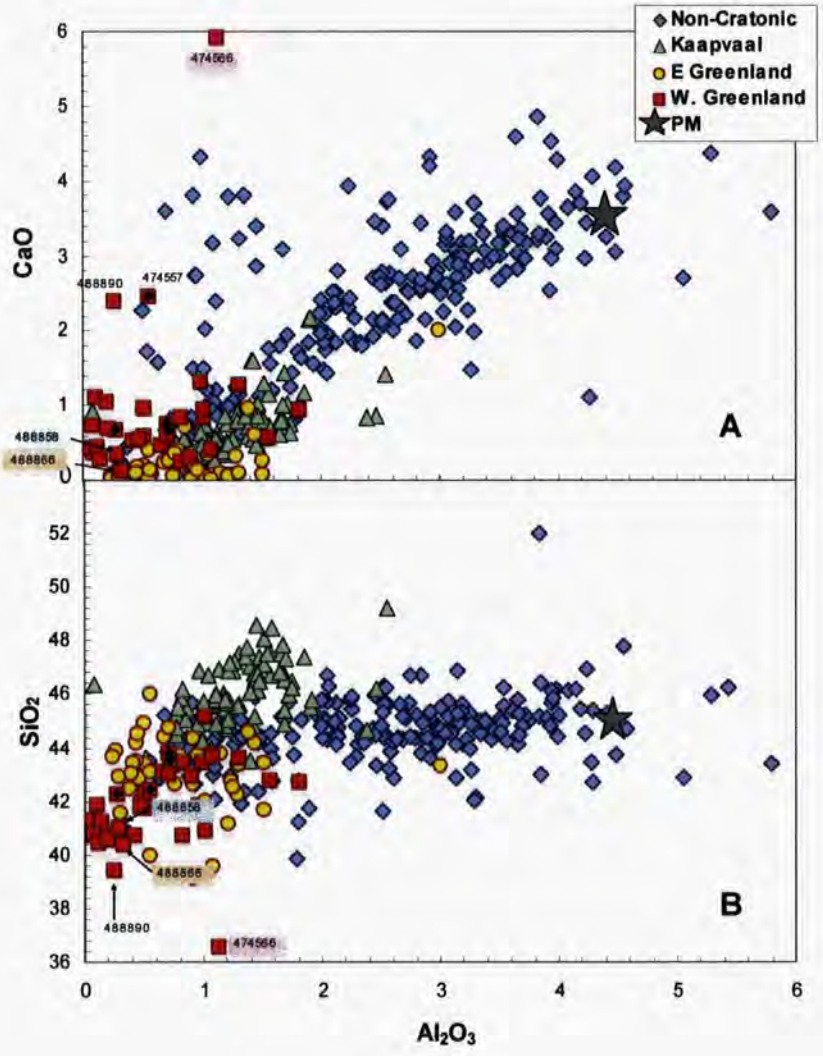


**Fig. 4.3** Whole rock $Al_2O_3$ vs **A**. CaO and **B**. $SiO_2$ for W.G, E. Greenland, Kaapvaal and non-cratonic peridotite xenolith suites. Data sources given in Figure 1.1.

### 4.3.4 $K_2O$ vs. $P_2O_5$ & $TiO_2$

Both the xenoliths and the host rock (UML) for the W.G. samples have been plotted on Figure 4.4, to investigate any host magma contamination. Most of the W.G. peridotite xenoliths are tightly compacted in the very low $P_2O_5$, $K_2O$ and $TiO_2$. Sample 474566 plots at the edge of the UML field, suggesting that this peridotite sample has been significantly metasomatised by the host magma. Samples 488890 and 474557 also have slightly elevated $TiO_2$, $P_2O_5$ and $K_2O$. This may also indicate that these samples have experienced some host magma metasomatism.

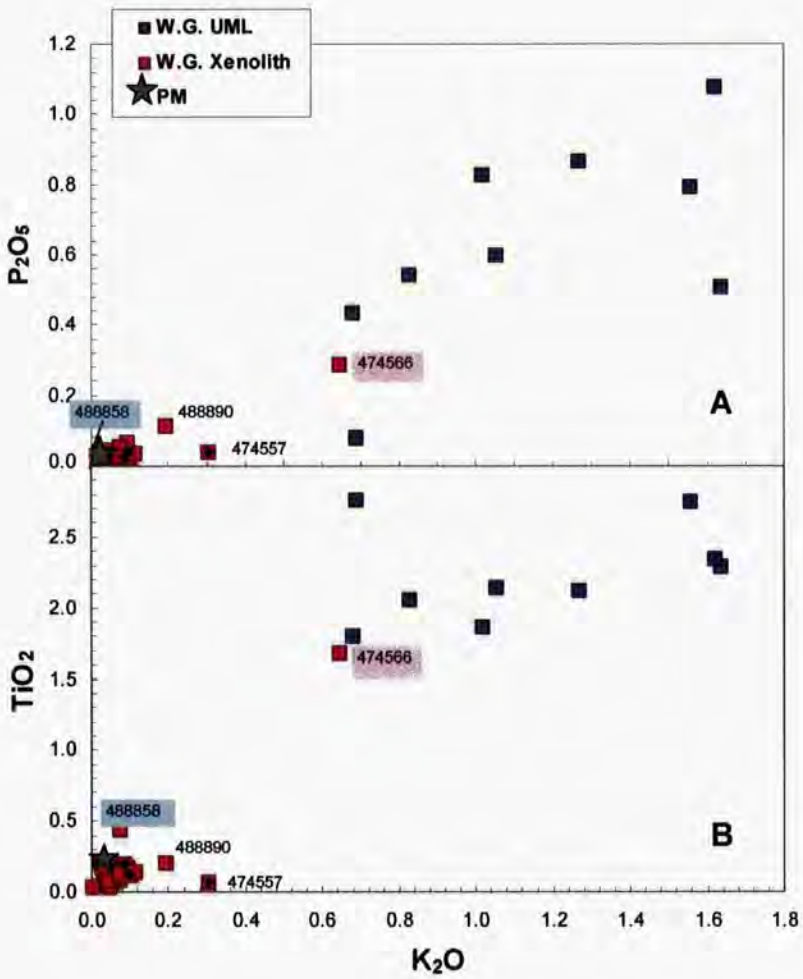


**Fig. 4.4** Whole rock $K_2O$ vs. **A.** $P_2O_5$ and **B.** $TiO_2$ for W.G. peridotite xenoliths (red squares) and W.G. UML (blue squares)

### 4.3.5 $Al_2O_3$ vs. V (ppm) and Cr (ppm)

**V**

Vanadium (V) is redox sensitive and its contents in peridotites vary with changes in oxygen fugacities (Canil, 2004). V against $Al_2O_3$ contents in garnet and spinel cratonic peridotites are generally very low (Fig. 4.5 inset), V is less than ~40 ppm (Canil, 2002). Abyssal and massif peridotite suites contain much higher contents of V ranging from ~50 to 100 ppm (Canil, 2002). The W.G. peridotite samples have scattered V contents, the lowest being ~13 ppm, to the highest at ~95 ppm. The majority of the samples are plotting within a range of approximately ~20 and ~60 ppm. Canil (2004) uses V contents to investigate late stage metasomatism on peridotite suites. If garnet has been added or subtracted it does not affect the V, but the addition or subtraction of clinopyroxene has effects on the V and Ti contents (Canil, 2004).

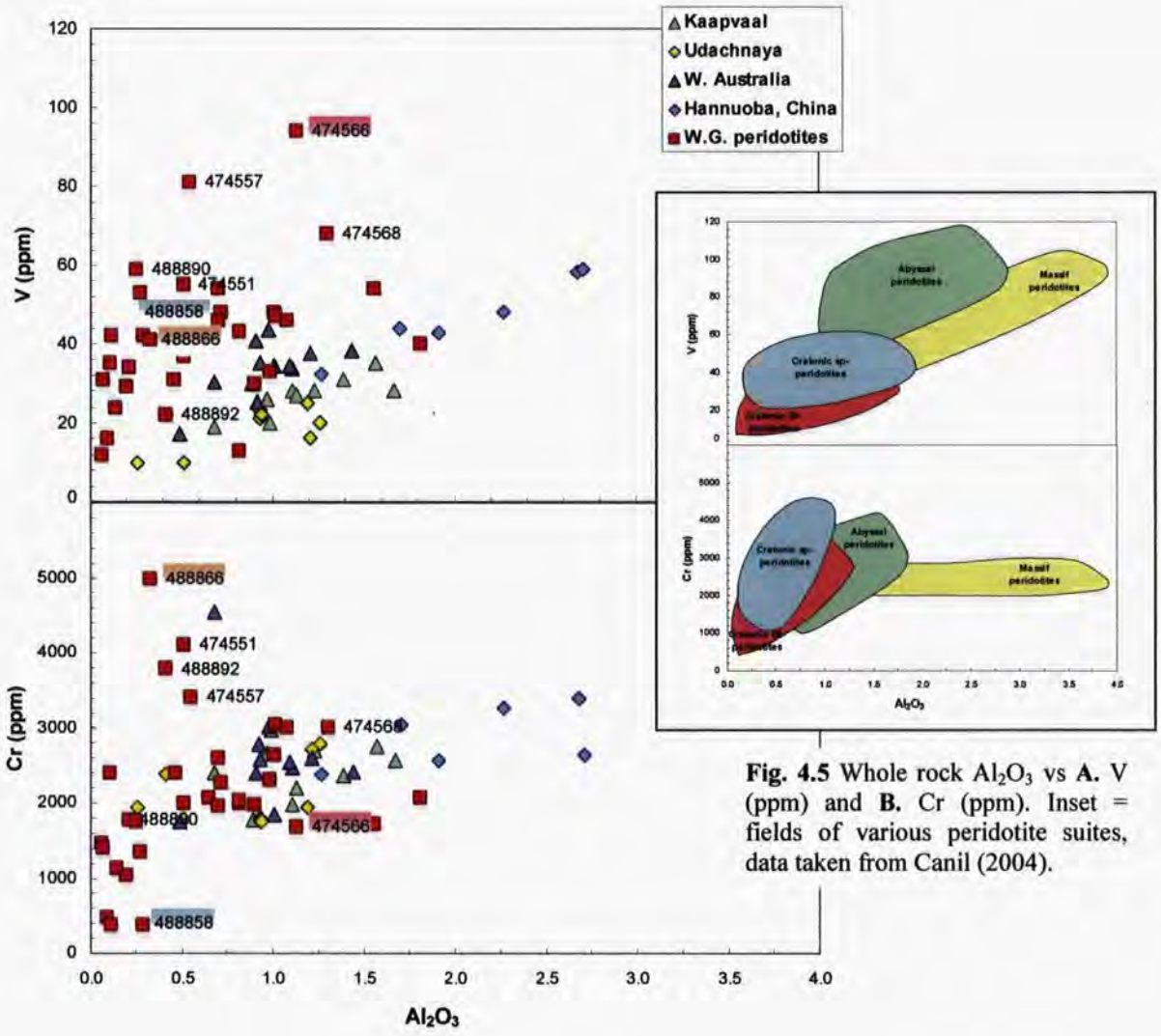


**Fig. 4.5** Whole rock $Al_2O_3$ vs **A.** V (ppm) and **B.** Cr (ppm). Inset = fields of various peridotite suites, data taken from Canil (2004).

Cr contents typically get more scattered with increasing depletion. Cr of massif peridotites is more confined to within 2000 to 3000 ppm (Canil, 2004). The scattering of the more depleted peridotites has been attributed to the 'nugget' effect of spinel. The spinels being mostly comprised of Cr would contribute considerably to the Cr contents.

The XRF results are essential to understanding the depleted nature of the W.G. peridotites and any subsequent metasomatism which has occurred. In the next chapter the W.G. peridotite xenoliths will be described in terms of their PGE and Re characteristics. PGE patterns normalised to whole rock chondrite will highlight any potential disturbances in I-PGE and P-PGE groups as well as documenting highly siderophile element behaviour in these rocks. Then the PGE systematics will be compared to major elements such as $Al_2O_3$. $Al_2O_3$ is not easily disturbed during serpentinisation and metasomatism and will provide an anchor to observe Pt and Pd depletions and additions in residual rocks. Finally the ages of the xenoliths will be examined.

# CHAPTER 5

# DESCRIPTION OF PGE AND Re GEOCHEMICAL DATA

# Chapter 5:

# Platinum Group Element & Re Data Results

## 5.1 Introduction

The platinum group elements comprise osmium, iridium, ruthenium, rhodium, platinum, and palladium (for the purpose of this study, rhodium is not measured because it is mono isotopic and will not be discussed throughout the text). Rhenium is not classed as a platinum group element, but it displays a similar behaviour as it prefers to be in a metal rather than a silicate and is part of the Re-Os isotope decay system. Rhenium will be referred to along with the platinum group elements (PGEs).

### I-PGE & P-PGE groups

Osmium, iridium, and ruthenium are classed as the iridium or I-PGE group, and display a compatible behaviour during melting (Pearson *et al.*, 2004). Platinum and palladium are classed as the platinum or P-PGE group and display incompatible behaviour, showing enrichment over I-PGEs in mantle melts. Therefore, I-PGE and P-PGE groups are commonly fractionated from each other (Fig. 5.1) (Pearson *et al.*, 2004). Rhenium is also an incompatible element and can be grouped along with the P-PGE group.

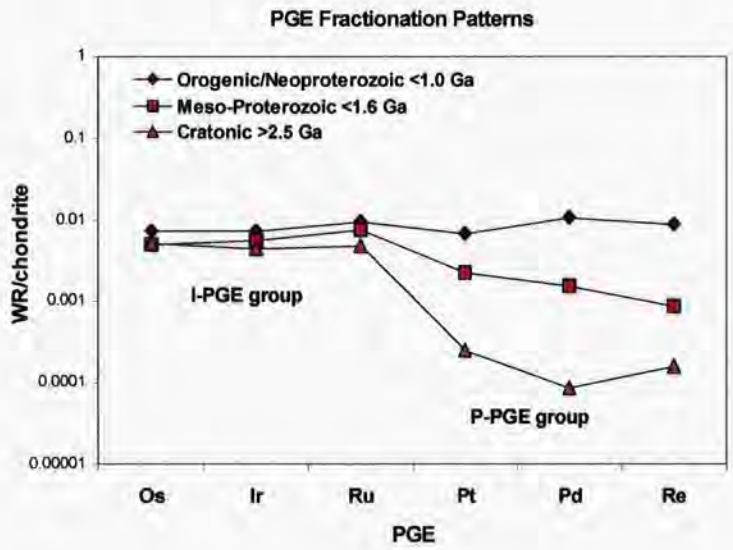


**Fig 5.1** Typical PGE fractionation patterns for various peridotite suites. *Data sources are for orogenic = sample GP13 Beni Bousera data set, Pearson et al., 1993. Meso-Proterozoic = sample 40-21 Slave Jericho data set, Kopylova & Caro, 2004. Cratonic = sample 8-7 Slave Jericho data set, Kopylova & Caro, 2004.*

### $^{187}Os/^{188}Os$ Ratios Explained

During mantle melting Re is moderately incompatible and prefers to be in the melt. Os is compatible and remains in the residue. Consequently, compared to the mantle the crust is enriched in Re and relatively depleted in Os, this is shown by the highlighted reservoirs in Figure 5.2 (Carlson, 2005). The isotope $^{187}Re$ decays by $\beta^-$ transmission to $^{187}Os$. The decay constant for $^{187}Re$ is $\lambda\ ^{187}Re = 1.666 \times 10^{-11}$ year$^{-1}$ this is based on a Re-Os isochron for group IIIA iron meteorites from Shen *et al* (1996); Smoliar *et al* (1996) (Fig. 5.3). Cratonic peridotites have experienced large degrees of partial melting, ~40% (Bernstein *et al.,* 2006). Hence Re is partitioned into the melt phase leaving the residue very depleted in Re. This removal of Re arrests the production of any more $^{187}Os$, and so the measured Os isotope ratio provides an estimate for the age of the peridotites (Pearson *et al.,* 2002). This Re-Os age dating technique is described in more detail in **Section 5.8.**

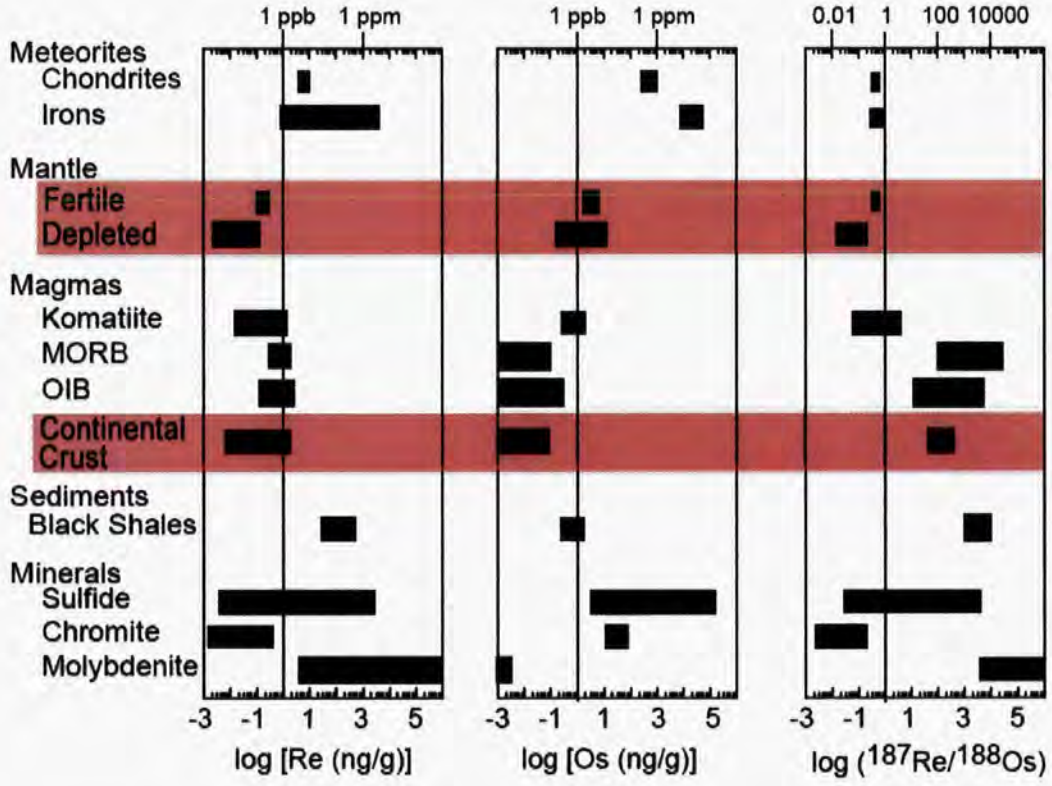


**Fig. 5.2** Re and Os concentrations and $^{187}Re/^{188}Os$ from various rocks and minerals (Carlson, 2005), reservoirs of particular interest have been highlighted.

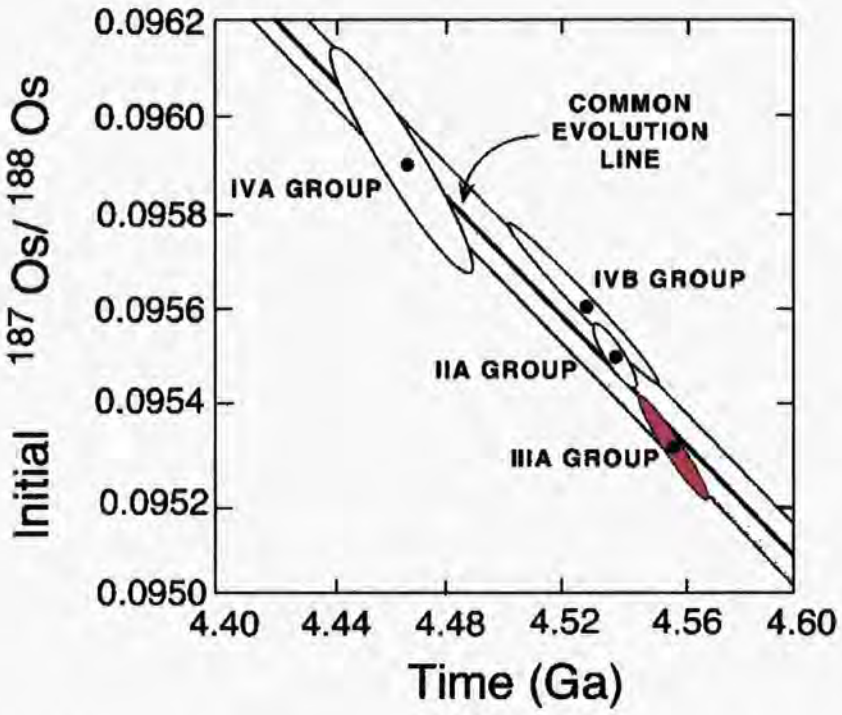


**Fig. 5.3** Plot of initial $^{187}Os/^{188}Os$ ratios vs. age. The evolution line is the best fit for the group isochrons (Shirey & Walker, 1998). Slope of the regression for group IIIA, gives a decay constant for $^{187}Re$ of $1.666 \times 10^{-11}$ $yr^{-1}$.

The Os isotope characteristics of different mantle reservoirs are shown in Table 5.1. The most depleted sub continental lithospheric mantle has the lowest $^{187}Os/^{188}Os$ ratio, commonly described as unradiogenic.

| Reservoir | $^{187}Os/^{188}Os$ |
|---|---|
| Chondrite | 0.127 |
| PUM | 0.129 |
| EMII | 0.136 |
| EMI | 0.152 |
| SCLM | 0.113 |
| DMM | 0.125 |
| HIMU | 0.150 |

**Table 5.1** $^{187}Os/^{188}Os$ for various terrestrial reservoirs (Shirey & Walker, 1998). PUM (primitive upper mantle), EMII (enriched mantle II), EMI (enriched mantle I), SCLM (sub continental lithospheric mantle), DMM (depleted MORB mantle), HIMU (high μ).

## 5.2 W. Greenland PGE and Re concentrations

### 5.2.1 PGE concentrations

PGE concentration plots of Ir against each platinum group element should show good correlations with I-PGEs (Os, Ir & Ru), and negative correlations for P-PGEs (Pd & Pt) for highly depleted residual peridotites. Ir varies from <1 to 5.4 ppb with an average of 2.3 ppb (Fig. 5.4 & 5.5). Os varies from <1 to 5.0 ppb with an average of 2.2 ppb. Os and Ir are well correlated generally with Os/Ir ~1. The relationship of Os and Ir for W.G. and other typical peridotites can be seen more effectively in Figure 5.5. Ru concentrations are scattered, ranging from <1 to 33.4 ppb, with an average of 5.4 ppb. Ru is much less correlated with Ir than Os, with data scattering widely either side of Ru/Ir = 1. Pd concentrations vary from <0.01 to 4.6 ppb with an average of 0.7 ppb. Pd is not correlated with Ir. Pt concentrations vary from <0.1 to 38.7 ppb with an average of 2.8 ppb.

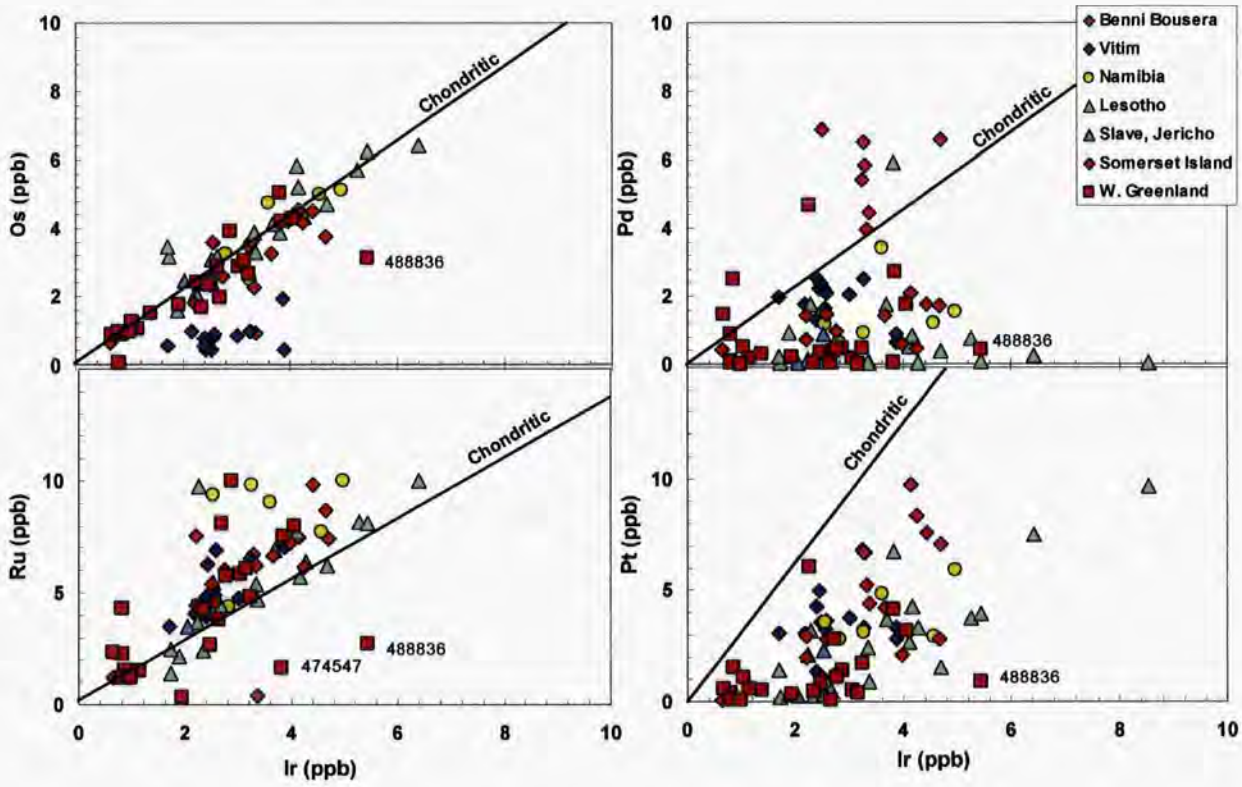


**Fig. 5.4** Concentrations of Os, Ru, Pt and Pd with Ir (in ppb) for Beni Bousera, Vitim, Namibia, Lesotho (Pearson *et al.*, 2004), Slave Jericho (Kopylova & Russel, 2000), Somerset Island (Irvine *et al.*, 2003) and W. Greenland (this Study). Chondritic ratio after McDonough and Sun (1995).

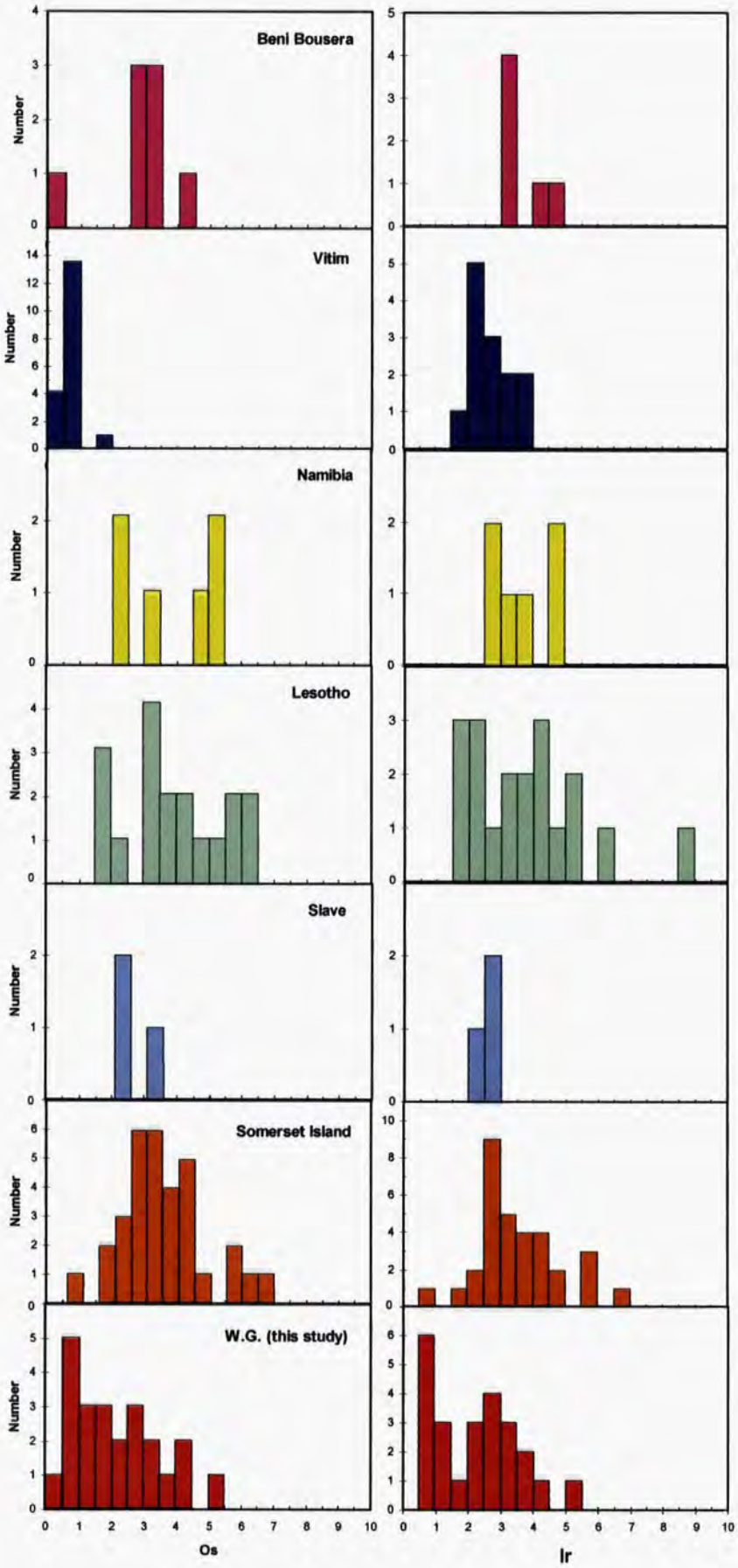


**Fig. 5.5** Frequncey distributions for Os ppb and Ir ppb for Beni Bousera, Vitim, Namibia, Lesotho, Slave, Somerset Island and W.G. peridotites suites. (For sources see Fig. 5.4).

### 5.2.2 Os and Re concentrations

Os concentrations for W.G. peridotites are widespread extending into the residue field, i.e. relatively high Os and low Re (Fig. 5.6). A relatively high proportion of samples have low Os, significantly less than primitive upper mantle (PUM), at low Re contents. Cratonic peridotites generally have higher Os contents when off-craton compared to spinel lherzolites which more commonly have lower Os contents at low Re, as typified by the Vitim suite (blue field Fig 5.6).

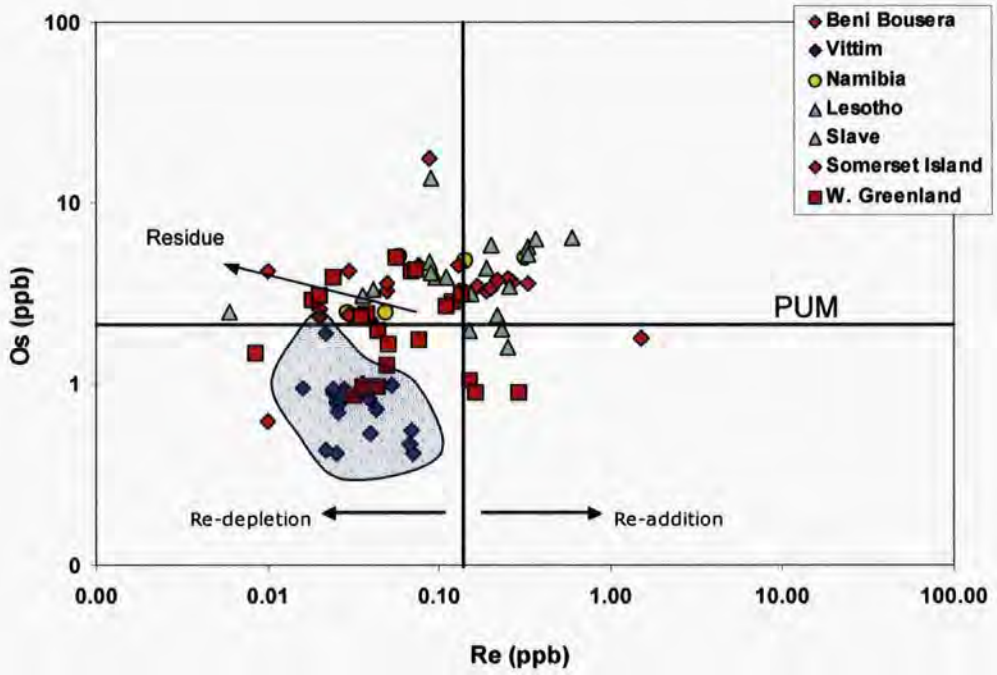


**Fig. 5.6**. Os ppb vs. Re ppb for Beni Bousera, Vitim, Namibia, Lesotho, Slave, Somerset Island and W.G. peridotites suites. Blue highlight is the Vitim suite. For data sources see Fig. 5.3.

## 5.3 W.G. PGE patterns – General characteristics

The W.G. peridotite xenolith samples have variably fractionated PGE patterns. Figure 5.7 shows all the W.G. samples together, normalised to chondrite. The most important distinctive feature to be observed in the W.G. peridotites is the presence in numerous samples that are very P-PGE depleted, similar to those observed in the Kaapvaal and Slave cratons (Pearson *et al.*, 2002 & 2004). These patterns are present in samples from both on and off craton localities. A wide variety of complex inter-element enrichments and depletions are super-imposed onto the general pattern of depletion. Before organizing the PGE patterns into distinguishing groups, we will examine how these PGE inter-element fractionations vary with indices of melt extraction such as $Al_2O_3$.

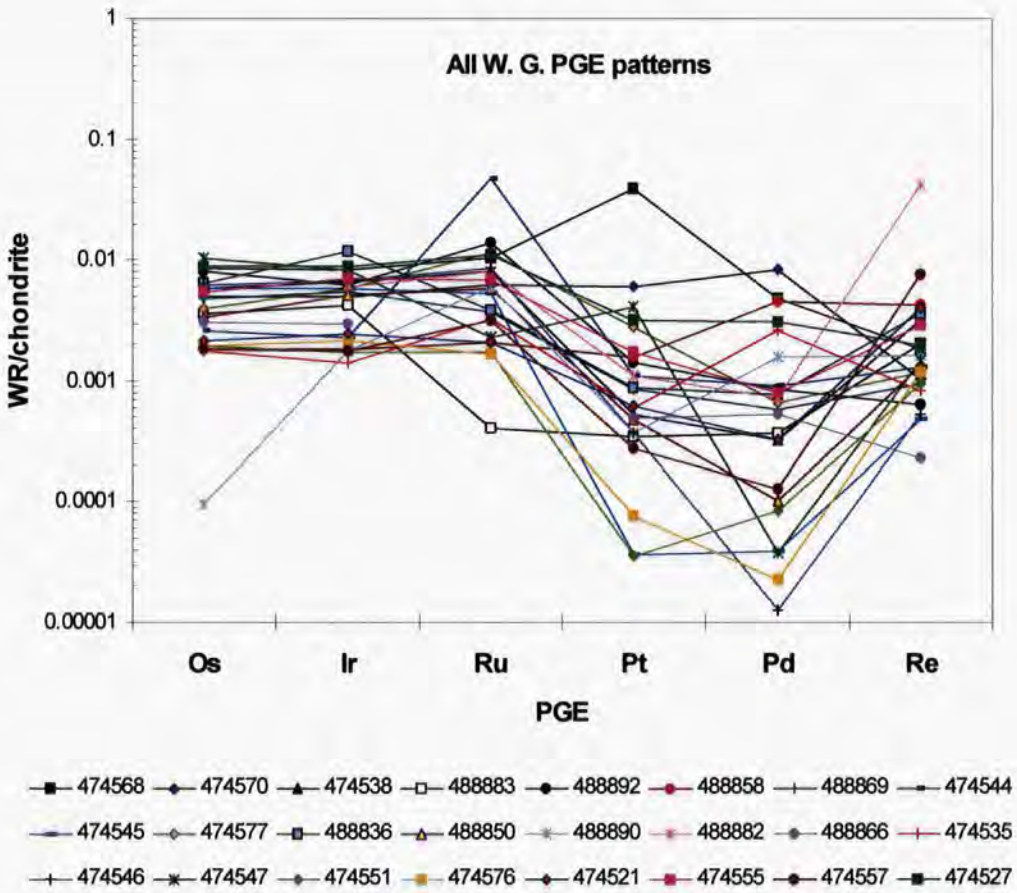


**Fig.5.7** Chondrite normalised PGE patterns for the on-craton peridotite xenolith samples from West Greenland. Chondrite normalised values from McDonough & Sun (1995).

## 5.4 (Pd/Ir)*n* vs. $Al_2O_3$

In many W.G. peridotites samples, Pd is severely depleted relative to Ir. Very low contents of Pd are indicative of mantle residues e.g. Barnes, 1985: Pearson *et al.*, 2002. This level of depletion should be reflected in the major element systematics of the W.G. peridotites. Highly depleted mantle residues commonly have low $Al_2O_3$ contents and high MgO (Fig. 4.1). Looking at the relationship between (Pd/Ir)*n* against $Al_2O_3$ for the W.G. samples will help to further clarify their origin. In Figure 5.8 a & b the W.G. samples have been separated into 3 groups. Group characteristics are summarised in Table 5.2. Group 1 show low (Pd/Ir)*n* low $Al_2O_3$. A theoretical partial melting trend taken from Pearson *et al* (2002) has been plotted on Figure 5.8 b. This melting trend depicts a starting composition of 300 ppm of total sulphur. With each percentage of melting more residual sulphide is driven off, until it disappears at 25% melting. Group 1 peridotites show high degrees of partial melting. Group 2 show low $Al_2O_3$, but have higher (Pd/Ir)*n* than Group 1. Group 3 are not following the melting trend and have high (Pd/Ir)*n* and low $Al_2O_3$.

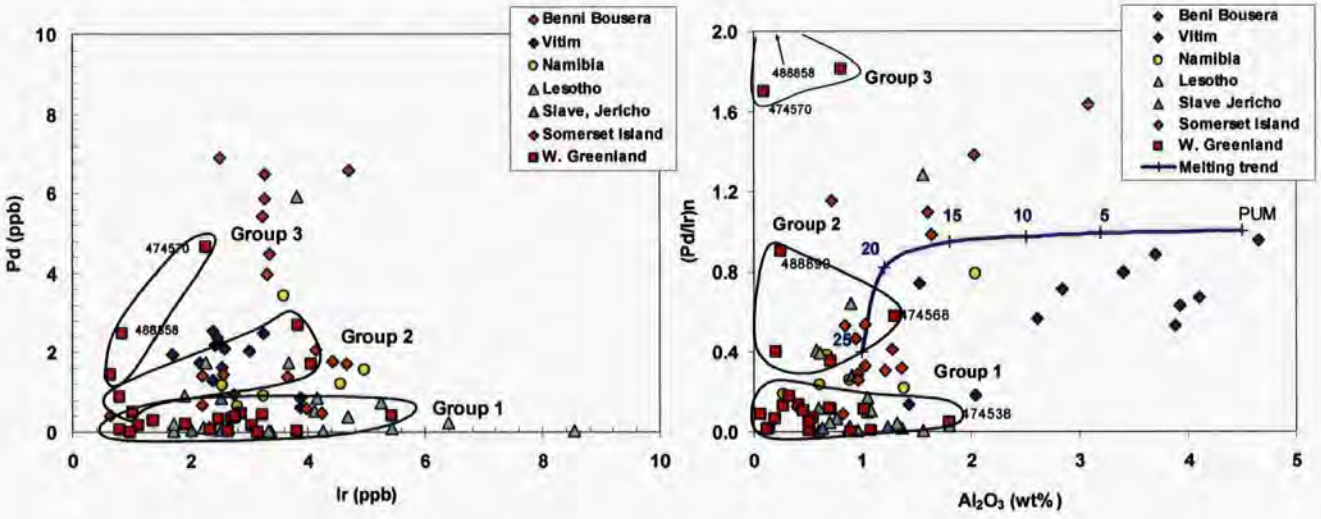


**Fig. 5.8 a)** Pd (ppb) vs. Ir (ppb). **b)** (Pd/Ir)n vs. $Al_2O_3$ for the Beni Bousera, Vitim, Namibia, Lesotho (Pearson *et al.*, 2004), Slave (Kopylova & Russel, 2000), Somerset Island (Irvine *et al.*, 2003) and West Greenland peridotite suite (this study).

**Table 5.2** Summary of the W.G. groups and their (Pd/Ir)*n* vs. $Al_2O_3$ contents

| Group | (Pd/Ir)*n Vs.* $Al_2O_3$ | Description |
|---|---|---|
| **Group 1** | ≤0.2 | High degree of partial melting |
| **Group 2** | 0.3-0.9 | Either less melting or Pd addition |
| **Group 3** | ≥1.0 | Enriched or fertile composition |

The PGE fractionation patterns for W.G. samples can now be placed into the three groups as seen earlier in the (Pd/Ir)*n* vs. $Al_2O_3$ plots. This will allow us to investigate the group's relative fractionation of I-PGE from P-PGE plus Re and their depletion of Pd relative to Pt.

## 5.5 W.G. PGE patterns – Group Characteristics

### 5.5.1 Group 1 PGE Fractionation Pattern

Considerable variations exist in the degree of fractionation of the P-PGEs from the I-PGEs (Fig. 5.9). All samples show a marked depletion of Pd, consistent with Figure 5.8b. Pd concentrations for Group 1 samples 474546 and 474576 are almost 3 orders of magnitude less than their I-PGEs. Pt is also depleted relative to I-PGEs but less so than Pd. Almost all samples apart from 488892 and 488866 show evidence of Re addition. Sample 488882 shows a greater enrichment of Re than the rest of the group. Minor fractionations are seen within the I-PGE group. The most obvious of these is with Ru. Sample 488883 is depleted by one order of magnitude compared with those typical of Group 1.

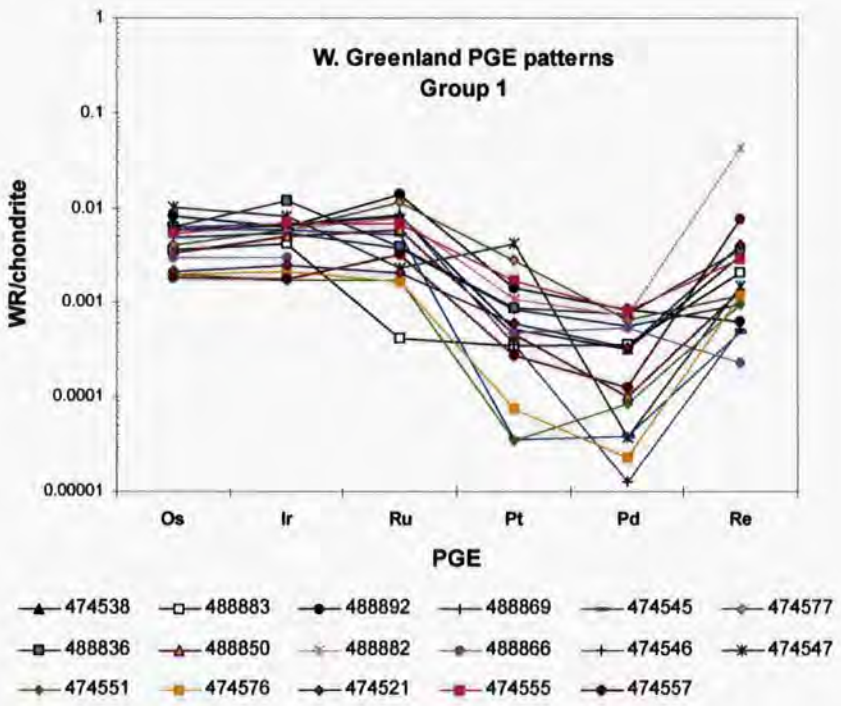


**Fig. 5.9** Chondrite normalised PGE patterns for Group 1 W.G. peridotites from West Greenland. Chondrite normalised values from McDonough & Sun (1995).

### 5.5.2 Group 2 PGE Fractionation Pattern

Pd and Re abundances are sub-chondritic to chondritic (Fig. 5.10), being depleted by less than one magnitude than I-PGEs. Pd contents for Group 2 peridotites are greater than the Pd contents in Group 1. Pt contents and hence (Pt/Ir)*n* for Group 2 are very fractionated compared to the Pd. The P-PGE group is fractionated from the I-PGE group, but there are also fractionations within the groups themselves. Samples 474544 and 488890 have high Ru contents. Sample 488890 also has an anomalously low Os content. Sample 474568 has the highest content of Pt out of the entire W.G. peridotite suite. This Pt anomaly is discussed in more detail in **Section 5.6**.

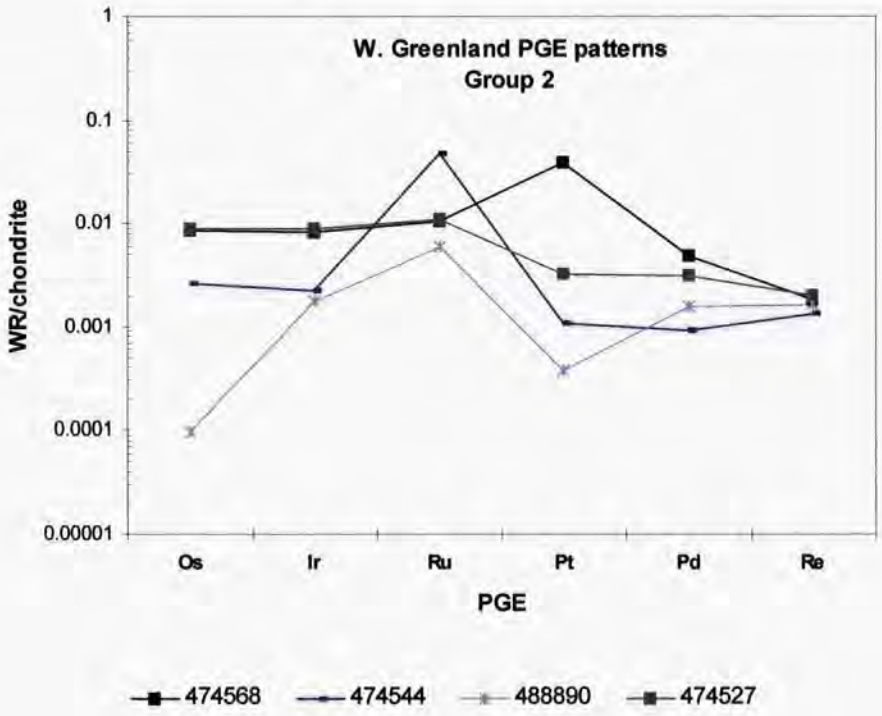


**Fig. 5.10** Chondrite normalised PGE patterns for Group 2 W.G. peridotites from West Greenland. Chondrite normalised values from McDonough & Sun (1995).

### 5.5.3 Group 3 PGE Fractionation Pattern

The PGE fractionation patterns for Group 3 peridotites are shown in Figure 5.11. The most striking observation is that the fractionation pattern is much flatter than those of either Group 1 or 2. Also there is a greater enrichment in Pd relative to Pt within the group and hence Pd/Pt in Group 3 is greater than Pd/Pt in Group 2. Re-depletions are seen in samples 474570 and 474535, while 488858 shows a Re-addition. A positive Ru anomaly is seen in sample 474535.

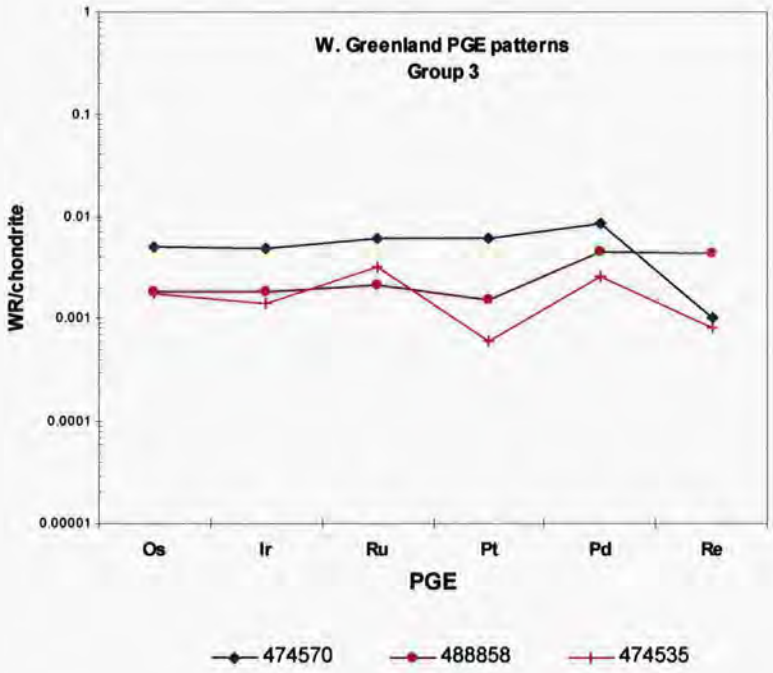


**Fig. 5.11** Chondrite normalised PGE patterns for Group 3 W.G. peridotites from West Greenland. Chondrite normalised values from McDonough & Sun (1995).

### 5.5.4 Grouping characteristics

Table 5.3 summarises the varying characteristics of the different peridotite samples and groups.

| Sample No. | Cratonic pattern | Ru Addition | Ru Depletion | Pt Addition | Pd Addition | Re Depletion |
|---|---|---|---|---|---|---|
| ***Group 1*** | | | | | | |
| 474557 | | | | | | |
| 488850 | | | | | | |
| 474576 | | | | | | |
| 488883 | | | | | | |
| 474551 | | | | | | |
| 474538 | | | | | | |
| 474521 | | | | | | |
| 474545 | | | | | | |
| 488892 | | | | | | |
| 474546 | | | | | | |
| 488836 | | | | | | |
| 474547 | | | | | | |
| 488869 | | | | | | |
| 488866 | | | | | | |
| 474555 | | | | | | |
| 488882 | | | | | | |
| 474577 | | | | | | |
| ***Group 2*** | | | | | | |
| 474568 | | | | | | |
| 474544 | | | | | | |
| 474527 | | | | | | |
| 488890 | | | | | | |
| ***Group 3*** | | | | | | |
| 488858 | | | | | | |
| 474570 | | | | | | |
| 474535 | | | | | | |

**Table 5.1**. Summarises the characteristics seen in the PGE fractionation patterns in Group 1, 2 and 3 for the W.G. peridotites.

## 5.6 Positive Pt anomaly in sample 474568

Sample 474568 of the W.G. peridotite suite falls into Group 2 in terms of its PGE characteristics. It shows an enrichment of Pt in the PGE fractionation pattern (Fig. 5.10). Figure 5.12 a), b) and c) shows the sample 474568 in photomicrographs. Figure 5.12 a), shows a group of intergranular sulphides (Pers. Com. Jean-Pierre Lorand). Figures b) and c) show a sulphide inclusion in an olivine (Pers. Com. Jean-Pierre Lorand). Positive Pt anomalies in a peridotite are not easily resolved by addition of Pt from secondary metasomatism alone; Pt fractionations are much more complicated than this and are discussed in more detail in the interpretation (Chapter 6). For now it is important to recognise that there are intergranular sulphides in this sample.

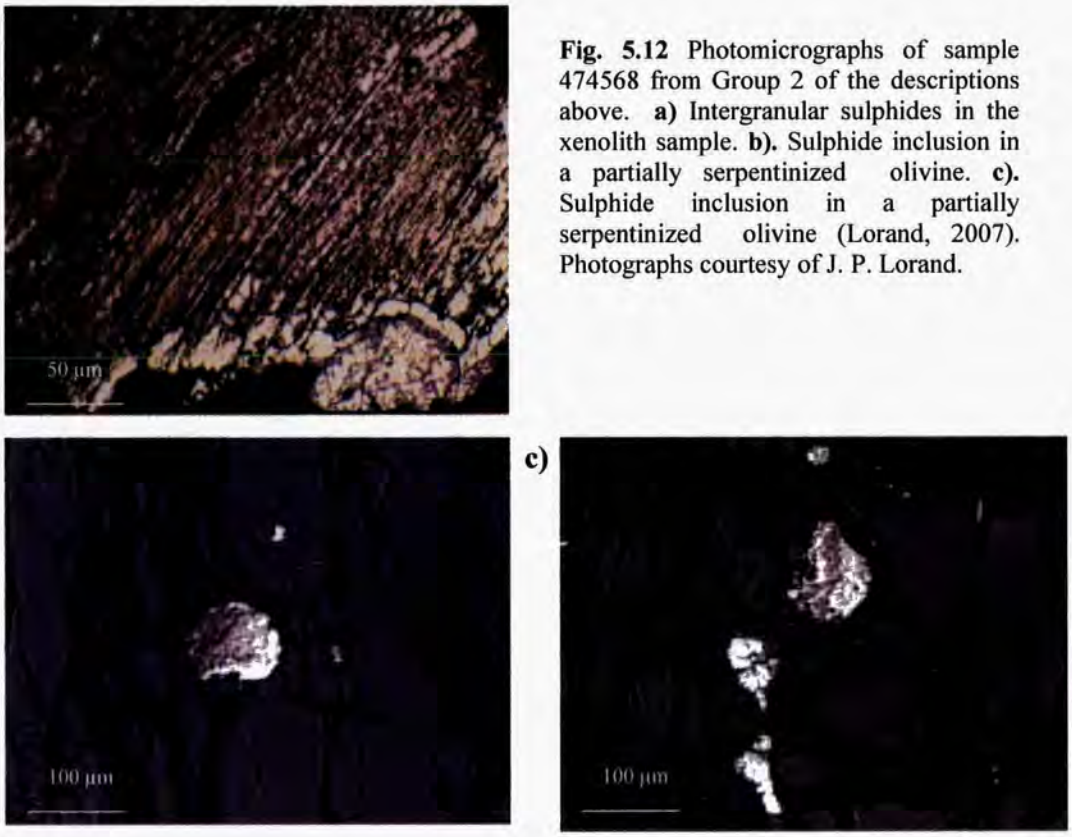


**Fig. 5.12** Photomicrographs of sample 474568 from Group 2 of the descriptions above. **a)** Intergranular sulphides in the xenolith sample. **b).** Sulphide inclusion in a partially serpentinized olivine. **c).** Sulphide inclusion in a partially serpentinized olivine (Lorand, 2007). Photographs courtesy of J. P. Lorand.

## 5.7 Os Isotope characteristics of W.G. peridotites

Gamma Os is used as a percentage deviation in the Os isotope composition of a given rock, from that of the bulk silicate Earth's $^{187}Os/^{188}Os$ value of 0. Increasing negative γOs (unradiogenic $^{187}Os/^{188}Os$) is typical of ancient depleted peridotites (Fig. 5.13). Typical cratonic peridotite γOs ranges from -6 to -18 , and typical non-cratonic γOs ranges from 4 to -6 (Pearson *et al.*, 2004). W.G. samples show a very large range in γOs ranging from -17 to 0 γOs (Fig. 5.14).

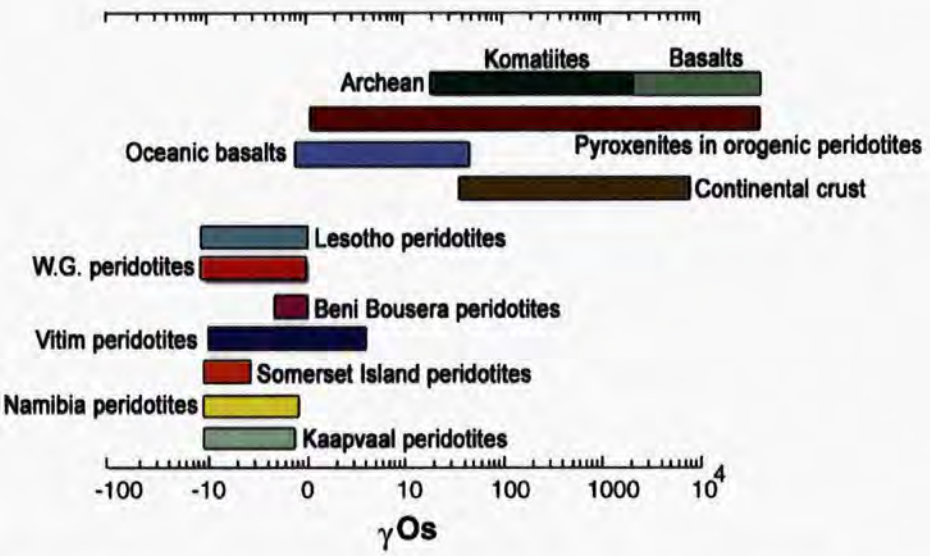


**Fig. 5.13** Variations in Os isotope given as γOs in various rock types (adapted from Pearson, 1999).

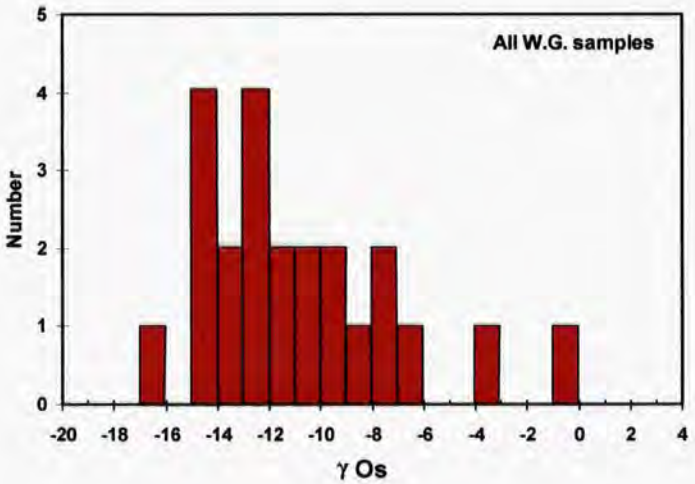


**Fig. 5.14** Frequency distribution of initial γOs values calculated at 600myr for the W.G. peridotite suite. γOs values for peridotite xenoliths are calculated at the time of their eruption.

## 5.8 Age determination

### 5.8.1 Model ages

Mantle derived xenoliths are very often deformed and altered due to their geological history and their subsequent journey to the Earth's surface. Most of the xenoliths original isotopic signature can be overprinted and disturbed during these events. Osmium isotopic signatures are relatively resilient to disturbance, due to the compatible behaviour of Os. Re is more incompatible than Os and prefers the melt phase. In theory, when the peridotite formed, all the Re would be depleted during large degrees of melt extraction, meaning that Os isotopic evolution is effectively arrested. Any Re now present in the xenolith is likely to have been added after the melting event and mostly from the host magma that brought the xenolith to the surface. This is indicated by the almost ubiquitous elevation of Re in extended PGE patterns. For this reason, Re-depletion ages, that assume zero Re/Os ($T_{RD}$), are more reliable than the Re-Os model ages ($T_{MA}$). However, in ancient Re-rich host magmas Os isotopic evolution is no longer arrested. $^{187}$Re is decaying to $^{187}$Os. $T_{RD\ erup.}$ takes into account any $^{187}$Os production since the eruption, and provides a more reliable estimation than $T_{RD}$ (Fig. 5.15).

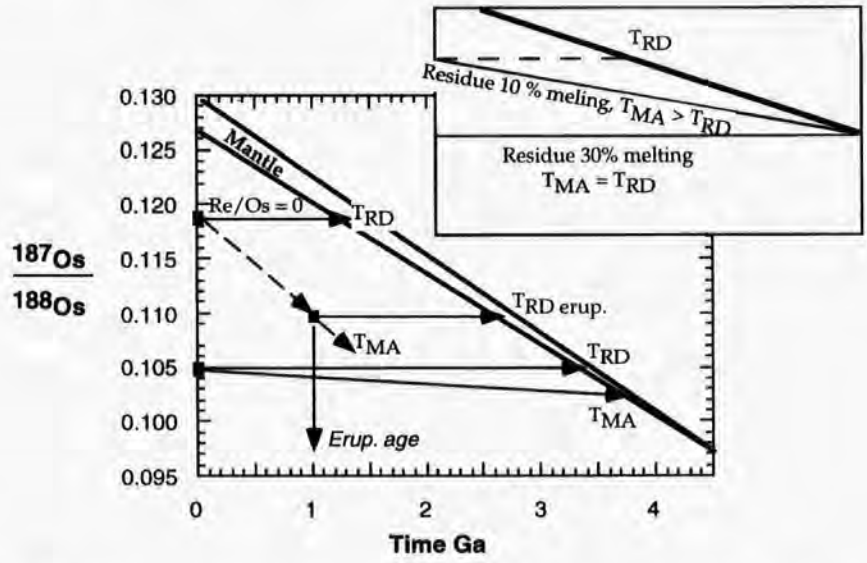


**Fig. 5.15** Os isotope evolution diagram showing the $T_{RD}$, $T_{MA}$ and $T_{RD\ erup}$ model age systematics (Pearson, 1999; Pearson *et al.*, 2002). Insert shows hypothetical effects of various degrees of melt extraction on the Os isotope evolution of a residual peridotite.

The equations for $T_{RD}$ and $T_{MA}$ calculations are: -

$$T_{RD} = \frac{1}{\lambda} \ln \{[(\frac{^{187}Os}{^{188}Os_{Bulk\ Earth(t)}} - \frac{^{187}Os}{^{188}Os_{Sample(t)}}) / \frac{^{187}Re}{^{188}Os_{Bulk\ Earth(t)}}] + 1 \}$$

$$T_{MA} = \frac{1}{\lambda} \ln \{[(\frac{^{187}Os}{^{188}Os_{Bulk\ Earth(t)}} - \frac{^{187}Os}{^{188}Os_{sample(t)}}) / \frac{^{187}Re}{^{188}Os_{Bulk\ Earth(t)}} - \frac{^{187}Re}{^{188}Os_{sample(t)}}] + 1\}$$

The Bulk Earth reservoir is taken as chondrite and '*t*' is the time of eruption.

### 5.8.2 W.G. Ages

Re-depletion ($T_{RD}$), Re-Os ($T_{MA}$) and $T_{RD\ erup}$ model ages for W.G. peridotites are presented in Figure 5.16. $T_{RD}$ ages (plot A) range from 0.5 - 3.3 Ga, with 7 samples out of the 24 having a $T_{RD}$ age of 3.0 Ga. $T_{MA}$ ages (plot C) range from 0.7 – 6.0 Ga, this must be considered an over estimate seeing as the age of the Earth is estimated at being 4.6 billion years old (Patterson, 1956: Allègre *et al.,* 1995). Therefore the $T_{MA}$ ages are not reliable. The $T_{RD\ erup}$ model ages for the W.G. peridotite samples take into account any production of $^{187}Os$ since the time of the UML eruption.

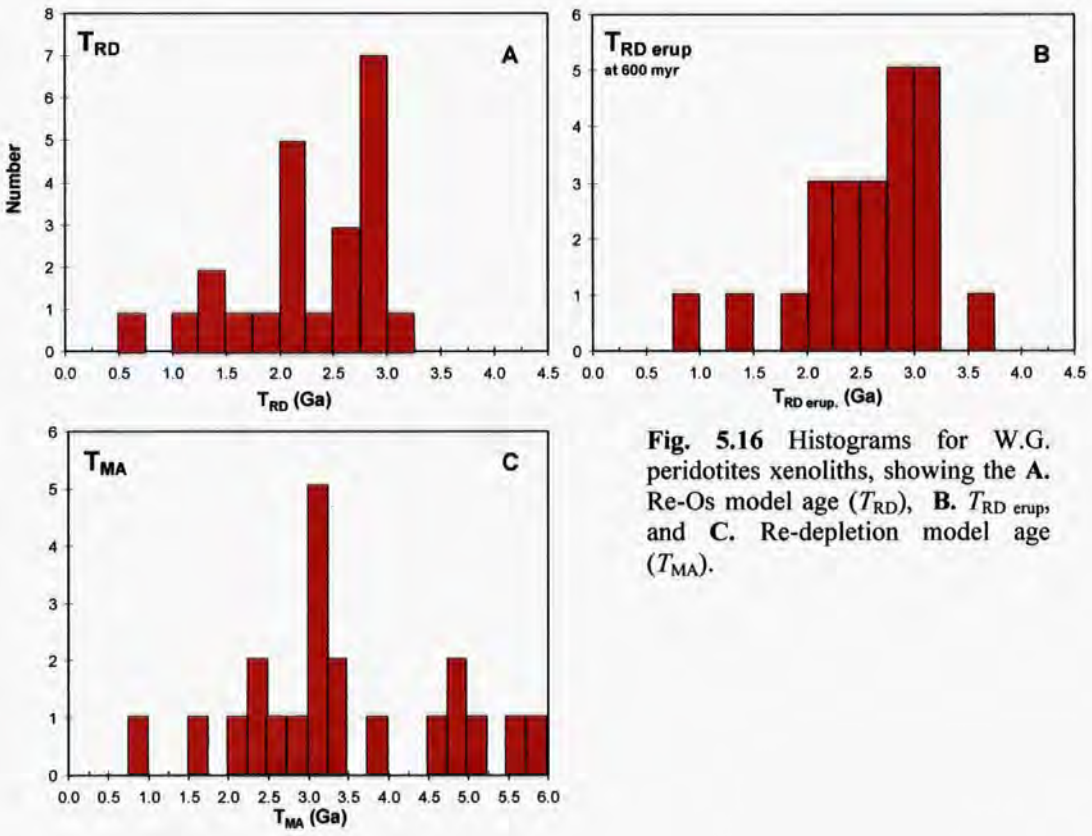


**Fig. 5.16** Histograms for W.G. peridotites xenoliths, showing the **A.** Re-Os model age ($T_{RD}$), **B.** $T_{RD\ erup}$, and **C.** Re-depletion model age ($T_{MA}$).

The W.G. peridotite samples were brought to the surface by ~600 Myr old UML dykes (Larsen & Rex, 1992). Since the UML eruption, substantial radiogenic Os may have accumulated from the decay of $^{187}Re$ to $^{187}Os$. For this reason, the isotopic compositions are corrected for the in-growth of $^{187}Os$ giving the $T_{RD\ erup.}$ age. $T_{RD\ erup}$ age is a more reliable age for the W.G. peridotite samples, as seen by Figure 5.16 B.

$T_{RD}$, $T_{RD\ erup}$ and $T_{MA}$ ages for the W.G. peridotites are shown in Table 5.4. It has already been established that Group 1 of the W.G. peridotites (discussed earlier) are the best representative group for indicating the most depleted peridotites, with the highest degrees of melting and the least alteration. Therefore Group 1 $T_{RD\ erup}$ ages should have the most reliable ages.

**Table 5.4** Model ages for the W.G. peridotite xenoliths

| Sample No. | $T_{RD}$ | $T_{RD\ erup}$ | $T_{MA}$ | Craton |
|---|---|---|---|---|
| ***Group 1 – High degrees of partial melting*** | | | | |
| **474557** | 1.5 | 3.6 | -0.6 | **off** |
| **488850** | 3.0 | 3.2 | 4.6 | on |
| **474576** | 2.9 | 3.2 | 5.9 | on |
| **488883** | 2.8 | 3.1 | 5.5 | on |
| **474551** | 2.9 | 3.1 | 4.8 | on |
| **474538** | 2.8 | 3.1 | 5.2 | on |
| **474521** | 2.0 | 3.0 | 3.3 | **off** |
| **474545** | 2.9 | 2.9 | 3.1 | on |
| **488892** | 2.8 | 2.9 | 3.0 | on |
| **474546** | 2.8 | 2.8 | 3.0 | on |
| **488836** | 2.5 | 2.8 | 4.9 | on |
| **474547** | 2.6 | 2.7 | 3.0 | on |
| **488869** | 2.6 | 2.7 | 3.1 | on |
| **488866** | 2.1 | 2.2 | 2.3 | on |
| **474555** | 1.8 | 2.1 | 3.3 | **off** |
| **488882** | 2.1 | 2.1 | 2.1 | on |
| **474577** | 1.7 | 1.9 | 2.3 | on |
| ***Group 2 – Less melting or Pd addition*** | | | | |
| **474568** | 2.5 | 2.6 | 3.0 | on |
| **474544** | 2.2 | 2.5 | 3.9 | on |
| **474527** | 2.2 | 2.3 | 2.7 | **off** |
| **488890** | No $^{187}Re$ data | | | on |
| ***Group 3 – Primitive or enriched*** | | | | |
| **488858** | 1.2 | 2.4 | -1.1 | on |
| **474570** | 1.3 | 1.4 | 1.5 | on |
| **474535** | 0.6 | 0.8 | 0.9 | on |

The $T_{RD\ erup}$ ages and Groups for the western Greenland samples are presented in Figure 5.17. This Figure shows that the majority of the Group 1 W.G. peridotites have ~3.0 Ga $T_{RD\ erup}$ ages.

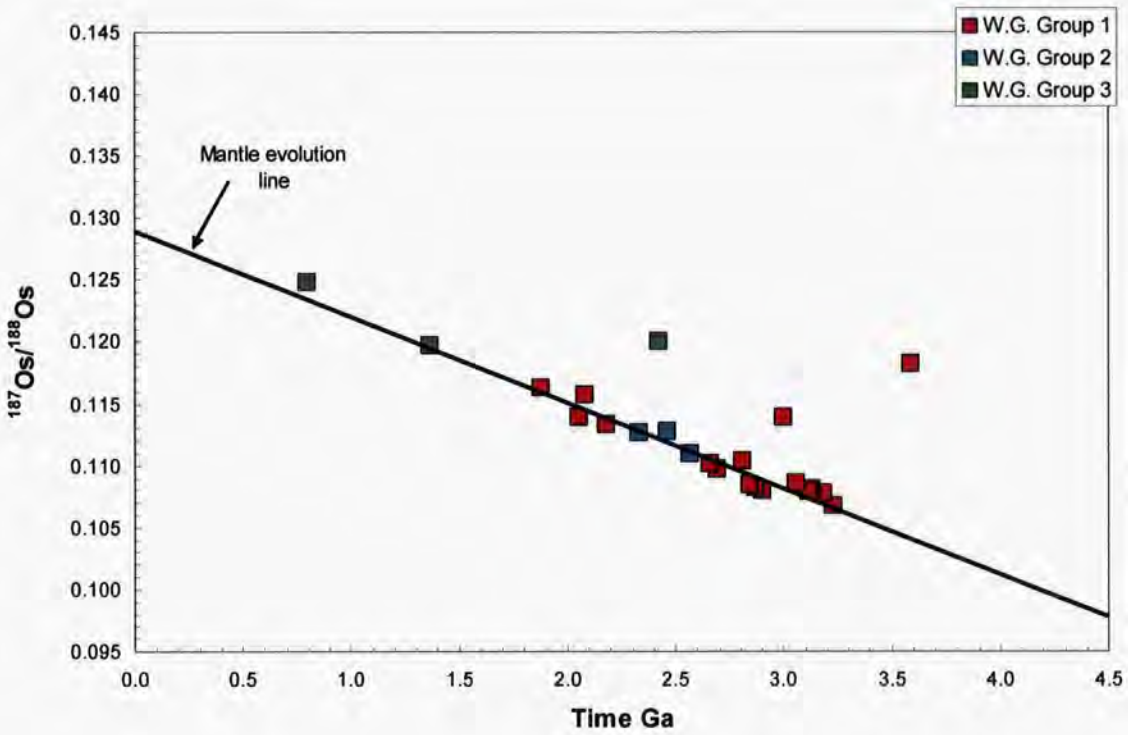


**Fig. 5.17** Os isotopic evolution diagram showing the $T_{RD\ erup}$ age and Groups for the W. Greenland peridotites. Mantle evolution line taken from Pearson *et al.*, (2002). Line also indicated by group IIIA on Fig. 5.3.

In chapters 4 and 5 the W. Greenland peridotite xenoliths have been described in terms of their major element contents and their PGE systematics respectively. In the next chapter the major elements and the PGE systematics of the W. Greenland peridotite suite will be investigated further. They will be interpreted and compared with other peridotite suites from around the world.

# CHAPTER 6

# SYNTHESIS

# Chapter 6:

# Synthesis

## 6.1 Major element constraints on peridotite genesis in W. Greenland

### 6.1.1 Whole Rock analyses

The W.G. peridotite xenoliths show a large range in major element composition. For Mg/Si vs Al/Si (Fig. 6.1) most W.G. samples overlap the range for cratonic peridotites. W.G. & E.G. peridotite suites display very similar bulk Earth compositions. The WG samples extend to much lower Al/Si and generally higher

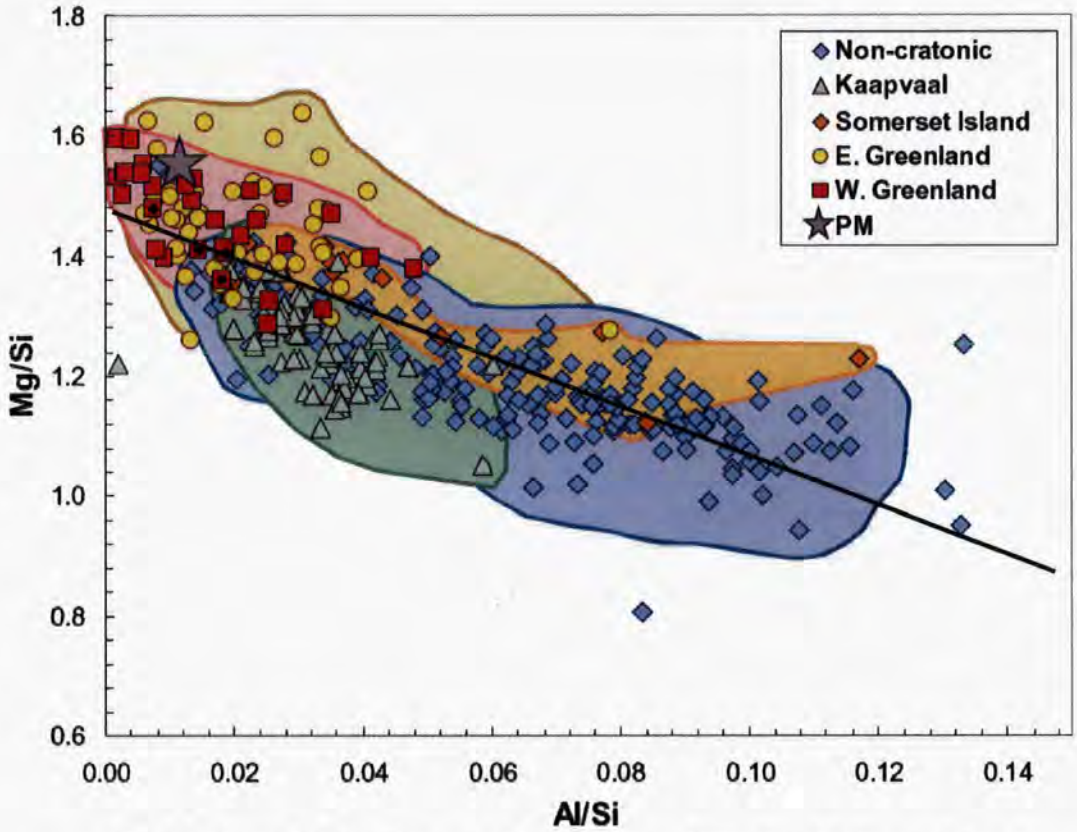


**Fig. 6.1** Plot of bulk Earth composition. Mg/Si vs Al/Si of peridotite xenolith suites. Yellow field = E. Greenland (Bernstein et al, 1998), red field = W. Greenland (this study), blue field = Non-cratonic (various authors Appendix E & F), orange field = Somerset Island (Irvine et al, 2003), and green field = Kaapvaal (Boyd et al, 1993; Pearson et al, 1995). PM = primitive mantle (McDonough & Sun, 1995).

Mg/Si values than other cratonic samples except those from other locations on the N. Atlantic craton, specifically from Greenland. Such high Mg and low Al are

consistent with an origin as residues from high degrees of partial melting (e.g., Boyd, 1989; Pearson, 2003). These characteristics in particular the high Mg and low Al are similar to those of typical cratonic peridotite compositions and give the first indication that the W.G. mantle may be of cratonic origin (Boyd, 1989; Pearson *et al.*, 2003).

### 6.1.2 Typical cratonic mantle

he Kaapvaal and Siberian peridotite suites have much higher contents of $SiO_2$ than W.G., E.G., Somerset Island and Tanzanian peridotites. Walter (1998) used a plot of $MgO/SiO_2$ vs $SiO_2$ (Fig. 6.2) to illustrate the differences between silica-rich low-T and silica-poor high T cratonic peridotites from the Kaapvaal craton. The olivine and

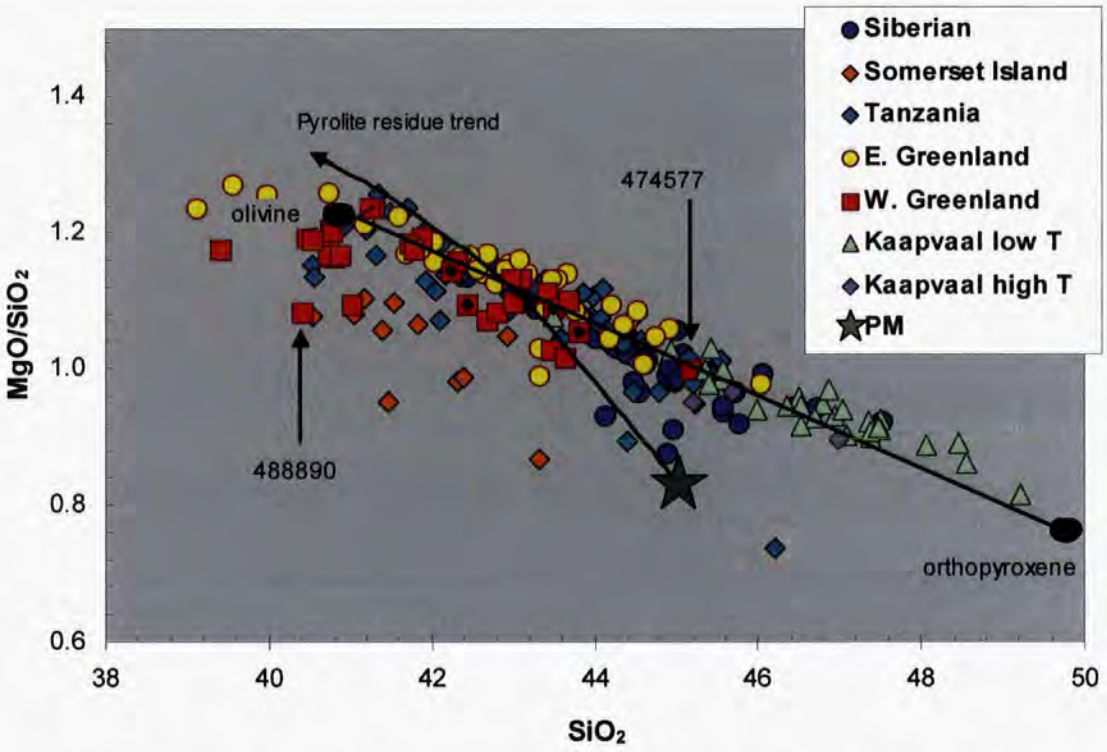


**Fig. 6.2** $MgO/SiO_2$ vs $SiO_2$ for cratonic peridotites. Straight black line is the olivine – orthopyroxene mixing trend. Curved black line is the pyrolite residue trend. Grey star is the primitive mantle. Sources see Fig 4.1.

orthopyroxene line in Figure 6.2 is a mixing trend between these two mineral end members. Low temperature Kaapvaal peridotites plot along the olivine – orthopyroxene mixing trend. This suggests that low temperature Kaapvaal peridotites with high $SiO_2$ were strongly affected by orthopyroxene addition. Peridotites from W. Greenland (and the N. Atlantic craton in general) plot to the silica-poor side of the opx-olivine mixing line, confirming the opx-poor characteristics observed in the field

and petrographically. Sample 474577 of the W.G. peridotite suite is separate from the rest of the W.G. field having very elevated $SiO_2$ and low $MgO/SiO_2$, lying close to the olivine-orthopyroxene mixing line, and so may be indicative of orthopyroxene addition. Sample 488890 is also separate from the rest of the field; this sample has very low $SiO_2$ and high $MgO/SiO_2$.

It has become increasingly apparent that the high levels of $SiO_2$ in the Kaapvaal and the Siberian peridotite suites are not typical of all Archean cratonic mantle (Bernstien *et al.*, 1998; Bernstein *et al.*, 2006). It has been suggested that the elevated amounts of $SiO_2$ are a result of orthopyroxene addition (Kelemen *et al.*, 1992; Kelemen *et al.*, 1998; Simon *et al.*, 2007). Simon *et al* (2007) suggest that this orthopyroxene addition took place in a Archean subduction zone environment. In contrast, the $SiO_2$ poor character of the W. Greenland peridotites and peridotites of the NAC in general indicates a lithospheric mantle with considerably less opx (Bernstein *et al*, 2006). The olivine-rich NAC peridotites also have high olivine Mg numbers, typical of those from the Kaapvaal craton and this has been taken by Bernstein *et al* (2006) to indicate that the NAC and Kaapvaal peridotites experienced very similar degrees of melt extraction but in the case of the Kaapvaal craton later opx enrichment took place. In this way the compositions of the NAC peridotites might be a better estimate of the pre- metasomatic bulk composition of cratonic lithospheric mantle (Bernstein *et al*, 2006). The olivine-rich, orthopyroxene poor peridotites reported in this thesis concur with this picture of the NAC lithospheric mantle and strongly support the views of Bernstein.

One anomaly in the NAC mantle is sample 474577 that has very low Mg/Si (Fig. 6.2) and hence may have experienced some $SiO_2$ enrichment, possibly from orthopyroxene addition. This sample is atypical of the NAC as a whole.

The $SiO_2$ poor nature of NAC samples is in keeping with that expected experimentally, for residues derived from melting pressures between 2 and 5 GPa (Walter, 2003; Canil, 2004). It seems likely that these compositions may be the typical residual mantle composition for cratons before substantial melt- and fluid-related modification takes place, such as the complex scenario suggested by Simon *et al* (2007) for the Kaapvaal craton peridotites.

### 6.1.3 The degree of partial melting in W.G. peridotites

The Ca- and Al-poor nature of W.G. peridotites plus their high olivine magnesium numbers (Mg#) clearly indicate an origin as residues from large fractions of partial melting, probably close to or above 40 % melt extraction (Fig. 6.3 A) (Bernstein *et al*, 2006). The olivine Mg# is a useful measure for observing the degree of partial

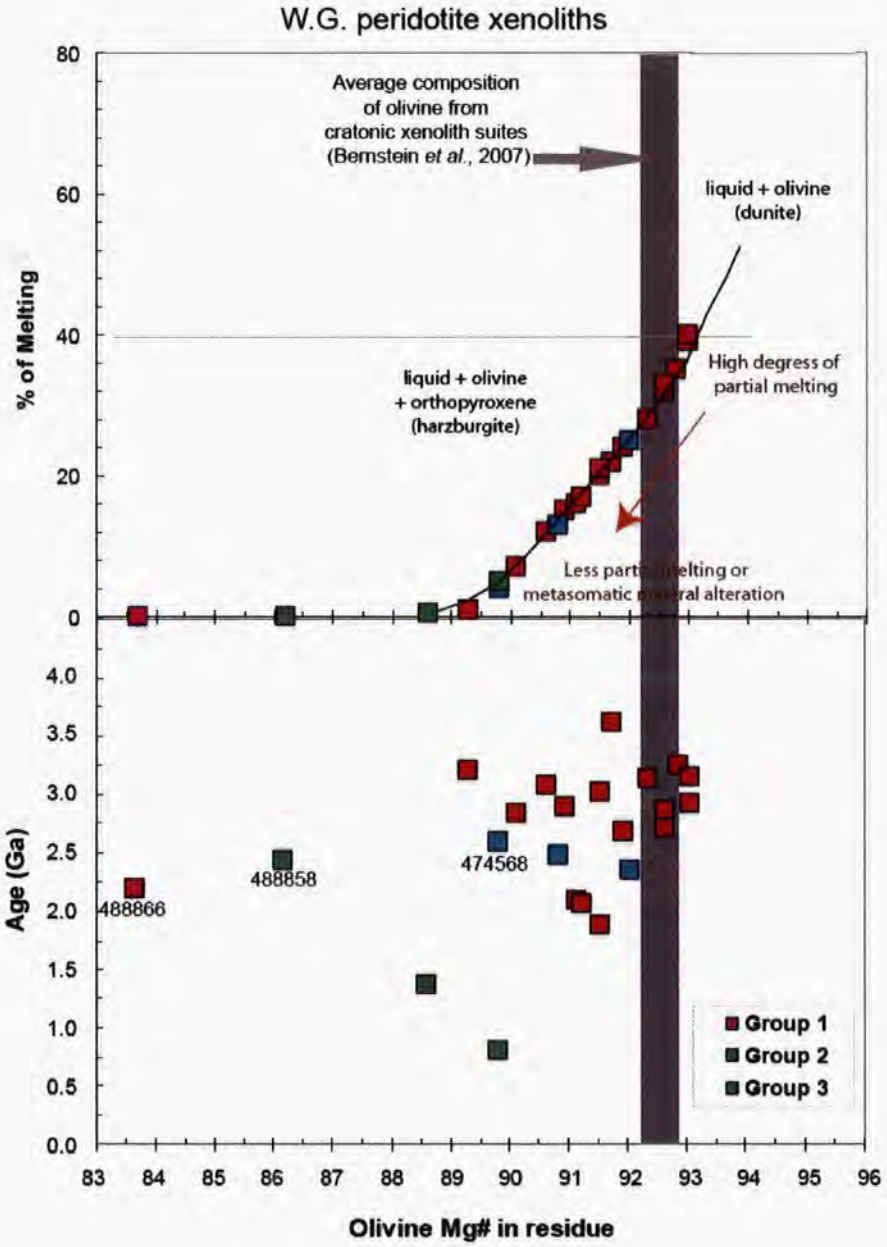


**Fig. 6.3 A**. Percentage of melting against olivine Mg number (Mg#) in a peridotite residue for the W.G. peridotites. Groups 1, 2 and 3, refer to the groupings made in Chapter 5 based on their PGE fractionation patterns. The black curve is taken from Bernstein *et al* (2007). **B**. Age (Ga) against olivine Mg number (#) for the W.G. peridotite suite.

melting which has occurred. High Mg# indicates a high degree of primary melt extraction. However, secondary processes such as metasomatism or serpentinization can modify the olivine Mg# of the residue (Pearson *et al.*, 2004).

Because P-PGEs are fractionated from I-PGEs during partial melting, (Pd/Ir)*n* can be used to evaluate the degree of partial melting. All the W.G. samples are characterised by very low $Al_2O_3$ which is indicative of residues from high degrees of partial melting. The very low (Pd/Ir)*n* values of the W.G. Group 1 peridotites are also consistent with residues for very large degree of melt extraction, and indicate in excess of 25% melt exstraction (Fig. 6.4). These large fractions of melt extraction characterise all the W.G. peridotites, even Group 3, samples whose Pd contents suggest lower degrees of melting have very low $Al_2O_3$ indicating that they too have experienced large degrees of partial melting, and have later been re-enriched in metasomatic Pd, giving higher (Pd/Ir)*n* ratios.

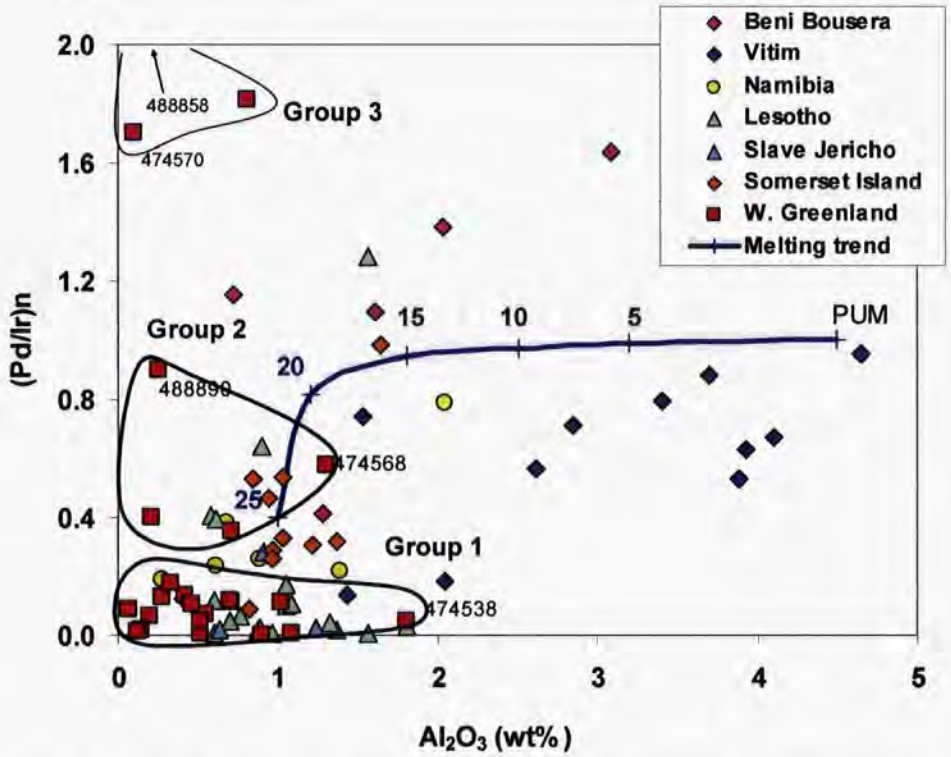


**Fig. 6.4** (Pd/Ir)n vs. $Al_2O_3$. W.G. peridotites are separated into 3 groups. Group 1 are residues from high degrees of partial melting. Group 2 have either experienced less partial melting than Group 1, or have been enriched in Pd. Group 3 have also either experienced less partial melting than Group 1 and 2, or have also experienced some enrichment of Pd. Melting trend taken from Pearson *et al* (2002).

### 6.1.4 Fe and Ti metasomatism

A large proportion of the W.G. peridotites have elevated FeO* contents relative to most other peridotites of the primitive mantle (Fig. 6.5 **A**). The W.G. peridotites plot much higher than E. Greenland, Kaapvaal and even non-cratonic peridotite suites. Similarly the W.G. samples also have higher contents of $TiO_2$ than the other peridotite suites (Fig. 6.5 B). Late stage metasomatism associated with UML magmatism may be responsible for the elevated contents of Fe and Ti (Boyd et al, 1993). Figure 6.5 C & D, shows the W.G. samples separated into their groups as described in Chapter 5, which were, Group 1 is highly depleted; Group 2 has P-PGE enrichments, and Group 3 has more P-PGE enrichment than Group 1 and 2. From Figure 6.5 C it is clear that Group 3 has experienced FeO* addition. Since highly depleted peridotites are characterised by low FeO* contents (Simon, 2004), it could be argued that the Fe has been introduced metasomatically to the W.G. peridotites. In Figure 6.5 D sample number 488858 is the only one with high $TiO_2$ from Group 3. The FeO* and $TiO_2$ anomalies may possibly be some mixture between ilmenite and melt addition.

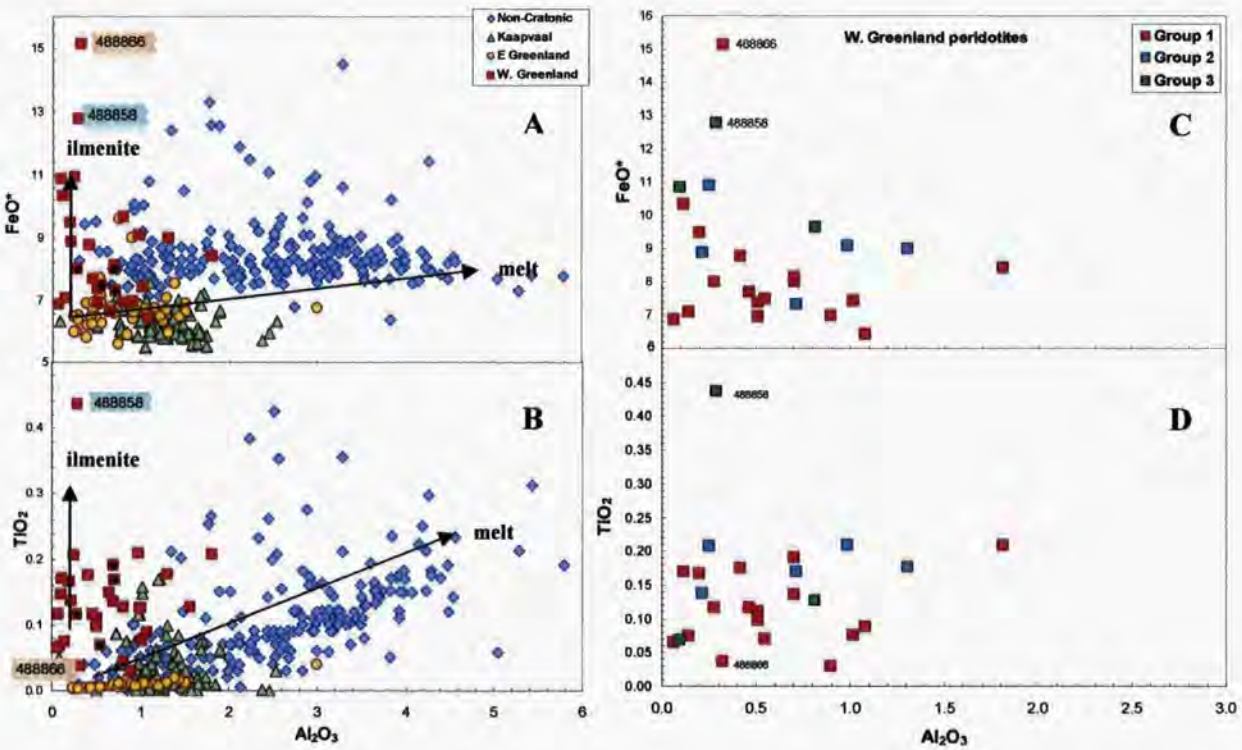


**Fig. 6.5** Plots of FeO* and $TiO_2$ against $Al_2O_3$. A & B. are for various peridotite suites including W.G. C & D are for the W.G. peridotites and they are separated into the groups defined in Chapter 5. Group 1 highly depleted, Group 2 less depleted, and Group 3 is enriched or fertile.

## 6.2 PGE systematics of the W.G. cratonic lithospheric mantle

After the initial formation of a residual peridotite any subsequent disturbance from melts or fluids will be reflected in the PGE patterns and the PGE-major-element systematics (Pearson *et al.*, 2004). The PGE and Re contents of the W.G. peridotite xenoliths were described in Chapter 5. The 24 samples of the peridotite suite were divided into 3 groups of similar characteristics which are summarised in Table 6.1.

Group 1 comprises 17 of the 24 samples and show typical highly P-PGE depleted patterns (Fig. 6.6) that are characteristic of cratonic peridotites. This is due to the fact that they are residues from large fractions of melting (>40%) (Bernstein *et al.*, 2006; Boyd, 1989; Pearson *et al.*, 2004). The cratonic extended PGE pattern of the W.G. peridotites shows some Re enrichment, closely resembling the N. Lesotho peridotites analysed by Irvine (2002) and Pearson et al., (2004). Re enrichment is probably due to small amounts of host dyke infiltration.

Group 2 and 3 peridotites show elevated contents of the P-PGEs compared to Group 1. This feature could be due to lower levels of melt depletion compared with the peridotites from Group 1, i.e. they are more fertile. Alternatively, Pt, Pd and Re have been added to the residual peridotites via metasomatism. From the investigation of the Mg-number and the (Pd/Ir)*n* vs. $Al_2O_3$ on all the W.G. peridotites (Fig. 6.3 & 6.4), it is clear that the peridotites were all once residues from ≥40% partial melting of a fertile mantle (Bernstein *et al.*, 2006). The lack of correlation between Mg# and Pd/Ir suggest that any elevated contents of Pt, Pd and Re are more likely to arise from metasomatic addition of fluids or melts. However, Guo *et al* (1999) notes that small amounts of Pt and Pd derived from immiscible sulphide melts, can get trapped in the residual mantle during partial melting, if this were the case for the W.G. peridotites for Group 2 and 3, then further investigations on the sulphides are needed to evaluate whether such trapped sulphides could account for the P-PGE enrichment. The additions of Pd and Re for Group 2 and 3 can be explained by metasomatic addition via sulphides, possibly during the formation of the ~2.0 Ga Kangâmiut dyke swarm and or from the host dyke during ascent through the crust. Unfortunately there was no scope for an in-depth investigation into the Pt and Pd anomalies found in this suite of peridotites. An investigation was conducted into sample No. 474568 in Group 2.

**Table 6.1** W.G. peridotite groups.

| Group 1 | Group 2 | Group 3 |
|---|---|---|
| ***Depleted/residual plus Re addition*** | ***Less depleted than Gp1 or Pt, Pd and Re addition*** | ***Metasomatised/ Pt, Pd and Re addition*** |
| Low $Al_2O_3$ Low (Pd/Ir)*n* | Low $Al_2O_3$ Med-Low (Pd/Ir)*n* | Low $Al_2O_3$ High (Pd/Ir)*n* |
| High degrees of partial melting | Less partial melting or Pt & Pd addition | Enriched by later melt |
| I-PGE>P-PGE | I-PGE>P-PGE (apart from Pt in sample 474568) | I-PGE = P-PGE |
| Age range is 1.75-3.75 Ga | Age range is 2.25-2.75 Ga | Age range is 0.75-2.50 Ga |

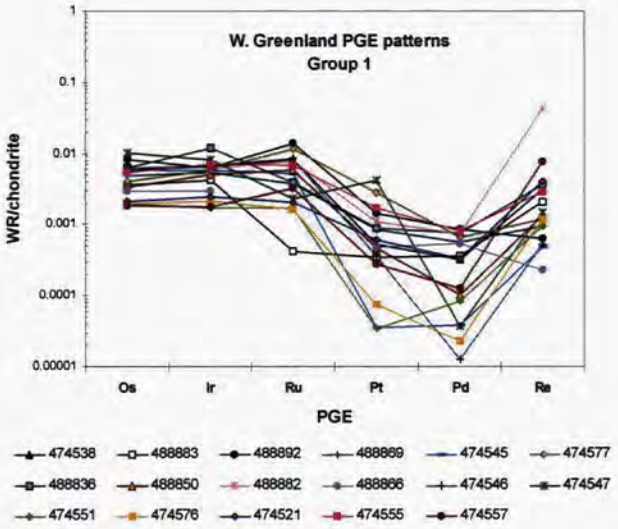


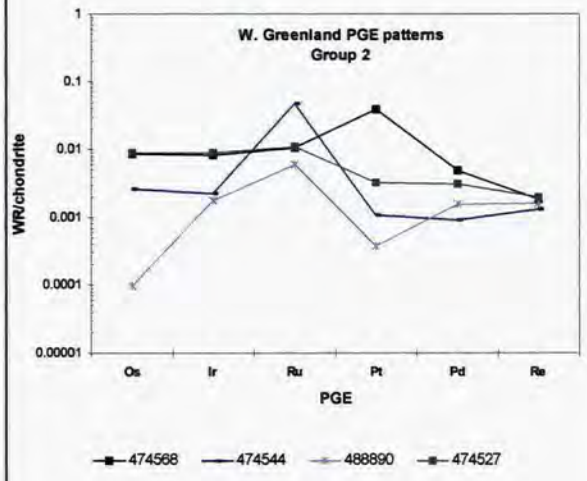


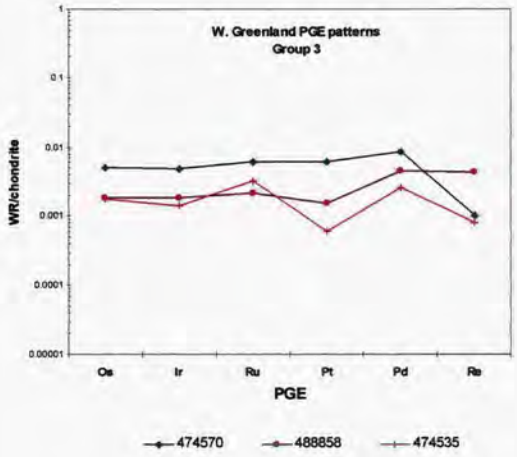

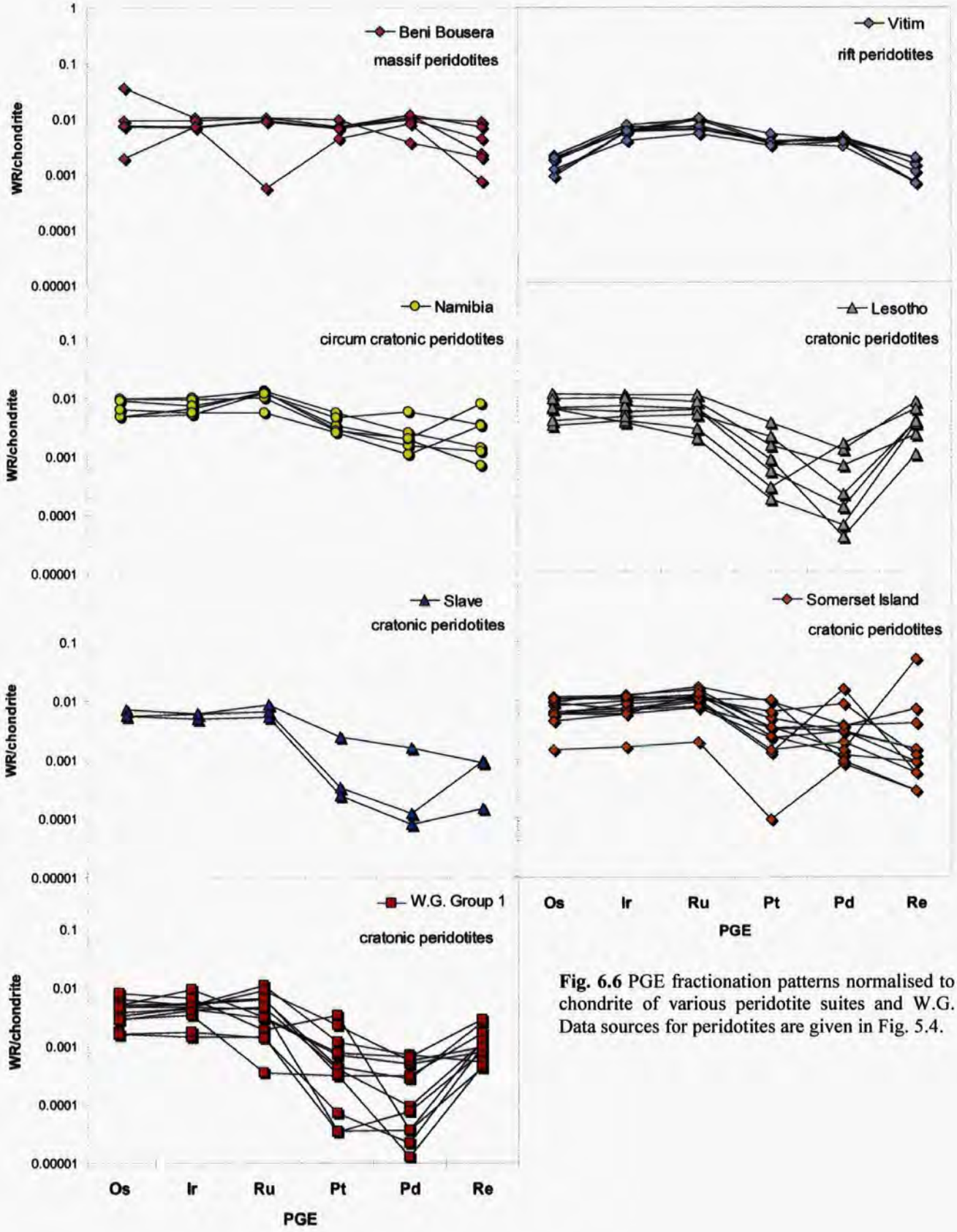


**Fig. 6.6** PGE fractionation patterns normalised to chondrite of various peridotite suites and W.G. Data sources for peridotites are given in Fig. 5.4.

## 6.3 Investigation of a positive Pt anomaly in sample 474568

Low melting temperature sulphides are incorporated into the melt phase during high degrees of partial melting. Os, Ir and Ru are compatible refractory sulphides + alloys and can stabilise in the residue, but Pd and Re act moderately incompatible and are incorporated into the melt phase (Bockrath *et al.*, 2004). The behaviour of Pt is much more complicated than Pd and Re. Pt can be incompatible and enter the melt phase during partial melting, but as a Pt-Ir alloy it can be chemically inert and behave as a highly refractory compatible element becoming trapped in the residue (Luguet *et al.*, 2004).

Under conditions where monosulphide solid solution (Mss) is melting Pd it is more incompatible than Pt, and usually begins to enter the melt phase first and Pd therefore shows higher levels of depletion than Pt (Fig. 5.9) (Luguet *et al.*, 2004). The characteristic depletion of Pt and Pd in PGE fractionation patterns is an expected feature of residual peridotites. The relative depletions observed in harzburgites and depleted lherzolites require $D^{solid/liquid}$ Re < $D^{solid/liquid}$ Pd < $D^{solid/liquid}$ Pt < 1 for peridotite-melt partition coefficients (Pearson et al., 2004; Becker *et al.*, 2006).

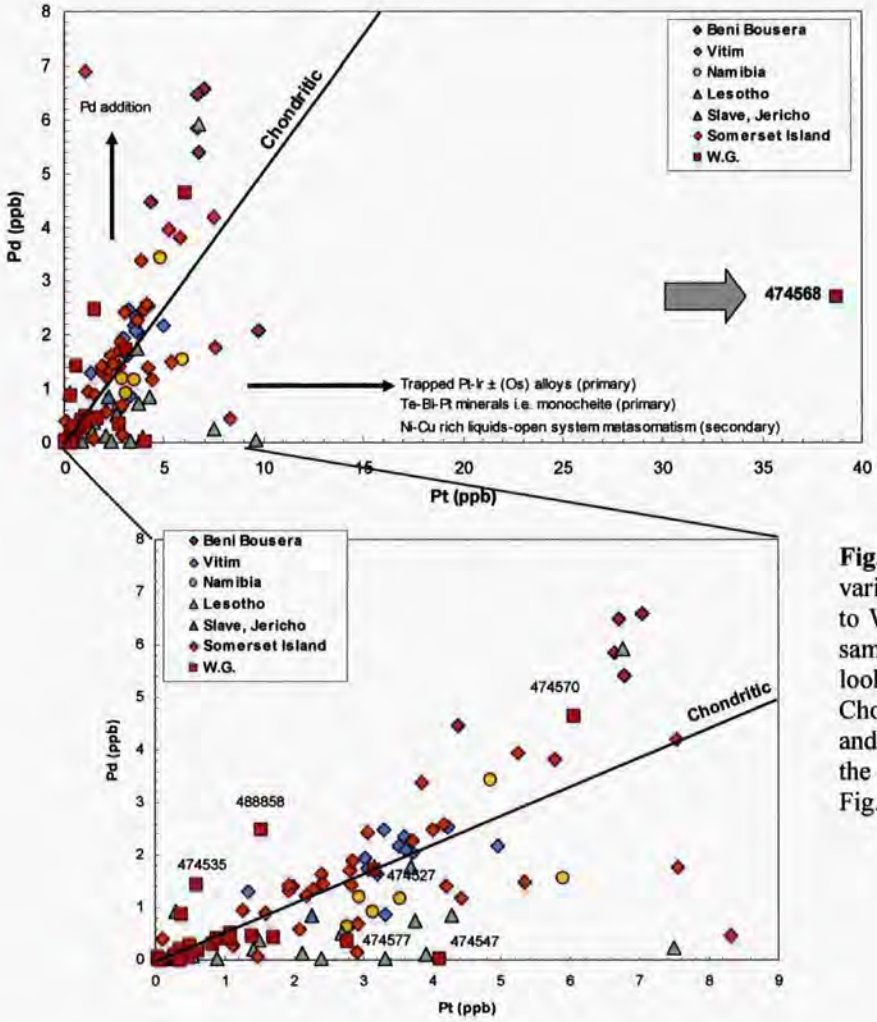


**Fig. 6.7** Pd (ppb) vs. Pt (ppb) for various peridotite suites compared to W.G. Grey arrow is indicating sample 474568. Inset is a closer look at the low Pd vs. Pt area. Chondritic ratio after McDonough and Sun (1995). Data sources for the various peridotites are given in Fig. 5.4.

Pd is well correlated with Pt for the majority of the W.G. peridotite suite (Fig. 6.7) and other peridotite suites worldwide. Both Pt and Pd levels are generally low in all these residual peridotites. However, sample 474568 is extremely enriched in Pt, well above any normal metasomatic disturbances. This requires some explanation. In some residual peridotites Pt and Pd can be significantly disturbed, (see numerous discussions on this subject by Luguet *et al.*, 2006 & 2007; Ohnenstetter, 1992; Lorand *et al.*, 2007; Becker *et al.*, 2006.

Refractory Pt-Ir alloys can get trapped in residual peridotites after high degrees of partial melting due to the desulfidation of base metal sulphides (BMS) in the fertile mantle (Luguet *et al.*, 2007; Lorand *et al.*, 2007). This may account for the positive Pt anomaly in 474568. Pt-Ir alloys are chemically inert and can be highly refractory during this primary melting process (Luguet *et al.*, 2007; Lorand *et al.*, 2007). Alternatively, Ohnenstetter (1999) has suggested that positive Pt anomalies in mantle peridotites can be due to a mineralizing process involving fluid transport and precipitation of platinum group minerals (PGM) in fractures, associated with open system metasomatism in late stage fluids.

Photomicrographs of sample 474568 (Fig. 5.12) in Chapter 5, show a group of intergranular sulphides, probably not formed during primary melting and melt trapping processes. It is likely that these sulphides are of metasomatic origin i.e. high temperature processes, because of their inclusion in silicate phases (Pers. Com. J.P. Lorand). Photomicrographs 2 and 3 show a sulphide inclusion in a partially serpentinized olivine. The inclusion was formally composed of Mss and pentlandite. Mss phases are only stable at high temperatures. When the temperature begins to drop, the Mss begins to decompose to pentlandite, Pt-alloys and or other sulphide phases (Luguet *et al*, 2004). The Mss in photomicrographs 2 and 3 of sample 474568 have now been replaced by microporus pentlandite by reacting with the low temperature serpentinization fluids (pers. com. J-P Lorand; Lorand and Grégoire, 2006). The presence of this secondary pentlandite can not contribute to positive Pt anomalies in PGE fractionation patterns (Luguet *et al*, 2004), it is formed by replacement, as Pentlandite has negative Pt anomalies. However, sample 474568 has the highest Pt anomaly of all the W.G. peridotite samples by ~1 order of magnitude above the I-PGE group. This suggests that the presence of pentlandite in this sample

is not dominating the PGE budget of the rock. Other means of creating a positive Pt anomaly must be considered for this sample.

A Pt-Ir alloy deposited by decomposition of Mss or deposited from a percolating melt will create a positive Pt anomaly (Luguet *et al.*, 2007). Another possibility for generating anomalously high Pt contents could be via a Pt 'nugget effect' during sampling and digestion. The powdered sample may have a small grain of Pt-alloy incorporated into the digestion process. In order to eliminate the 'nugget effect' from this sample, it would be necessary to repeat another digestion of this sample and probably using a larger sample size. Unfortunately this was not possible due to the time constraints of this study. The presence of some Pt-Ir alloy phases seems the most likely explanation for this unusual Pt enrichment and a further SEM/TEM study to search for such phases seems warranted.

## 6.4 Timing of the stabilisation of the craton in S.W. Greenland

The residual signature and high degree of partial melting observed in the Group 1 peridotites for W.G., offer the best opportunities for constraining the true ages and therefore the stabilisation of the W.G. lithospheric mantle, because melt depletion may have frozen in unradiogenic Os isotope signatures.

Archean Re-depletion ages of ~3.0 Ga dominate the Group 1 peridotites for W.G. (Fig. 6.8). There is no obvious distinction between the Re-Os ages of xenoliths found on or off the craton (Fig. 6.9 & Fig. 6.10). This suggests that the Archean lithospheric mantle beneath the craton also extends beneath the reworked Archean terrane (RAT). However, a Re enrichment is seen in all W.G. samples, suggesting some Re addition from the host magma. This Re enrichment places some doubt on the true Re-Os model ages for W.G. peridotites, and makes it likely that they are minimum ages.

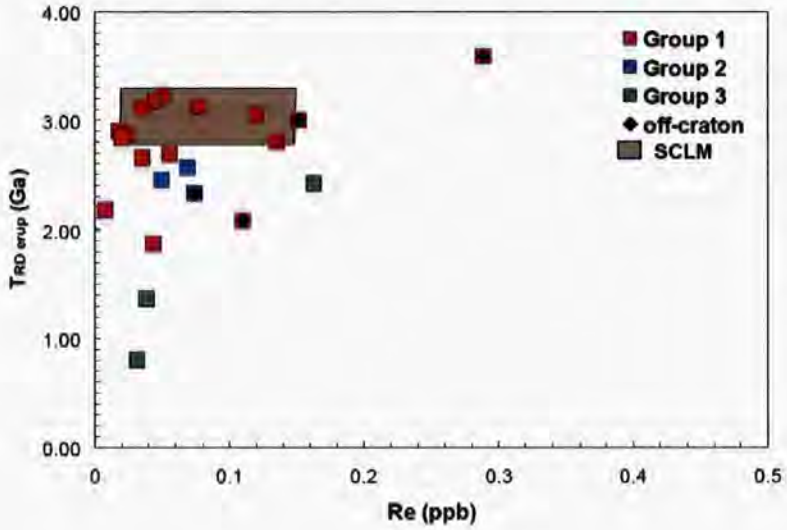


**Fig. 6.8** $T_{RD\ erup}$ (Ga) model age vs. Re (ppb). Sub continental lithospheric mantle (SCLM) taken from Shirey & Walker, 1998). One data point has anomalously high Re (ppb) and the oldest age.

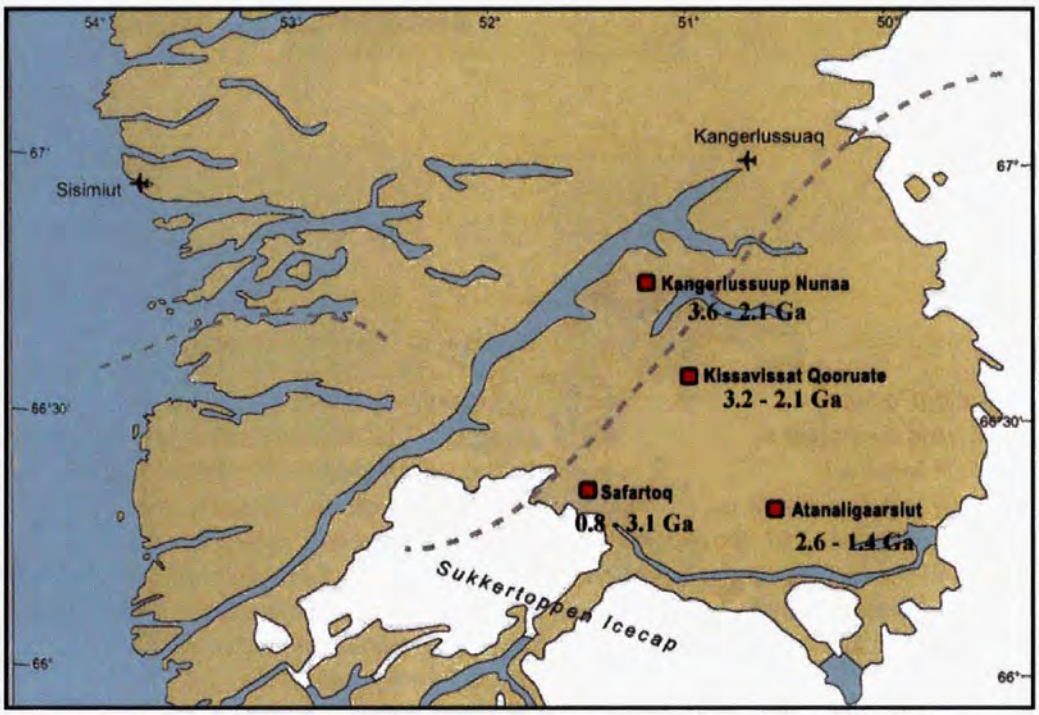


**Fig. 6.9** Age ranges (Ga) for the W.G. peridotite xenoliths collected at the four localities

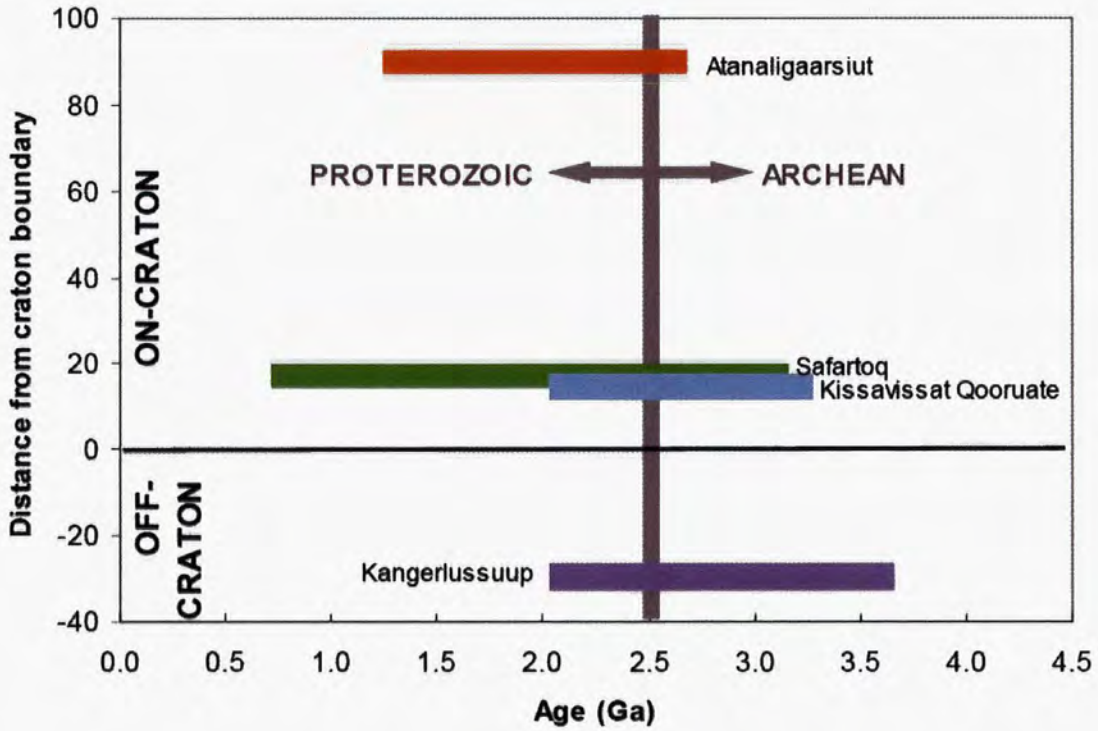


**Fig. 6.10** Age ranges for the W.G. peridotite samples plotted against distance in km from the craton boundary. The grey line represents 2.5 Ga crust, older represents Archean crust and younger represents Proterozoic crust.

## 6.5 Diamond Potential in W.G.

Recent field studies by GEUS in W.G. have returned 111 micro- and 9 macro-diamonds from Garnet Lake in the Safartoq area in 2004, and 124 micro- and 4 macro-diamonds from Safartoq - Maniitsoq (south) in 2003 (Secher & Jensen, 2004).

Many reconnaissance investigations have taken place in the Safartoq area; these are ground geophysics, mapping, helicopter borne geophysics, regional till and stream sediment research (Secher & Jensen, 2004). In constraining the diamond potential of this region it is important to determine lithospheric ages for both on and off the craton, as UML dykes occur in both these areas. This study is the first investigation into the age and timing of the stabilisation of the Archean lithospheric mantle beneath western Greenland. Specifically what lies beneath the re-worked Archean terrane? Is it all re-worked Archean, or new Proterozoic mantle, or undisturbed Archean lithosphere? The possible variations are illustrated in the 4 scenarios of Figure 6.11. In each scenario the plan view is the same, i.e. a central block of Archean crust surrounded by re-worked crust, but the cross section through the crust and mantle and the diamond potential is different. From the Re-Os age dating carried out by this research, Archean ~3.0 Ga mantle extends beneath the re-worked Archean terrane, indicating that scenario 3 from Figure 6.11 is representative of the lithospheric mantle beneath W.G.

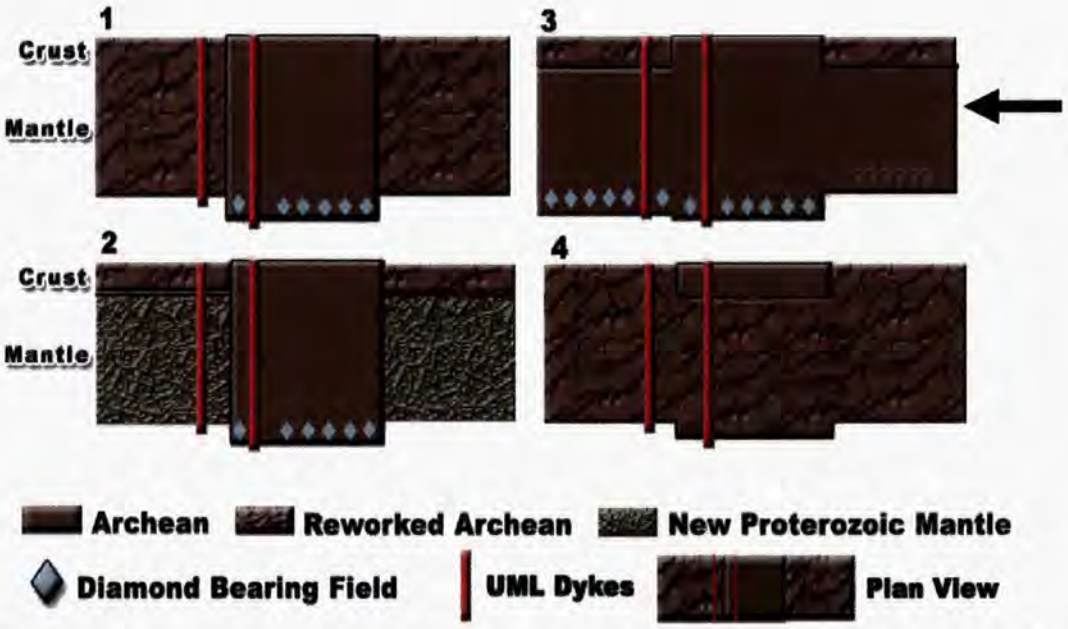


**Fig. 6.11**. In each of these four diagrams the crust on the surface appears the same, but the lithospheric mantle and diamond potential is different in each case. The scenario that appears to represent the lithospheric mantle beneath W.G. is No. 3. This would suggest the there is diamond potential in this area, both on and immediately at the edge of the 'craton' as defined by the area of re-worked Archean crust.

A better understanding of the depth of the Archean lithospheric mantle beneath W.G. is important in evaluating whether the UML dykes have come from the diamond stability field (>150 km) or not. Pressure and temperature work on peridotites xenoliths carried out by Sand (2007) has indicated that the depth of the lithosphere beneath W.G. extends to a depth of 220 km (Fig. 6.12 A).

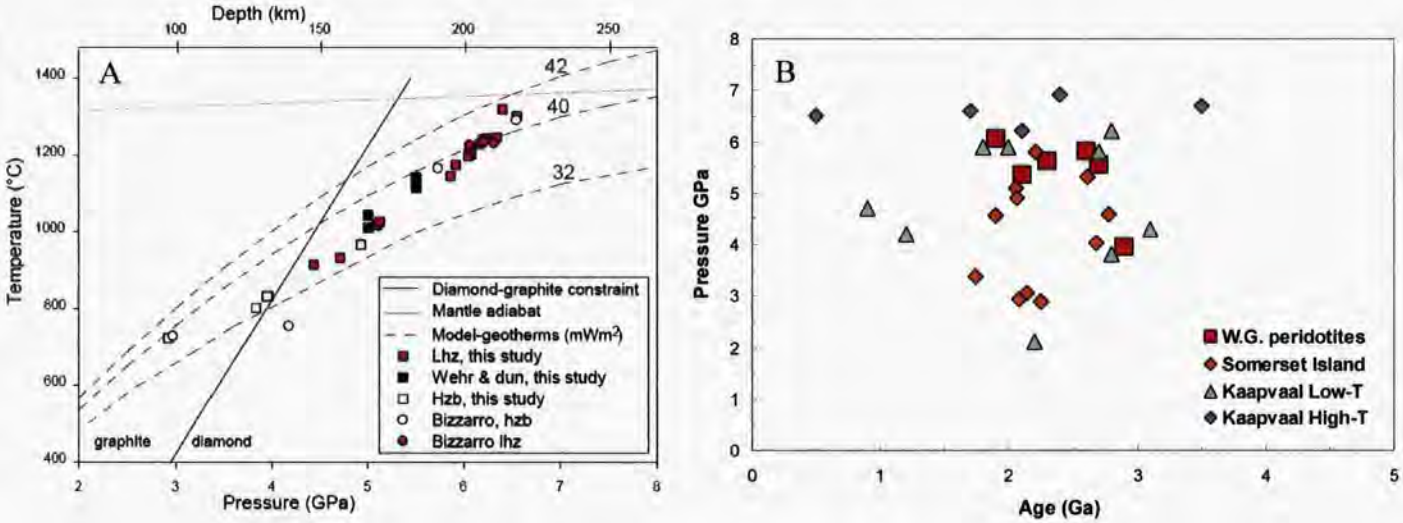


**Fig. 6.12 A**. Pressure and depth vs. temperature for W.G. samples taken fron Sand (2007). **B**. Pressure (GPa) vs. Re-depletion ages (Ga) for W. G. peridotites and various other peridotite suites. (Data sources are Somerset Island = Irvine *et al.*, 2003, Kaapvaal low-T & high-T = Pearson *et al.*, 1995a) (W.G. pressure data was provided by Sand (2007)). There are only limited samples where pressure data is available for their corresponding ages.

A limited number of peridotites on which pressure and temperature determinations have been made have been analysed for Re-Os isotopes to determine their age (Gig 6.12 B). These samples show a range of pressures between 4 and 6 GPa. Sand (2007) suggests samples which are between 5.7 and 6.5 GPa have come from a depth range between 190 and 220 km. Although there is a range of ages in the samples determined for pressure and temperature, probably because these are clinopyroxene bearing lherzolites that have undergone metasomatism, Archean (>2.5 Gyr) Re-depletion ages are evident in both the shallowest and deepest samples. This indicates the presence of Archean mantle right into the diamond stability field in this region. The large proportion of samples in the depth range of 150-220km (Sand, 2007) suggests that a significant proportion of the xenoliths are being sampled from mantle in the diamond stability field. So from a diamond potential perspective, relating to the age of the Archean mantle beneath both areas, there is potential for diamond exploration.

# CHAPTER 7

# CONCLUSION

# Chapter 7:

# Conclusions

600 My old ultra-mafic lamproite (UML) dykes in the region between Kangerlussuaq and Safartoq of S.W. Greenland have erupted a remarkable collection of mantle xenoliths. This suite of peridotite xenoliths is particularly useful for Re-Os analysis because they are found in dykes that have intruded within the edge of an Archean craton, and the surrounding reworked Archean terrane. The aim of this research was to constrain the age of the lithospheric mantle beneath both these terranes, and to explore whether the Archean lithospheric mantle extends beneath the reworked Archean terrane. This study is a small part of a more extensive ongoing investigation by the Geological Survey of Denmark (GEUS) into the likely diamond potential of the area.

After careful investigation the W.G. peridotites were separated into 3 distinct groups based on their major element and PGE and Re contents. Group 1 are depleted residues from high degrees of partial melting probably up to ~40%. They have major element and PGE inter-element fractionation patterns characteristic of Archean mantle. These are, very low $Al_2O_3$ contents and Mg# of olivine ranging up to >93, plus PGE patterns that are significantly depleted in both Pt and Pd. The samples have minimum Re-Os ages ranging from 1.8 to 3.0 Ga. Thermobarometry investigations by Sand (2007) have revealed equilibration pressures for some of these samples of between 5-7 GPa, with a maximum depth of 220 km at 600 Ma (Sand, 2007). The xenoliths have therefore come from the diamond stability field. There is no distinct difference in the geochemical signatures of the xenoliths found on or off the craton. Re-depletion ages >2.5 Gyr for samples both on and off the craton edge indicate that old Archean lithospheric mantle extends beneath both the re-worked Archean terrane and the Archean craton. Groups 2 and 3 of the W.G. peridotites show more complicated disturbances in their geochemistry. Group 2 show positive anomalies in Ru, Pt, Pd and Re, Group 3 have relatively flat, unfractionated patterns. The additions of Pd and Re for Group 2 and 3 can be explained by metasomatic addition via sulphides, possibly during the formation of the ~2.0 Ga Kangâmiut dyke swarm and or from the host dyke during ascent through the crust. However, large positive Pt anomalies can

be more complicated to resolve. The most likely explanation for a large Pt anomaly found in one sample is the formation of anomalous amounts of refractory Pt-rich alloy phases in this sample.

The W.G. peridotite xenoliths that were placed into Group 1 most closely retain evidence of the original partial melting process and subsequent stabilisation of the W.G. mantle lithosphere. Therefore, the oldest Re-Os age data for Group 1 should be the most reliable age for the stabilisation of the lithospheric mantle beneath W.G. which is ~3.0 Ga.

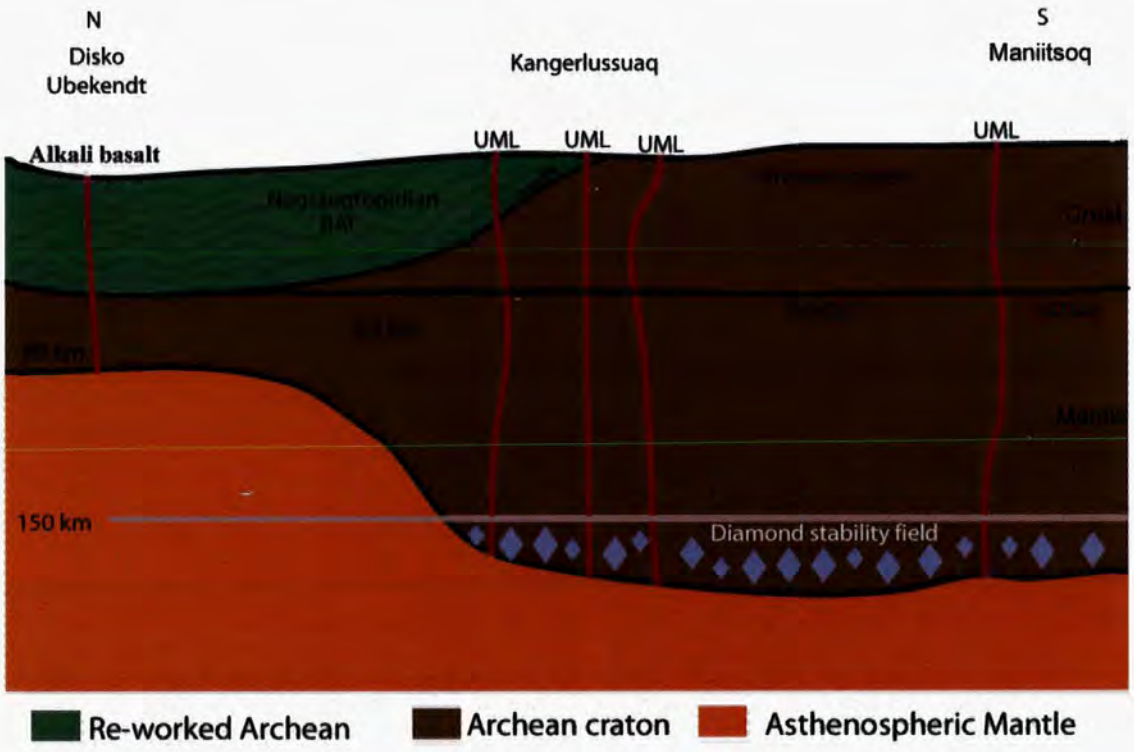


**Fig. 7.1** Illustrates the Archean craton extending below the Nagssugtoqidian reworked Archean terrane. Disko alkali basalt from Bernstein *et al.*, 2006

## 7.2 Diamond potential

Thermobarometry work by Sand (2007) has shown that numerous peridotite samples from the Kangerlussuaq and Safartoq areas of W.G. have come from the diamond stability field plus shallower parts of the W.G. lithosphere. This plus the Archean ages found in this study therefore provide 2 main requirements for diamond potential one is very deep lithosphere and the second is Archean age. Work already carried out

by GEUS on some of the ultra-mafic dykes in this region have already returned micro and macro-diamonds (Fig. 7.2).

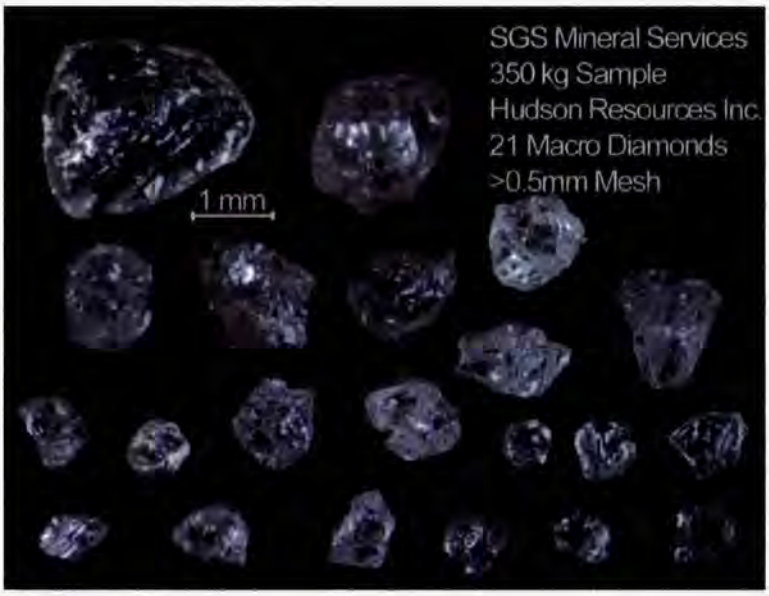


**Fig. 7.2** Diamonds already discovered by Hudson Resources in SW Greenland. (HR website)

Further work is needed on the indicator minerals within the xenoliths to further constrain their relation to the diamond potential, and also on the mineralogy of the host dyke to understand its composition. There is still an ongoing debate as to whether the ultra-mafic dykes that brought these xenoliths to the surface in W.G. are kimberlitic or ultramafic lamprophyre. UML dykes are becoming increasingly more significant to the diamond exploration industry for hosting diamonds (Tappe *et al.*, 2004).

### 7.3 Future work

More peridotite xenoliths need to be collected and analysed from the off-craton area in W.G. In this study only 4 samples were analysed from UML dykes in the reworked Archean terrane. Although the major element and Re-Os data for these 4 samples is informative, it may not give a true representation of the area as a whole.

Analysing the trace element characteristics for the W.G. peridotite xenoliths would help to more firmly establish the depth of melting

Investigations into the FeO* content of the W.G. peridotite samples would resolve the large positive anomalies seen in the major element compositions.

A mineralogical investigation on the host dyke is needed to classify its composition. Is it a lamprophyre or a kimberlite?

# REFERENCES

## References

**Allègre, Claude. J., Manhès, Gérard. & Göpel, Christa.** 1995. The age of the Earth. *Geochimica et Cosmochimica Acta*, Vol. 59, No. 8, Pp 1445-1456

**Becker, H., Horan, M.F., Walker, R.J., Gao, S., Lorand, J.P. & Rudnick, R.L.** 2006. Highly siderophile element composition of the Earth's primitive upper mantle: Constraints from new data on peridotite massif xenoliths. *Geochimica et Cosmochimica Acta*. Vol. 70, Pp. 4528-4550

**Bedini, R.M., Bodinier, J.-L., Dautria, J.-M. & Morten, L.** 1997. Evolution of LILE-enriched small melt fractions in the lithospheric mantle: a case study from the East African Rift. *Earth and Planetary Science Letters*. Vol. 153, Pp 67-83

**Bennett, Victoria C., Nutman, Allen P. & Esat, Tezer M.** 2002. Constraints on mantle evolution from 187Os/188Os isotopic compositions of Archean ultramafic rocks from southern West Greenland (3.8 Ga) and Western Australia (3.46 Ga). *Geochimica et Cosmochimica Acta*, Vol. 66, No. 14, Pp. 2615-2630.

**Bernstein, Stefan., Kelemen, Peter B. & Brooks, C. Kent.** 1998. Depleted spinel harzburgite xenoliths in Tertiary dykes from East Greenland: Restites from high degree melting. *Earth and Planetary Science Letters*. 154, Pp 221-235.

**Bernstein, Stefan., Hanghøj, Karen., Kelemen, Peter B. & Brooks, C.Kent.** 2006. Ultra-depleted, shallow cratonic mantle beneath West Greenland: dunitic xenoliths from Ubekendt Ejland. *Contributions to mineralogy and petrology*, Vol. 152, No. 3, Pp. 335-347.

**Bernstein, Stefan., Kelemen, Peter B. & Hanghøj, Karen.** 2007. Consistent olivine Mg# in cratonic mantle reflects Archaean mantle melting to the exhaustion of orthopyroxene. *Geology*, Vol. 35, Pp. 459-462

**Bockrath, C., Ballhaus, C. & Holzheid, A.** 2004 Fractionation of Platinum-Group Elements during partial melting. *Science*, Vol. 305, Pp 1951-1953

**Boucher, D.R.** 2000. 1999 Assessment work report on the mini-bulk sampling programme, Sarfartoq exploration licence, Kalaallit Nunaat, 18 pp. Unpublished report, Monopros Ltd. For Dia Met Minerals Ltd., Kelowna, B.C., Canada (in archives of *Geological Survey of Denmark and Greenland*, GEUS Report File 21742).

**Burton, Kevin W., Schiano, Pierre., Birck, Jean-Louis. & Allegre, Claude J.** 1999. Osmium isotope disequilibrium between minerals in a spinel-lherzolite. *Earth and Planetary Science Letters*. 172, Pp 311-322.

**Boyd, F.R., Gurney, J.J. & Richardson, S.H.** 1985. Evidence for a 150-200km thick Archean lithosphere from diamond inclusion thermobarometry. *Nature*, Vol. 315, Pp 387-389.

**Boyd, F.R., Pearson, D.G., Nixon, P.H. & Mertzman, S.A.** 1993. Low-calcium garnet harzburgites from southern Africa: their relations to craton structure and diamond crystallization. *Contributions to Mineral Petrology*, Vol. 113, Pp. 352-366

**Boyd, F.R., Pokhilenko, N.P., Pearson, D.G., Mertzman, S.A., Sobolev, N.V. & Flinger, L.W.** 1997. Coposition of the Siberian cratonic mantle: evidence from Udachnaya peridotite xenoliths. *Contributions to Mineral Petrology*, Vol. 128, Pp. 228-246

**Boyd, F. R., Pearson, G. P., Hoal, B. G., Nixon, P. H., Kingston, M. J. & Mertzman, S. A.** 2004. Garnet Lherzolites from Louwrensia, Namibia: bulk composition and *P/T* relations. *Lithos*, Vol. 77, Pp 573-592.

**Bridgewater, D., Escher, A. & Watterson, J.** 1973. Dyke swarms and the persistence of major geological boundaries in Greenland. In. *The Early Precambrian of Scotland and Related rocks of Greenland.* Edited by R.G. Park & Tarney. Pp. 137-141. Published by the Department of Geology, University of Keele, Newcastle, Staffordshire.

**Cadman, A.C., Tarney, J., Bridgewater, D., Mengel, F., Whitehouse, M.J. and Windley, B.F.** 2001. The petrogenesis of the Kangâmiut dyke swarm, W. Greenland. *Precambrian Research*, Vol. 105, Pp. 183-203.

**Canil, Dante.** 2002. Vanadium in peridotites, mantle redox and tectonic environments: Archean to present. *Earth and Planetary Science Letters*. Vol. 195, Pp. 75-90.

**Canil, Dante**. 2004. Mildly incompatible elements in peridotites and the origins of mantle lithosphere. *Lithos*. Vol. 77, Pp. 375-393.

**Carlson, Richard W**. 2005. Application of the Pt-Re-Os isotopic systems to mantle geochemistry and geochronology. *Lithos*. 82. Pp 249-272

**Connelly, J.N., van Gool, J.A.M. & Megel, F.C**. 2000 Temporal evolution of a deeply eroded orogen: The Nagssugtoqidian Orogen, West Greenland. *Canadian Journal of Earch Sciences*, Vol. 37, Pp. 1121-1142.

**Dale, Christopher. W., Luguet, A., Macpherson, C.G., Pearson D.G., Hickey-Vargas R**. (In review) Extreme platinum-group element fractionation and variable Os isotope compositions in Philippine Sea Plate basalts: tracing mantle source heterogeneity. *Chemical Geology Special Publication* – Highly Siderophile Element Volume (In Press)

**Dautria, J.M. & Girod, M**. 1987. Cenozoic volcanism associated with swells and rifts. In: *Mantle Xenoliths*. Edited by Peter H. Nixon. John Wiley & Sons Ltd. Pp.195-214.

**Davies, G.F**. 1995. Punctuated tectonic evolution of the Earth. *Earth and Planetary Science Letters*. 136. Pp. 363-379

**Dupuy, C., Dostal, J., Dautria, J.M. & Girod,** M. 1986. Geochemistry of spinel peridotite inclusions in basalts from Hoggar, Algeria. *Journal of African Earth Sciences*, Vol. 5, Issue 3, Pp. 209-215

**Dupuy, C., Dostal, J. & Bodinier, J.L**. 1987. Geochemistry of spinel peridotite inclusions in basalts from Sardinia. *Mineralogical Magazine*, Vol. 51, Pp. 561-568

**Embey-Isztin, A., Scharbert, H.G., Dietrich, H. & Poultidis, H**. 1989. Petrology and Geochemistry of Peridotite Xenoliths in Alkali Basalts from the Transdanubian Volcanic Region, West Hungary. *Journal of Petrology*, Vol. 30, No. 1, Pp. 79-105.

**Ernst, W.G**. 2007. Speculations on evolution of the terrestrial lithosphere-asthenosphere system - Plumes and plates. *Gondwana Research* Vol. 11 Pp. 38-49.

**Frey, F.A. & Green, D.H**. 1974. The Mineralogy, Geochemistry and origin of lherzolite inclusions in Victorian Basanites. *Geochimica et Cosmochimica Acta*, Vol. 38, No. 8. Pp 1023-1059.

**Griffin, W.L., Sutherland, F.L. & Hollis, J.D**. 1987. Geothermal profile and crust-mantle transition beneath east-central Queensland:Volcanology, xenolith petrology and seismic data. *Journal of Volcanology and Geothermal Research*, Vol. 31, Issue 3-4, Pp. 177-203.

**Griffin, W.L., O'Reilly, S.Y., Abe, N., Aulbach, S., Davies, R.M., Pearson, N.J., Doyle, B.J. & Kivi, K**. 2003. The origin evolution of Archean lithospheric mantle. *Precambrian Research*. Vol. 127, Pp. 19-41.

**Guo, Jingfeng., Griffin, William. L. & O'Reilly, Suzanne. Y.** 1999. Geochemistry and Origin of sulphide minerals in mantle xenoliths: Qilin Southeast China. *Journal of Petrology*. Vol. 40, No. 7, Pp. 1125-1149.

**Hanghøj, Karen., Kelemen, Peter., Bernstein, Stefan., Blusztajn, Jerzy. & Frei, Robert**. 2001. Osmium isotopes in the Wiedemann Fjord mantle xenoliths: A unique record of cratonic mantle formation by melt depletion in the Archean. Geochemistry, Geophysics, Geosystems. *American Geophysical Union*. Vol. 2, January 3rd. Paper No. 2000GC00085.

**Holgate, S.A**. 2005. *The mantle sources of West Greenland kimberlites: Implications for diamond exploration*. Masters Thesis. Department of Earth Sciences, University of Durham.

**Hudson Resources Website**. http://www.hudsonresources.ca/files/350kg_Caustic.pdf

**Hunter, R.H. & Upton, B.G.J**. 1987. The British Isles- a Palaeozoic mantle sample. In: *Mantle Xenoliths*. Edited by Peter H. Nixon. John Wiley & Sons Ltd. Pp. 107-118.

**Irvine, Gordon J., Pearson D. Graham., Kjarsgaard, B.A., Carlson, R.W., Kopylova, M.G. & Dreibus, G**. 2003. A Re-Os isotope and PGE study of kimberlite-derived peridotite xenoliths from Smoerset Island and a comparison to the Slave and Kaapvaal cratons. *Lithos*, 71, Pp 461-488.

**Jagoutz, E., Palme, H., Baddenhausen, Hildegard., Blum, K., Cendales, M., Dreibus, Gerlind., Spettel, B., Lorenz, V. & Wänke, H**. 1979. The abundances of major, minor and trace elements in the earth's mantle as derived from primitive ultramafic nodules. *Proceedings of the 10th Lunar Planetary Science Conference*, Pp2031-2050

**Jaques, A.L., O'Neill, H. St. C., Smith, C.B., Moon, J. & Chappell, B.W**. 1990. Diamondiferous peridotite xenoliths from the Argyle (AK1) lamproite pipe, Western Australia. *Contributions to Mineralogy and Petrology*. Vol. 104, No. 3, Pp 255-276

**Jensen, S.M., Secher, K., Rasmussen, T.M., Tukiainen, T., Krebs, J.D. & Schjøth, F.** 2003. Distribution and magnetic signatures of kimberlitic rocks in the Sarfartoq region, southern West Greenland. *8th International Kimberlite Conference*, Victoria, B.C., Canada. Extended abstracts CD-ROM. Pp. 5.

**Keleman, Peter. B., Dick, Henry. J.B. & Quick, James. E**. 1992. Formation of harzburgite by pervasive melt/rock reaction in the upper mantle. *Nature*. Vol. 358, Pp. 635-641.

**Koylova, Maya G. & Russell, James K**. 2000. Chemical stratification of cratonic lithosphere: constraints from the Northern Slave craton, Canada. *Earth and Planetary Science Letters*. 181. Pp 71-87.

**Larsen, L.M. & Rex, D.C**. 1992. A review of the 2500 Ma span of alkaline ultramafic , potassic and carbonatitic magmatism in West Greenland. *Lithos* Vol. 28, Pp 367-402.

**Larsen, Lotte Melchior. & Rønsbo, Jørn**. 1993. Conditions of origin of kimberlites in West Greenland: new evidence from the Sarfartoq and Sukkertoppen regions. *Rapp. Grønlands Geol*. Vol. 159, Pp. 115-120.

**Lee, C.T. & Rudnick, R.L**. 1999. Compositionally stratified cratonic lithosphere: petrology and geochemistry of peridotite xenoliths from the Labait volcano, Tanzania. In Gurney, J.J. et al (eds): *Proceedings of the VIIth International Kimberlite Conference 2*. Pp. 503–521. Cape Town: Red Roof Design cc.

**Leitch, A.M**. 2004. Archean Plate Tectonics. Abstract. *American Geophysical Union* Spring meeting. 2004.

**Lithoprobe. 2007**. The Growth of Canada. Website URL = http://www.lithoprobe.ca/media/slideset/slides/growth5.asp

**Lorand, Jean-Pierre & Grégoire**. 2006. Petrogenesis of base metal sulphide assemblages of some peridotites from the Kaapvaal craton (South Africa). *Contributions to mineralogy and Petrology*. Vol. 151, Pp. 521-538

**Lorand, J-P., Luguet, Ambre., Alard, Olivier., Antoine, Bezos. & Meisel, Thomas**. 2007. Abundance and distribution of platinum-group elements in orogenic lherzolites; a case stud in a Fontete Rouge lherzolite (French Pyrénées). *Chemical Geology*. In Press

**Luguet, Ambre., Lorand, Jean-Pierre., Alard, Olivier. & Cottin, Jean-Yves**. 2004. A multi-technique study of platinum group element systematic in some ligurian ophiolite peridotites, Italy. *Chemical Geology*. Vol. 175, Pp. 175-194.

**Luguet, Ambre., Shirey, Steven. B., Lorand, Jean-Pierre., Horan, Mary. F. & Carlson, Richard. W**. 2007. Residual platinum-group minerals from highly depleted harzburgites of the Lherz massif (France) and their rols in HSE fractionation of the mantle. *Geochimica et Cosmochimica Acta*. Vol. 71, Pp. 3082-3097.

**Luhr, James. F. & Aranda-Gomez, Jose. J**. 1997 Mexican peridotite xenoliths and tectonic terranes: Correlations among vent location, texture, temperature, pressure and oxygen fugacity. *Journal of Petrology*, Vol. 38, No. 8, Pp. 1075-1112.

**Marker, M., Mengel, F. & van Gool, J**. 1995. Evolution of the Palaeoproterozoic Nagssugtoqidian Orogen. *DLC investigations in West Greenland*. In report Geological Survey of Denmark and Greenland. Vol. 165, Pp. 100-105.

**McDonough, W.F. & Sun, Shen. Su**. 1995. The composition of the Earth. *Chemical Geology*, Vol. 120, Pp. 223-253.

**McGregor, V.R., Nutman, A.P. & Friend, C.R.L**. 1986. The Archean geology of the Godthaabsfjord region, southern West Greenland. *Lun. Planet. Inst.* Tech. Report 86-04, Pp. 113-169.

**Meisel, Thomas., Moser, Johann., Fellner, Norbert., Wegscheider, Wolfhard. & Schoenberg, Ronny**. 2001 Simplified method for the determination of Ru, Pd, Re, Os, Ir and Pt in chromites and other geological materials by isotope dilution ICP-MS and acid digestion. *The Analyst*. Vol. 126, Pp. 322-328.

**Meisel, Thomas., Walker, Richard J., Irving, Anthony J. & Lorand, Jean-Pierre**. 2001. Osmium isotopic compositions of mantle xenoliths: A global perspective. *Geochimica et Cosmochimica Acta*, Vol. 65, No. 8. Pp 1311-1323.

**Menzies, M.A. & Hawkesworth, C.J.** 1987. Upper mantle processes and composition. In: *Mantle Xenoliths*. Edited by Peter H. Nixon. John Wiley & Sons Ltd. Pp. 725-738.

**Mitchell, R.H., Scott Smith, B.H. & Larsen, L.M.** 1999. Mineralogy of ultramafic dykes from the Sarfartoq, Sisimiut and Maniitsoq areas, West Greenland. In Gurney, J.J. et al (eds): *Proceedings of the VIIth International Kimberlite Conference 2*. Pp574-583. Cape Town: Red Roof Design cc.

**Morton, L.** 1987. Italy: a review of xenolithic occurrences and their comparison with Alpine peridotites. In: *Mantle Xenoliths*. Edited by Peter H. Nixon. John Wiley & Sons Ltd. Pp. 135-148

**Myers, J.S.** 1984. The Nagssugtoqidian mobile belt of Greenland. *In Precambrian tectonics illustrated*. Edited by A. Kröner and R. Greiling. Pp. 237-250.

**Nielsen, T.F.D., Jebens, M., Jensen, S.M. & Secher, K.** 2006 Archetypal kimberlite from the Maniitsoq region, southern West Greenland and analogy to South Africa. *Geological Survey of Denmark and Greenland Bulletin*. Vol. 10, Pp. 45-48.

**Nixon, P.H.** 1987. *Mantle Xenoliths*, Published by Wiley, Chichester.

**Ohnenstetter, M.** 1992. Platinum group element enrichment in the upper mantle peridotites of the Monte Maggiore Ophiolite Massif (Corsica, France): Mineralogical evidence for ore-fluid metasomatism. *Mineralogy and Petrology*. Vol. 46, Pp. 85-107

**Patterson, Claire.** 1956. Age of meteorites and Earth. *Geochimica et Cosmochimica Act. Vol 10, No. 4, Pp. 230-237.*

**Pearson, D.G., Davies, G.R. & Nixon, P.H.** 1993. Geochemical constraints on the petrogenesis of diamond facies pyroxenites from the Beni Bousera peridotite massif, north Morocco. *Journal of Petrology*. Vol. 34, Pp. 125-172.

**Pearson, D.G., Carlson, R.W., Shirey, S.B., Boyd, F.R. & Nixon, P.H.** 1995a. Stabilisation of Archaean lithospheric mantle: A Re-Os isotope study of peridotite xenoliths from the Kaapvaal craton. *Earth and Planetary Science Letters*. 134. Pp 341-357.

**Pearson, D.G., Shirey, S.B., Carlson, R.W., Boyd, F.R., Pokhilenko, N.P. & Shimizu, N.** 1995b. Re-Os, Sm-Nd and Rb-Sr isotope evidence for thick Archean lithospheric mantle beneath the Siberian craton modified by multistage metasomatism. *Geochimica et Cosmochimica Acta*, Vol. 59, No. 5. Pp. 959-977.

**Pearson, D.G., & Woodland S.J.** 2000. Solvent extraction/anion exchange separation and determination of PGEs (Os, Ir, Pt, Pd, Ru) and Re-Os isotopes in geological samples by isotope dilution ICP-MS. *Chemical Geology* (Including isotope science), 165, Pp 87-107

**Pearson, D.G., Irvine, G.J., Carlson, R.W., Kopylova, M.G. & Ionov, D.A.** 2002. The development of lithospheric keels beneath the earliest continents: time constraints using PGE and Re-Os isotope systematics. *The Early Earth: Physical, Chemical and Biological Development*. Geological Society, London, Special Publications. Vol 199, Pp. 65-90.

**Pearson, D.G., Irvine, G.J., Ionov, D.A., Boyd, F.R. & Dreibus, G.E.** 2004. Re-Os isotope systematics and platinum group element fractionation during mantle melt extraction: a study of massif and xenolith peridotite suites. *Chemical Geology*, Vol. 208, Pp. 29-59

**Pearson, D.G., Canil, D. & Shirey, S.B.** 2004. Mantle samples included in volcanic rocks: xenoliths and diamonds. In *The Treatise on Geochemistry*. Published by Elsevier/Pergamon. Edited by Heinrich D.Holland & Karl K.Turekian. Volume 2 of 10. ISBN: 0080437516. Pp. 171-275

**Peltonen, Petri. & Brügmann**. 2006. Origin of layered continental mantle (Karelian craton, Finland): Geochemical and Re-Os isotope constraints. *Lithos*, Vol. 89, Pp. 405-423.

**Press, S., Witt, G., Seck, H.A., Ionov, D. & Kovalenko, V.I**. 1986. Spinel peridotite xenoliths from the Tariat Depression, Mongolia: Major element chemistry and mineralogy of a primitive mantle xenolith suite. *Geochimica et Cosmochimica Acta*, Vol. 50, Pp 2587-2599.

**Qi, Q.U., Taylor, Lawrence. A. & Zhou, Xinmin**. 1995. Petrology and Geochemistry of Mantle Peridotite Xenoliths from SE China. *Journal of Petrology*, Vol. 36, No. 1, Pp. 55-79.

**Rudnick, Roberta. L., McDonough, William. F. & Chappell, Bruce. W**. 1993. Carbonatite metasomatism in the northern Tanzanian mantle: petrographic and geochemical characteristics. *Earth and Planetary Science Letters*, Vol. 114, Pp. 463-475

**Sand. Kariina.Krarup**. 2007. A geotherm for the cratonic lithospheric mantle in southern West Greenland: thermal implications for diamond potential. *Masters Thesis. Geological Survey of Denmark and Greenland*. Copenhagen

**Saunders, A.D., Fitton, J.G., Kerr, A.C., Norry, M.J. & Kent, R.W**. 1997. The North Atlantic Igneous Province. *AGU. Geophysical Monograph*. Large igneous provinces: continental, oceanic and planetary flood volcanism. Vol. 100, Pp 45-93.

**Schmidberger, S.S. & Francis, D**. 1999. Nature of the mantle roots beneath the North American craton: mantle xenolith evidence from Somerset Island kimberlites. *Lithos*. 48. Pp 195-216.

**Secher, Karsten. & Jensen, Sven. Monrad**. 2004. Diamond exploration in Greenland. *Geology and Ore: Exploration and mining in Greenland. No.4 December*. GEUS: Geological Survey of Denmark and Greenland.

**Shen, JJ., Papanastassiou, D.A. & Wasserburg, G.J.** 1996. Precise Re-Os determinations and systematics of iron meteorites. *Geochimica et Cosmochimica Acta*. Vol. 60, Pp. 288-2900.

**Shirey, S.B. & Walker, R.J**. 1995. Carius tube digestions for low-blank rhenium-osmium chemistry analysis. *Anal. Chem*. vol. 67, Pp. 2136-2141.

**Shirey, Stephen B. & Walker, Richard J**. 1998. The Re-Os isotope system in cosmochemistry and high-temperature geochemistry. *Annu. Rev. Earth Planet. Sci*. Vol. 26, Pp 423-500.

**Simon, Nina, S.C., Carlson, R.W., Pearson, D.G. & Davies, G.R**. 2007. The Origin and Evolution of the Kaapvaal Cratonic Lithospheric Mantle. *Journal of Petrology*, Vol. 48, No. 3, Pp. 589-625.

**Simon, Nina, S.C.** 2004 *A petrological and geochemical study of xenoliths from the Kaapvaal craton*. PhD Thesis. Vrije Universiteit Amsterdam. Supervisors: P.A.M. Anderson., G.R. Davies & D.G. Pearson.

**Smoliar, M.L., Walker, R.J. & Morgan, J.W**. 1996. Re-Os ages of group IIA, IIIA, IVA, and IVB iron meteorites. *Science*. Vol 271. Pp. 1099-1102.

**Song, Yan. & Frey, Frederick. A**. 1989. Geochemistry of peridotite xenoliths from Hannuoba, Eastern China: Implications for subcontinental mantle heterogeneity. *Geochimica et Cosmochimica Acta*, Vol. 53. Pp. 97-113.

**Stolz, A.J. & Davies, G.R**. 1988. Chemical and isotopic evidence from spinel lherzolite xenoliths for episodic metasomatism of the upper mantle beneath southeast Australia. *Journal of Petrology Special Lithosphere* Issue. Pp. 303-330.

**Tappe, Sebastian., Jenner, George. A., Foley, Stephen. F., Heaman, Larry., Besserer, Dean., Kjarsgaard, Bruce. A. & Ryan, Bruce**. 2004. Torngat ultramafic lamprophyres and their relation to the North Atlantic Akaline Province. *Lithos* Vol. 76, Pp. 491-518.

**van Gool, Jeroen, A.M., Connelly, James. N., Marker, Morgens. & Mengel, Flemming. C**. 2002. The Nagssugtoqidian orogen of West Greenland: tectonic evolution and regional correlations from a West Greenland perspective. *Canadian Journal of Earth Sciences*. Vol. 39, Pp. 665-686.

**Vaselli, O., Downes, H., Thirlwall, M., Dobosi, G., Coradossi, N., Seghedi, I., Szakacs, A. & Vannucci, R**. 1995. Ultramafic Xenoliths in Plio-Pleistocene Alkali Basalts from the Eastern Transylvanian Basin: Depleted Mantle

Enriched by Vein Metasomatism. *Journal of Petrology*, Vol. 36, No. 1, Pp. 23-53.

**Walter, Michael J**. 1998. Melting of Garnet Peridotite and the Origin of Komatiite and Depleted Lithosphere. *Journal of Petrology*. Vol 39, Number 1, Pp 29-60.

**Westerlund, K.J., Shirey, S.B., Richardson, S.H., Carlson, R.W., Gurney, J.J. & Harris, J.W.** 2006. A subduction wedge origin for Paleoarchean peridotite diamonds and harzburgites from the Pands Kimberlite, Slave craton: evidence from Re-Os isotope systematics. *Contributions to Mineralogy and Petrology*. Vol. 152, No. 3, Pp. 275-294.

**Windley, B.F.** 1977. *The Evolving Continents*. 1st Edition. Wiley, New York. Pp. 16-19.

**Wittig, Nadine., Webb, Michelle., Pearson, D.G., Nowell, G.M., Jensen, S.M. & Sand, K.K**. 2007. Archetypal Archean lithosphere from West Greenland implicates shallow melting at ~3.0Ga. Abstract. *Goldschmidt 2007*.

**Yaxley, Gregory. M., Crawford, Anthony. J. & Green, David. H**. 1991. Evidence for carbonatite metasomatism in spinel peridotite xenoliths from Western Victoria, Australia. *Earth and Planetary Science Letters*. Vol. 107, Issue 2, Pp 305-317.

# Appendices

# Appendices


**WESTREN GREENLAND DATA**

Appendix A – Rock samples

A (I) *Western Greenland Rock sample list* ..... 87

Appendix B – Major Element Data

(I) *Western Greenland Peridotite suite* ..... 88
(II) *Western Greenland Peridotite ratios* ..... 89
B (III) *Western Greenland Peridotite Trace Elements* ..... 90
(IV) *Western Greenland UML suite* ..... 91
(V) *Western Greenland UML Trace Elements* ..... 92

Appendix C – Platinum Group Element Data

(I) *Western Greenland PGE ppb data* ..... 93
C (II) *Western Greenland PGE ratios & Ages* ..... 94

**CRATONIC DATA-OTHER PERIDOTITE SUITES**

Appendix D – Major Element Data

(I) *Kaapvaal Peridotite suite* ..... 95
(II) *Canadian Peridotite suite* ..... 99
(III) *Tanzanian Peridotite suite* ..... 101
D (IV) *Siberian Peridotite suite* ..... 103
(V) *East Greenland Peridotite suite* ..... 105
(VI) *West Australian Peridotite suite* ..... 107

**NON-CRATONIC DATA – NON EUROPEAN**

Appendix E – Major Element Data

(I) *African Peridotite suite* ..... 108
(II) *Australian Peridotite suite* ..... 110
(III) *Mongolian Peridotite suite* ..... 112
E (IV) *Chinese Peridotite suite* ..... 113
(V) *Beni Bousera Peridotite suite* ..... 114
(VI) *Vitim* ..... 115

**NON-CRATONIC DATA- EUROPEAN**

Appendix F – Major Element Data

(I) *Hungarian Peridotite suite* ..... 116
(II) *Romanian Peridotite suite* ..... 117
F (III) *Italian Peridotite suite* ..... 118
(IV) *British Peridotite suite* ..... 119

**PGE DATA- OTHER PERIDOTITE SUITES**

Appendix G – Platinum Group Element Data

(I) *Kaapvaal PGE ppb data* ..... 120
(II) *Beni Bousera ppb data* ..... 121
(III) *Vitim ppb data* ..... 122
G (IV) *Slave & Namibia ppb data* ..... 123
(V) *Lesotho ppb data* ..... 124
(VI) *Somerset Island ppb data* ..... 125

# Appendix A

## Western Greenland
## Rock Samples

## Appendix A (I)

### Western Greenland peridotite xenolith sample descriptions

| GEUS No. | Field number | Sample description | Grid Reference | Comments | Date |
|---|---|---|---|---|---|
| 474521 | L4a | Large lherzolite xenolith in float | N66° 44' 38.2/W51° 09' 65.6. | Hyperbyssal kimberlite with xenolith and ilmenite. a) harz xeno. b) lherz xeno. N66o 44' 52.8/51o 09' 89.0 = "sill" xenoliths. | 19/07/2004 |
| 474527 | L6a | very large (>10 kg) garnet/lherz xen, "sheared" high T? from Naroii dyke of Diamet | N66° 44' 45.1/W51° 10' 59.0 | none | 19/07/2004 |
| 474535 | P1 | 2 fragments of very large (25 kg) garnet lz xenolith | N66° 21' 10.7/W51° 27' 47.6 | none | 13/07/2004 |
| 474536 | P2 | spinel/chromite lherz large 30 15 x 10 cm | N66° 21' 10.7/W51° 27' 47.6 | none | 14/07/2004 |
| 474538 | P4 | fist-sized garnet lherzolite | N66° 21' 10.7/W51° 27' 47.6 | none | 15/07/2004 |
| 474544 | P10 | fist sized garnet-harz/lherz abundant garnet | N66° 21' 10.7/W51° 27' 47.6 | none | 16/07/2004 |
| 474545 | P11 | large 15 x 10 cm garnet harz | N66° 21' 10.7/W51° 27' 47.6 | none | 17/07/2004 |
| 474546 | P12 | garnet harz fist sized | N66° 21' 10.7/W51° 27' 47.6 | none | 18/07/2004 |
| 474547 | P13 | garnet harz fist sized | N66° 21' 10.7/W51° 27' 47.6 | none | 19/07/2004 |
| 474551 | P17 | garnet, lz, scarce garnet | N66° 21' 10.7/W51° 27' 47.6 | none | 20/07/2004 |
| 474555 | L1a | large garnet lherz- 3 fragments | ? | none | 20/07/2004 |
| 474557 | L1c | fist sized peridotite xenolith | ? | none | 21/07/2004 |
| 474566 | P-dyke | none | ? | none | 23/07/2004 |
| 474568 | Hardy 1 | Xenolith | N66° 23' 17.9/W50° 42' 52.1 | none | 15/07/2004 |
| 474570 | Anna | none | ? | none | 15/07/2004 |
| 474573 | P18 | none | N66° 21' 10.7/W51° 27' 47.6 | none | 17/07/2004 |
| 474574 | P19 | none | N66° 21' 10.7/W51° 27' 47.6 | none | 18/07/2004 |
| 474575 | P20 | none | N66° 21' 10.7/W51° 27' 47.6 | none | 19/07/2004 |
| 474576 | P21 | none | N66° 21' 10.7/W51° 27' 47.6 | none | 20/07/2004 |
| 474577 | P-dyke 3 | Xenolith | ? | none | 15/07/2004 |
| 488836 | | 10 x 5 + 8 x 3 cm sp. Lz. In same block. Poss same sample | N66° 28' 29/W 50° 56' 49 | Ilmenite bearing kimberlite (26) the rest are xenoliths. Some with garnet. Strong serpentinisation in most nodules have lead to black colour - very difficult to see garnet or cpx. 2 samples with chromite and garnet to take back to Durham. | 14/07/2004 |
| 488850 | | 3 fragments large coarse lherz | N66° 28' 29/W 50° 56' 49 | | 14/07/2004 |
| 488858 | | 2 altered lherz in hand specimen | N66° 28' 29/W 50° 56' 49 | | 14/07/2004 |
| 488866 | | dunite loose block in granite - poss refer to carbonatite cumulate?? | | | 14/07/2004 |
| 488869 | | 5 fragments altered lherz diff samples | N66° 28' 33.5/W50° 56' 57.5 | Lower portion of main Francois dyke. Sunny and cool. 1/2 km from camp on lake edge. Good exposeures of xenoliths bearing float in broad shallow gully at small mossy lake behind prominent granite "Kopje" ~0.5 km below base of main gully. Good garnet bearing (purple) +1 chromite, dunite Lherzolite lots of ilmenite locally in kimberlite. Several locations ~5-10 m apart in small gully leading from lake (minor stream to NE). Superb blocks packed with ~70 - 90% peridotite xenoliths (N66o 28' 31/W50o 56' 57.7) Tracing of main Fancois dyke indicates continuity from upper main gully to within 50m of lake shore and then probably extends across lake - evidenced via loose blocks walking towards outcrop in gully to N. Host is altered granite. | 16/07/2004 |
| 488882 | | single 10 x 10 x 8 cm lherz xenolith | N66° 28' 33.5/W50° 56' 57.5 | | 16/07/2004 |
| 488883 | | 7 fragments of single large lherz xenoliths | N66° 28' 33.5/W50° 56' 57.5 | | 16/07/2004 |
| 488888 | | 9 x 6 chromite/lherz xenolith | N66° 28' 33.5/W50° 56' 57.5 | | 16/07/2004 |
| 488890 | | 4 lherz/dunite xenoliths | N66° 28' 33.5/W50° 56' 57.5 | | 16/07/2004 |
| 488892 | | large chromite lherz xenolith | N66° 28' 33.5/W50° 56' 57.5 | | 16/07/2004 |

# Appendix B

## Western Greenland
## Major Elements

## Appendix B (I) W.G.

Anhydrous Major element oxides Western Greenland peridotite xenolith suite (This Study)

| Sample | $Na_2O$ | MgO | $Al_2O_3$ | $SiO_2$ | CaO | $TiO_2$ | MnO | FeO* | $K_2O$ | $P_2O_5$ | Total | LOI |
|---|---|---|---|---|---|---|---|---|---|---|---|---|
| **474521** | 0.0810 | 48.3453 | 0.2778 | 42.2496 | 0.6830 | 0.1158 | 0.1088 | 7.9986 | 0.0995 | 0.0405 | 100.00 | 1.16 |
| **474527** | 0.1151 | 47.3349 | 0.7160 | 43.4986 | 0.6636 | 0.1696 | 0.1078 | 7.3190 | 0.0471 | 0.0283 | 100.00 | 1.05 |
| **474535** | 0.0346 | 47.5576 | 0.8146 | 40.7457 | 0.8469 | 0.1281 | 0.1281 | 9.6567 | 0.0542 | 0.0335 | 100.00 | 1.15 |
| **474536** | 0.0457 | 49.9355 | 0.1051 | 41.8936 | 1.1118 | 0.1463 | 0.0983 | 6.5781 | 0.0411 | 0.0446 | 100.00 | 1.14 |
| **474538** | 0.0915 | 45.6446 | 1.8103 | 42.7003 | 0.9337 | 0.2083 | 0.1327 | 8.4225 | 0.0469 | 0.0092 | 100.00 | 1.14 |
| **474544** | 0.0474 | 49.0026 | 0.2122 | 40.7831 | 0.6994 | 0.1375 | 0.1197 | 8.8855 | 0.0759 | 0.0367 | 100.00 | 1.19 |
| **474545** | 0.0812 | 47.9866 | 1.0801 | 43.6884 | 0.4130 | 0.0882 | 0.1056 | 6.4409 | 0.0754 | 0.0406 | 100.00 | 1.16 |
| **474546** | 0.0352 | 48.6110 | 0.9000 | 42.9755 | 0.3059 | 0.0293 | 0.0996 | 6.9687 | 0.0492 | 0.0258 | 100.00 | 1.17 |
| **474547** | 0.0707 | 48.9456 | 0.5088 | 42.3244 | 0.9551 | 0.0978 | 0.0848 | 6.9528 | 0.0318 | 0.0283 | 100.00 | 1.18 |
| **474551** | 0.0556 | 49.3954 | 0.5116 | 41.7436 | 0.5995 | 0.1112 | 0.1057 | 7.3807 | 0.0634 | 0.0334 | 100.00 | 1.11 |
| **474555** | 0.1207 | 46.1628 | 0.7058 | 43.8150 | 0.7661 | 0.1910 | 0.1153 | 8.0135 | 0.0856 | 0.0241 | 100.00 | 1.10 |
| **474557** | 0.1231 | 46.3816 | 0.5460 | 42.4546 | 2.4613 | 0.0694 | 0.1197 | 7.4987 | 0.3065 | 0.0392 | 100.00 | 1.12 |
| **474566** | 0.0807 | 48.2757 | 0.8159 | 43.4366 | 0.2478 | 0.0438 | 0.0991 | 6.9485 | 0.0426 | 0.0092 | 100.00 | 1.15 |
| **474566** | 0.0977 | 41.6183 | 1.1317 | 36.5567 | 5.9125 | 1.6774 | 0.1892 | 11.8850 | 0.6470 | 0.2845 | 100.00 | 1.22 |
| **474568** | 0.1770 | 44.6618 | 0.9836 | 43.4747 | 1.3122 | 0.2091 | 0.0852 | 9.0743 | 0.0221 | 0.0000 | 100.00 | 1.11 |
| **474568** | 0.1127 | 44.3436 | 1.3034 | 43.6406 | 1.2753 | 0.1769 | 0.0856 | 9.0079 | 0.0315 | 0.0225 | 100.00 | 1.13 |
| **474570** | 0.0813 | 47.5095 | 0.0945 | 40.8202 | 0.3730 | 0.0681 | 0.1260 | 10.8693 | 0.0559 | 0.0020 | 100.00 | 1.02 |
| **474573** | 0.0580 | 47.6211 | 1.0079 | 40.8827 | 0.8385 | 0.1264 | 0.1345 | 9.2520 | 0.0510 | 0.0278 | 100.00 | 1.16 |
| **474574** | 0.0578 | 48.7545 | 0.6524 | 43.1054 | 0.4765 | 0.1492 | 0.0948 | 6.6422 | 0.0312 | 0.0359 | 100.00 | 1.16 |
| **474575** | 0.0917 | 46.3292 | 1.5607 | 42.8054 | 0.5699 | 0.1273 | 0.1101 | 8.3208 | 0.0527 | 0.0321 | 100.00 | 1.15 |
| **474576** | 0.0679 | 48.2362 | 0.1154 | 40.4598 | 0.4481 | 0.1697 | 0.1075 | 10.3319 | 0.0272 | 0.0362 | 100.00 | 1.13 |
| **474577** | 0.0793 | 45.0835 | 1.0156 | 45.1786 | 0.9420 | 0.0759 | 0.1200 | 7.4235 | 0.0510 | 0.0306 | 100.00 | 1.13 |
| **488836** | 0.0233 | 48.2509 | 0.1989 | 40.5321 | 1.0469 | 0.1663 | 0.1466 | 9.4769 | 0.0942 | 0.0640 | 100.00 | 1.16 |
| **488850** | 0.0345 | 50.9367 | 0.1413 | 41.2561 | 0.2919 | 0.0747 | 0.0988 | 7.0775 | 0.0448 | 0.0437 | 100.00 | 1.15 |
| **488858** | 0.0346 | 44.8310 | 0.2887 | 41.0381 | 0.3477 | 0.4366 | 0.1120 | 12.7865 | 0.0751 | 0.0497 | 100.00 | 1.15 |
| **488866** | 0.0109 | 43.7464 | 0.3256 | 40.4144 | 0.1172 | 0.0369 | 0.2030 | 15.1315 | 0.0033 | 0.0109 | 100.00 | 1.09 |
| **488869** | 0.0447 | 49.1236 | 0.4619 | 41.7936 | 0.5592 | 0.1163 | 0.1107 | 7.6915 | 0.0738 | 0.0246 | 100.00 | 1.12 |
| **488882** | 0.0454 | 47.1079 | 0.7027 | 43.0130 | 0.6040 | 0.1362 | 0.1090 | 8.1318 | 0.1147 | 0.0352 | 100.00 | 1.14 |
| **488883** | 0.0708 | 51.0607 | 0.0602 | 41.2955 | 0.4321 | 0.0649 | 0.1003 | 6.8683 | 0.0449 | 0.0024 | 100.00 | 1.18 |
| **488888** | 0.1035 | 48.3260 | 0.0725 | 40.7455 | 0.7396 | 0.1162 | 0.1472 | 9.6298 | 0.1012 | 0.0184 | 100.00 | 1.15 |
| **488890** | 0.0235 | 46.3023 | 0.2527 | 39.4212 | 2.3909 | 0.2069 | 0.1728 | 10.9253 | 0.1939 | 0.1105 | 100.00 | 1.18 |
| **488892** | 0.1145 | 49.0545 | 0.4158 | 40.7532 | 0.5304 | 0.1753 | 0.1168 | 8.7719 | 0.0607 | 0.0069 | 100.00 | 1.15 |
| **PM** | 0.3600 | 37.8000 | 4.4500 | 45.0000 | 3.5500 | 0.2000 | 0.1350 | 8.0500 | 0.0290 | 0.0210 | 99.60 | |

FeO* : Total Fe given as FeO*. Corrected for LOI. Analyses were performed by X.R.F. at Geological Survey of Denmark (GEUS). Oxides in wt%.
PM: Primitive Mantle (McDonough and Sun, 1995).

## Appendix B (II) W.Greenland

Major element oxide ratios Western Greenland peridotite xenolith suite (This Study)

| SAMPLE | MgO/SiO2 | Al/Si | Ca/Al | Mg/Si | Ca/Si | Mg# |
|---|---|---|---|---|---|---|
| **474521** | 1.144278 | 0.007444 | 3.319737 | 1.476424 | 0.024712 | 91.5 |
| **474527** | 1.088194 | 0.018634 | 1.251688 | 1.404062 | 0.023324 | 92.0 |
| **474535** | 1.167181 | 0.022632 | 1.403959 | 1.505976 | 0.031775 | 89.8 |
| **474536** | 1.191959 | 0.002841 | 14.281964 | 1.537946 | 0.040571 | 93.1 |
| **474538** | 1.068952 | 0.047994 | 0.696541 | 1.379233 | 0.033430 | 90.6 |
| **474544** | 1.201540 | 0.005890 | 4.451044 | 1.550308 | 0.026216 | 90.8 |
| **474545** | 1.098383 | 0.027987 | 0.516373 | 1.417208 | 0.014452 | 93.0 |
| **474546** | 1.131132 | 0.023708 | 0.458926 | 1.459463 | 0.010880 | 92.6 |
| **474547** | 1.156440 | 0.013609 | 2.535129 | 1.492117 | 0.034500 | 92.6 |
| **474551** | 1.183305 | 0.013875 | 1.582318 | 1.526780 | 0.021954 | 92.3 |
| **474555** | 1.053585 | 0.018236 | 1.465910 | 1.359406 | 0.026732 | 91.1 |
| **474557** | 1.092497 | 0.014559 | 6.087876 | 1.409614 | 0.088631 | 91.7 |
| **474566** | 1.111406 | 0.021265 | 0.410080 | 1.434011 | 0.008721 | 92.5 |
| **474566** | 1.138458 | 0.035047 | 7.055010 | 1.468916 | 0.247256 | 86.2 |
| **474568** | 1.027307 | 0.025613 | 1.801548 | 1.325501 | 0.046142 | 89.8 |
| **474568** | 1.016108 | 0.033812 | 1.321223 | 1.311051 | 0.044674 | 89.8 |
| **474570** | 1.163874 | 0.002622 | 5.329004 | 1.501708 | 0.013971 | 88.6 |
| **474573** | 1.164823 | 0.027909 | 1.123522 | 1.502933 | 0.031356 | 90.2 |
| **474574** | 1.131054 | 0.017133 | 0.986464 | 1.459362 | 0.016901 | 92.9 |
| **474575** | 1.082322 | 0.041275 | 0.493130 | 1.396485 | 0.020354 | 90.8 |
| **474576** | 1.192202 | 0.003230 | 5.242735 | 1.538260 | 0.016932 | 89.3 |
| **474577** | 0.997895 | 0.025449 | 1.252546 | 1.287551 | 0.031877 | 91.5 |
| **488836** | 1.190438 | 0.005555 | 7.107376 | 1.535983 | 0.039485 | 90.1 |
| **488850** | 1.234645 | 0.003879 | 2.788634 | 1.593023 | 0.010816 | 92.8 |
| **488858** | 1.092426 | 0.007965 | 1.625883 | 1.409522 | 0.012951 | 86.2 |
| **488866** | 1.082445 | 0.009121 | 0.486145 | 1.396643 | 0.004434 | 83.7 |
| **488869** | 1.175386 | 0.012512 | 1.634869 | 1.516562 | 0.020455 | 91.9 |
| **488882** | 1.095202 | 0.018496 | 1.160604 | 1.413103 | 0.021466 | 91.2 |
| **488883** | 1.236471 | 0.001651 | 9.691117 | 1.595378 | 0.015995 | 93.0 |
| **488888** | 1.186043 | 0.002013 | 13.782669 | 1.530312 | 0.027751 | 89.9 |
| **488890** | 1.174553 | 0.007258 | 12.775426 | 1.515488 | 0.092719 | 88.3 |
| **488892** | 1.203699 | 0.011551 | 1.722413 | 1.553094 | 0.019895 | 90.9 |

Analyses were performed by X.R.F. at Geological Survey of Denmark (GEUS). Oxides in wt%.

## Appendix B (III) W. Greenland

Trace elements Western Greenland peridotite xenolith suite (This Study)

| Sample | Ba | Rb | Nb | La | Ce | Sr | Zr | Y | V | Cr | Ni | Cu | Zn | Mo | Sn |
|---|---|---|---|---|---|---|---|---|---|---|---|---|---|---|---|
| **474521** | 38 | 0 | 7 | 18 | 0 | 97 | 0 | 0 | 53 | 1360 | 2286 | 9 | 49 | 0 | 0 |
| **474527** | 8 | 0 | 0 | 29 | 0 | 68 | 0 | 0 | 48 | 2269 | 2318 | 19 | 53 | 0 | 0 |
| **474535** | 97 | 0 | 0 | 51 | 0 | 73 | 0 | 0 | 43 | 2029 | 2556 | 13 | 56 | 0 | 0 |
| **474536** | 52 | 0 | 1 | 24 | 0 | 85 | 0 | 0 | 35 | 2403 | 2534 | 6 | 41 | 0 | 0 |
| **474538** | 0 | 0 | 0 | 47 | 0 | 84 | 0 | 0 | 40 | 2073 | 2211 | 12 | 48 | 0 | 0 |
| **474544** | 72 | 0 | 9 | 0 | 0 | 89 | 0 | 0 | 34 | 1786 | 2444 | 12 | 34 | 0 | 0 |
| **474545** | 55 | 0 | 0 | 0 | 0 | 62 | 0 | 0 | 46 | 3018 | 2145 | 3 | 38 | 0 | 0 |
| **474546** | 61 | 0 | 7 | 0 | 0 | 60 | 0 | 0 | 30 | 1980 | 2438 | 7 | 26 | 0 | 0 |
| **474547** | 49 | 0 | 0 | 0 | 0 | 124 | 0 | 0 | 37 | 1993 | 2427 | 6 | 38 | 0 | 0 |
| **474551** | 74 | 0 | 2 | 0 | 0 | 84 | 0 | 0 | 55 | 4118 | 2537 | 11 | 47 | 0 | 0 |
| **474555** | 84 | 0 | 9 | 0 | 0 | 82 | 0 | 0 | 54 | 1970 | 2425 | 12 | 37 | 0 | 0 |
| **474557** | 42 | 8 | 6 | 0 | 0 | 117 | 5 | 0 | 81 | 3420 | 2306 | 14 | 37 | 0 | 0 |
| **474566** | 0 | 0 | 0 | 79 | 0 | 69 | 0 | 0 | 13 | 2003 | 2361 | 19 | 37 | 0 | 0 |
| **474566** | 359 | 9 | 88 | 84 | 100 | 456 | 66 | 0 | 94 | 1693 | 1515 | 36 | 74 | 0 | 0 |
| **474568** | 0 | 0 | 0 | 90 | 0 | 67 | 0 | 0 | 33 | 2321 | 2233 | 16 | 40 | 0 | 0 |
| **474568** | 23 | 0 | 0 | 0 | 0 | 72 | 0 | 0 | 68 | 3018 | 2225 | 9 | 44 | 0 | 0 |
| **474570** | 0 | 0 | 0 | 108 | 0 | 98 | 0 | 0 | 16 | 485 | 2765 | 12 | 76 | 0 | 0 |
| **474573** | 0 | 0 | 0 | 2 | 0 | 61 | 0 | 0 | 48 | 2641 | 2460 | 13 | 55 | 0 | 0 |
| **474574** | 14 | 0 | 0 | 27 | 0 | 56 | 0 | 0 | 39 | 2071 | 2196 | 7 | 38 | 0 | 0 |
| **474575** | 19 | 0 | 2 | 40 | 0 | 68 | 0 | 0 | 54 | 1731 | 2147 | 18 | 55 | 0 | 0 |
| **474576** | 30 | 0 | 5 | 19 | 0 | 93 | 0 | 0 | 42 | 393 | 2302 | 7 | 70 | 0 | 0 |
| **474577** | 7 | 0 | 5 | 5 | 0 | 75 | 0 | 0 | 47 | 3053 | 2150 | 11 | 28 | 0 | 0 |
| **488836** | 112 | 0 | 14 | 0 | 0 | 134 | 0 | 0 | 29 | 1048 | 2445 | 14 | 37 | 0 | 0 |
| **488850** | 23 | 0 | 6 | 0 | 0 | 72 | 0 | 0 | 24 | 1136 | 2494 | 9 | 26 | 0 | 0 |
| **488858** | 24 | 2 | 13 | 58 | 0 | 79 | 0 | 0 | 42 | 394 | 1851 | 38 | 61 | 0 | 0 |
| **488866** | 8 | 3 | 12 | 7 | 0 | 68 | 4 | 0 | 41 | 4995 | 2059 | 6 | 119 | 0 | 0 |
| **488869** | 32 | 0 | 5 | 0 | 0 | 71 | 0 | 0 | 31 | 2402 | 2519 | 11 | 34 | 0 | 0 |
| **488882** | 134 | 0 | 7 | 0 | 0 | 76 | 0 | 0 | 46 | 2602 | 2267 | 15 | 35 | 0 | 0 |
| **488883** | 0 | 0 | 0 | 64 | 0 | 80 | 0 | 0 | 12 | 1472 | 2505 | 7 | 36 | 0 | 0 |
| **488888** | 40 | 0 | 0 | 79 | 0 | 105 | 0 | 0 | 31 | 1412 | 2206 | 9 | 58 | 0 | 0 |
| **488890** | 177 | 8 | 20 | 26 | 0 | 236 | 20 | 0 | 59 | 1758 | 2005 | 21 | 58 | 0 | 0 |
| **488892** | 0 | 0 | 0 | 69 | 0 | 87 | 0 | 0 | 22 | 3800 | 2539 | 9 | 48 | 0 | 0 |

Analyses were performed by X.R.F. at Geological Survey of Denmark (GEUS). Elements in pp

## Appendix B (IV) UML

Major element anhydrous oxides Western Greenland UML suite (Holgate, 2005).

| Sample | $Na_2O$ | MgO | $Al_2O_3$ | $SiO_2$ | CaO | $TiO_2$ | MnO | FeO* | $K_2O$ | $P_2O_5$ | Total |
|---|---|---|---|---|---|---|---|---|---|---|---|
| **474514** | 0.128 | 29.084 | 3.017 | 33.789 | 15.113 | 2.646 | 0.234 | 13.506 | 1.898 | 0.585 | 100.000 |
| **474515** | 0.141 | 28.207 | 3.146 | 33.649 | 13.970 | 3.225 | 0.260 | 14.646 | 1.830 | 0.926 | 100.000 |
| **474516** | 0.083 | 26.754 | 2.960 | 32.384 | 18.042 | 2.773 | 0.271 | 13.532 | 1.926 | 1.275 | 100.000 |
| **474517** | 0.072 | 42.217 | 1.409 | 36.125 | 3.198 | 3.321 | 0.200 | 12.532 | 0.834 | 0.092 | 100.000 |
| **474560** | 0.060 | 38.795 | 1.028 | 34.019 | 9.509 | 2.160 | 0.239 | 12.849 | 0.819 | 0.520 | 100.000 |
| **483838** | 0.113 | 39.498 | 1.690 | 32.784 | 10.897 | 2.851 | 0.195 | 10.909 | 0.719 | 0.343 | 100.000 |
| **483840** | 0.071 | 38.975 | 1.943 | 35.067 | 8.474 | 3.114 | 0.219 | 11.390 | 0.427 | 0.320 | 100.000 |
| **483842** | 0.132 | 39.878 | 1.880 | 30.304 | 11.995 | 3.145 | 0.219 | 11.471 | 0.586 | 0.390 | 100.000 |
| **483843** | 0.094 | 38.908 | 3.203 | 28.784 | 8.737 | 4.917 | 0.268 | 14.262 | 0.629 | 0.200 | 100.000 |
| **483844** | 0.158 | 40.085 | 1.835 | 32.332 | 10.303 | 2.757 | 0.200 | 10.909 | 1.049 | 0.371 | 100.000 |
| **483845** | 0.070 | 44.066 | 0.669 | 35.398 | 5.699 | 2.555 | 0.172 | 10.934 | 0.120 | 0.317 | 100.000 |
| **483847** | 0.103 | 46.639 | 0.966 | 33.635 | 4.789 | 2.279 | 0.190 | 11.094 | 0.250 | 0.055 | 100.000 |
| **483848** | 0.224 | 40.966 | 1.363 | 28.879 | 13.830 | 2.385 | 0.220 | 10.938 | 0.113 | 1.081 | 100.000 |
| **483849** | 0.076 | 40.014 | 2.197 | 30.128 | 8.736 | 4.027 | 0.269 | 13.431 | 0.682 | 0.440 | 100.000 |
| **483850** | 0.120 | 39.072 | 1.656 | 30.043 | 14.059 | 2.801 | 0.213 | 11.108 | 0.604 | 0.324 | 100.000 |
| **483857** | 0.140 | 41.824 | 1.719 | 31.164 | 8.823 | 3.275 | 0.229 | 12.265 | 0.116 | 0.445 | 100.000 |
| **483860** | 0.118 | 41.426 | 1.356 | 31.627 | 8.740 | 2.779 | 0.211 | 12.237 | 0.599 | 0.907 | 100.000 |
| **483861** | 0.071 | 39.952 | 1.284 | 31.617 | 13.462 | 2.229 | 0.185 | 10.465 | 0.205 | 0.530 | 100.000 |
| **483862** | 0.197 | 34.709 | 1.734 | 21.927 | 23.328 | 4.854 | 0.244 | 12.481 | 0.062 | 0.465 | 100.000 |
| **483863** | 0.079 | 43.567 | 1.525 | 32.701 | 6.219 | 3.580 | 0.212 | 11.922 | 0.112 | 0.083 | 100.000 |
| **483864** | 0.103 | 38.433 | 1.869 | 29.715 | 7.898 | 7.265 | 0.227 | 13.519 | 0.570 | 0.401 | 100.000 |
| **488810** | 0.084 | 36.986 | 1.559 | 32.093 | 12.342 | 2.471 | 0.226 | 12.597 | 0.994 | 0.648 | 100.000 |
| **488822** | 0.099 | 31.832 | 2.411 | 30.888 | 17.376 | 2.620 | 0.213 | 11.917 | 1.573 | 1.071 | 100.000 |
| **488823** | 0.097 | 36.230 | 1.847 | 32.532 | 11.801 | 2.583 | 0.241 | 12.667 | 1.277 | 0.724 | 100.000 |
| **488825** | 0.074 | 33.130 | 1.858 | 31.834 | 16.549 | 2.295 | 0.194 | 11.781 | 1.263 | 1.021 | 100.000 |

FeO* : Total Fe given as FeO*. Corrected for LOI. Analyses were performed by X.R.F. at Geological Survey of Denmark (GEUS). Oxides in wt%.

## Appendix B (V) UML

Trace elements Western Greenland UML suite (Holgate, 2005))

| Sample | V | Cr | Ni | Cu | Zn | Rb | Sr | Y | Zr | Nb | Mo | Sn | Ba | La | Ce |
|---|---|---|---|---|---|---|---|---|---|---|---|---|---|---|---|
| **474514** | 214 | 1527 | 878 | 134 | 111 | 82 | 1062 | 28 | 198 | 109 | 0 | 0 | 805 | 77 | 119 |
| **474515** | 221 | 1687 | 752 | 123 | 107 | 79 | 833 | 38 | 412 | 124 | 0 | 0 | 712 | 149 | 134 |
| **474516** | 237 | 1358 | 706 | 120 | 103 | 91 | 1076 | 43 | 408 | 131 | 0 | 0 | 712 | 175 | 156 |
| **474517** | 102 | 1488 | 1431 | 72 | 77 | 23 | 267 | 0 | 53 | 130 | 0 | 0 | 527 | 94 | 89 |
| **474560** | 166 | 2345 | 1289 | 48 | 94 | 27 | 910 | 0 | 75 | 115 | 0 | 0 | 548 | 116 | 109 |
| **483838** | 160 | 1591 | 1399 | 110 | 72 | 0 | 695 | 0 | 95 | 155 | 0 | 0 | 1042 | 270 | 100 |
| **483840** | 144 | 1531 | 1381 | 122 | 69 | 0 | 477 | 0 | 104 | 170 | 0 | 0 | 1090 | 157 | 106 |
| **483842** | 166 | 1721 | 1235 | 99 | 71 | 0 | 1065 | 0 | 143 | 179 | 0 | 0 | 1927 | 246 | 107 |
| **483843** | 217 | 2232 | 1166 | 234 | 89 | 14 | 722 | 11 | 272 | 278 | 0 | 0 | 1984 | 312 | 305 |
| **483844** | 128 | 1402 | 1255 | 105 | 65 | 23 | 923 | 0 | 95 | 177 | 0 | 0 | 1709 | 222 | 91 |
| **483845** | 119 | 1528 | 1699 | 52 | 47 | 0 | 621 | 0 | 56 | 128 | 0 | 0 | 817 | 174 | 31 |
| **483847** | 111 | 1431 | 1564 | 83 | 56 | 0 | 572 | 0 | 104 | 117 | 0 | 0 | 842 | 133 | 56 |
| **483848** | 125 | 1485 | 1232 | 82 | 67 | 0 | 1620 | 0 | 138 | 232 | 0 | 0 | 2506 | 286 | 268 |
| **483849** | 163 | 1816 | 1132 | 103 | 63 | 9 | 1459 | 0 | 153 | 220 | 0 | 0 | 1447 | 236 | 138 |
| **483850** | 149 | 1399 | 1209 | 90 | 69 | 1 | 915 | 0 | 130 | 112 | 0 | 0 | 1239 | 169 | 77 |
| **483857** | 158 | 1485 | 1262 | 103 | 75 | 0 | 989 | 0 | 168 | 208 | 0 | 0 | 1591 | 238 | 217 |
| **483860** | 132 | 1186 | 1216 | 85 | 72 | 0 | 906 | 0 | 169 | 208 | 0 | 0 | 1688 | 212 | 81 |
| **483861** | 118 | 1282 | 1448 | 53 | 66 | 0 | 868 | 0 | 100 | 120 | 0 | 0 | 921 | 232 | 93 |
| **483862** | 235 | 1051 | 530 | 55 | 73 | 0 | 1882 | 29 | 212 | 240 | 0 | 0 | 1252 | 320 | 280 |
| **483863** | 174 | 1348 | 1399 | 103 | 66 | 0 | 525 | 0 | 79 | 97 | 0 | 0 | 969 | 219 | 56 |
| **483864** | 269 | 1721 | 1287 | 106 | 78 | 1 | 897 | 13 | 172 | 287 | 0 | 0 | 1119 | 311 | 214 |
| **488810** | 142 | 1586 | 1164 | 51 | 89 | 41 | 1105 | 7 | 124 | 149 | 0 | 0 | 770 | 142 | 176 |
| **488822** | 144 | 1435 | 937 | 88 | 88 | 68 | 1298 | 20 | 148 | 156 | 0 | 0 | 1158 | 173 | 207 |
| **488823** | 178 | 1700 | 1168 | 84 | 90 | 53 | 975 | 9 | 113 | 141 | 0 | 0 | 925 | 153 | 177 |
| **488825** | 147 | 1337 | 1017 | 87 | 85 | 50 | 1181 | 10 | 223 | 127 | 0 | 0 | 631 | 100 | 148 |

Analyses were performed by X.R.F. at Geological Survey of Denmark (GEUS). Elements in ppm..

# Appendix C

# Western Greenland
# Platinum Group Elements

## Appendix C (I) W. Greenland

PGE element concentrations for Western Greenland peridotite xenolith suite

| | Measured | | | | | | Chondrite normalised | | | | | |
|---|---|---|---|---|---|---|---|---|---|---|---|---|
| **Samp No.** | **Os (ppb)** | **Ir (ppb)** | **Ru (ppb)** | **Pt (ppb)** | **Pd (ppb)** | **Re (ppb)** | **Os (ppb)** | **Ir (ppb)** | **Ru (ppb)** | **Pt (ppb)** | **Pd (ppb)** | **Re (ppb)** |
| **474521** | 1.0446 | 1.1398 | 1.4909 | 0.6002 | 0.1820 | 0.1518 | 0.0021 | 0.0025 | 0.0021 | 0.0006 | 0.0003 | 0.0040 |
| **474527** | 4.2898 | 4.0602 | 7.9618 | 3.1621 | 1.7298 | 0.0742 | 0.0088 | 0.0088 | 0.0112 | 0.0032 | 0.0031 | 0.0020 |
| **474535** | 0.8640 | 0.6564 | 2.3405 | 0.5940 | 1.4415 | 0.0313 | 0.0018 | 0.0014 | 0.0033 | 0.0006 | 0.0026 | 0.0008 |
| **474538** | 2.8579 | 3.0480 | 5.8000 | 0.5120 | 0.1770 | 0.1198 | 0.0059 | 0.0066 | 0.0081 | 0.0005 | 0.0003 | 0.0032 |
| **474544** | 1.2550 | 1.0395 | 33.4081 | 1.0807 | 0.5047 | 0.0494 | 0.0026 | 0.0023 | 0.0468 | 0.0011 | 0.0009 | 0.0013 |
| **474545** | 2.8770 | 2.6408 | 3.7921 | 0.0359 | 0.0211 | 0.0183 | 0.0059 | 0.0058 | 0.0053 | 0.0000 | 0.0000 | 0.0005 |
| **474546** | 3.0600 | 3.1569 | 6.0698 | 0.3601 | 0.0070 | 0.0199 | 0.0063 | 0.0069 | 0.0085 | 0.0004 | 0.0000 | 0.0005 |
| **474547** | 5.0238 | 3.8176 | 1.6366 | 4.1146 | 0.0209 | 0.0557 | 0.0103 | 0.0083 | 0.0023 | 0.0041 | 0.0000 | 0.0015 |
| **474551** | 0.9638 | 0.7992 | 1.2304 | 0.0345 | 0.0464 | 0.0354 | 0.0020 | 0.0017 | 0.0017 | 0.0000 | 0.0001 | 0.0009 |
| **474555** | 2.6719 | 3.2265 | 4.8334 | 1.7155 | 0.4468 | 0.1101 | 0.0055 | 0.0070 | 0.0068 | 0.0017 | 0.0008 | 0.0029 |
| **474557** | 0.8925 | 0.8015 | 2.2639 | 0.2703 | 0.0708 | 0.2896 | 0.0018 | 0.0017 | 0.0032 | 0.0003 | 0.0001 | 0.0076 |
| **474568** | 4.1940 | 3.8480 | 7.5259 | 38.7340 | 2.7005 | 0.0689 | 0.0086 | 0.0084 | 0.0105 | 0.0390 | 0.0049 | 0.0018 |
| **474570** | 2.4190 | 2.2570 | 4.3958 | 6.0460 | 4.6462 | 0.0384 | 0.0050 | 0.0049 | 0.0062 | 0.0061 | 0.0084 | 0.0010 |
| **474576** | 0.9611 | 0.9809 | 1.1797 | 0.0745 | 0.0125 | 0.0444 | 0.0020 | 0.0021 | 0.0017 | 0.0001 | 0.0000 | 0.0012 |
| **474577** | 1.9499 | 2.7007 | 8.1162 | 2.7771 | 0.3588 | 0.0440 | 0.0040 | 0.0059 | 0.0114 | 0.0028 | 0.0006 | 0.0012 |
| **488836** | 3.1087 | 5.4371 | 2.7410 | 0.8810 | 0.4213 | 0.1353 | 0.0064 | 0.0118 | 0.0038 | 0.0009 | 0.0008 | 0.0036 |
| **488850** | 1.6502 | 2.3422 | 4.2211 | 0.4672 | 0.0559 | 0.0507 | 0.0034 | 0.0051 | 0.0059 | 0.0005 | 0.0001 | 0.0013 |
| **488858** | 0.8902 | 0.8497 | 1.5064 | 1.5336 | 2.4896 | 0.1630 | 0.0018 | 0.0019 | 0.0021 | 0.0015 | 0.0045 | 0.0043 |
| **488866** | 1.4795 | 1.3758 | Neg No. | 0.4827 | 0.2945 | 0.0085 | 0.0030 | 0.0030 | Neg No. | 0.0005 | 0.0005 | 0.0002 |
| **488869** | 2.3519 | 2.4773 | 2.6577 | 0.8340 | 0.3148 | 0.0353 | 0.0048 | 0.0054 | 0.0037 | 0.0008 | 0.0006 | 0.0009 |
| **488882** | 21000.6870 | 2.7628 | 5.7303 | 1.0724 | 0.3989 | 1.5884 | 43.2113 | 0.0060 | 0.0080 | 0.0011 | 0.0007 | 0.0418 |
| **488883** | 1.7609 | 1.9270 | 0.2914 | 0.3457 | 0.2009 | 0.0773 | 0.0036 | 0.0042 | 0.0004 | 0.0003 | 0.0004 | 0.0020 |
| **488890** | 0.0466 | 0.8042 | 4.2792 | 0.3674 | 0.8740 | 0.0615 | 0.0001 | 0.0018 | 0.0060 | 0.0004 | 0.0016 | 0.0016 |
| **488892** | 3.9073 | 2.8700 | 9.9970 | 1.3978 | 0.4706 | 0.0241 | 0.0080 | 0.0063 | 0.0140 | 0.0014 | 0.0008 | 0.0006 |

Chondrite normalised = measured value / value for chondrite PGE elements

## Appendix C (II) W.Greenland PGE

PGE for Western Greenland peridotite xenolith suite

| | | | | | | | Myr | | | Gyr | | |
|---|---|---|---|---|---|---|---|---|---|---|---|---|
| Samp No. | $^{187}Os/^{188}Os$ | $^{187}Re/^{188}Os$ | (Pd/Ir)*n* (ppb) | (Re/Ir)*n* (ppb) | γOs | Mg# | $T_{RD}$ | $T_{RD\ Erup}$ | $T_{MA}$ | $T_{RD}$ | $T_{RD\ Erup}$ | $T_{MA}$ |
| **474521** | 0.113990 | 0.698598 | 0.15968 | 1.60869 | -13 | 91.5 | 2046 | 2998 | 3308 | 2.0 | 3.0 | 3.3 |
| **474527** | 0.112733 | 0.083137 | 0.42604 | 0.22074 | -9 | 92.0 | 2217 | 2331 | 2745 | 2.2 | 2.3 | 2.7 |
| **474535** | 0.1247802 | 0.174639 | 2.19591 | 0.57672 | -0.4 | 89.8 | 552 | 797 | 935 | 0.6 | 0.8 | 0.9 |
| **474538** | 0.108576 | 0.201371 | 0.05807 | 0.47476 | -14 | 90.6 | 2781 | 3054 | 5188 | 2.8 | 3.1 | 5.2 |
| **474544** | 0.112842 | 0.189326 | 0.48555 | 0.57440 | -10 | 90.8 | 2202 | 2461 | 3920 | 2.2 | 2.5 | 3.9 |
| **474545** | 0.108017 | 0.030574 | 0.00800 | 0.08376 | -13 | 93.0 | 2857 | 2898 | 3073 | 2.9 | 2.9 | 3.1 |
| **474546** | 0.1084369 | 0.031298 | 0.00223 | 0.07628 | -13 | 92.6 | 2800 | 2843 | 3018 | 2.8 | 2.8 | 3.0 |
| **474547** | 0.1097824 | 0.053281 | 0.00546 | 0.17628 | -12 | 92.6 | 2618 | 2691 | 2985 | 2.6 | 2.7 | 3.0 |
| **474551** | 0.1078785 | 0.176611 | 0.05809 | 0.53562 | -14 | 92.3 | 2876 | 3114 | 4845 | 2.9 | 3.1 | 4.8 |
| **474555** | 0.115726 | 0.198114 | 0.13848 | 0.41214 | -8 | 91.1 | 1808 | 2080 | 3348 | 1.8 | 2.1 | 3.3 |
| **474557** | 0.118250 | 1.560720 | 0.08833 | 4.36440 | -17 | 91.7 | 1460 | 3587 | -555 | 1.5 | 3.6 | -0.6 |
| **474568** | 0.110947 | 0.078943 | 0.70179 | 0.21628 | -11 | 89.8 | 2460 | 2568 | 3009 | 2.5 | 2.6 | 3.0 |
| **474570** | 0.119720 | 0.076368 | 2.05857 | 0.20551 | -4 | 88.6 | 1257 | 1363 | 1530 | 1.3 | 1.4 | 1.5 |
| **474576** | 0.107816 | 0.221675 | 0.01278 | 0.54620 | -15 | 89.3 | 2884 | 3183 | 5888 | 2.9 | 3.2 | 5.9 |
| **474577** | 0.116342 | 0.108460 | 0.13285 | 0.19670 | -7 | 91.5 | 1723 | 1873 | 2304 | 1.7 | 1.9 | 2.3 |
| **488836** | 0.110469 | 0.209116 | 0.07749 | 0.30056 | -12 | 90.1 | 2525 | 2809 | 4881 | 2.5 | 2.8 | 4.9 |
| **488850** | 0.106755 | 0.147663 | 0.02385 | 0.26166 | -15 | 92.8 | 3027 | 3226 | 4582 | 3.0 | 3.2 | 4.6 |
| **488858** | 0.120077 | 0.880974 | 2.92998 | 2.31713 | -10 | 86.2 | 1208 | 2422 | -1144 | 1.2 | 2.4 | -1.1 |
| **488866** | 0.1133116 | 0.027742 | 0.21406 | 0.07497 | -9 | 83.7 | 2138 | 2176 | 2285 | 2.1 | 2.2 | 2.3 |
| **488869** | 0.110217 | 0.072137 | 0.12707 | 0.17217 | -11 | 91.9 | 2559 | 2658 | 3070 | 2.6 | 2.7 | 3.1 |
| **488882** | 0.1139149 | 0.000364 | 0.14440 | 6.94441 | -8 | 91.2 | 2056 | 2056 | 2058 | 2.1 | 2.1 | 2.1 |
| **488883** | 0.108130 | 0.210863 | 0.10426 | 0.48454 | -14 | 93.0 | 2842 | 3127 | 5523 | 2.8 | 3.1 | 5.5 |
| **488890** | 0.1250400 | | 1.08672 | 0.92330 | | | | | | | | |
| **488892** | 0.108240 | 0.029567 | 0.16397 | 0.10122 | -13 | 90.9 | 2827 | 2867 | 3033 | 2.8 | 2.9 | 3.0 |

Chondrite normalised = measured value / value for chondrite PGE elements

## Appendix D (I) Kaapvaal

Major element oxides Kaapvaal cratonic peridotite xenolith suite

| Sample | $Na_2O$ | MgO | $Al_2O_3$ | $SiO_2$ | CaO | $TiO_2$ | MnO | FeO* | Total | Ref |
|---|---|---|---|---|---|---|---|---|---|---|
| **FRB 135** | 0.0617 | 43.9400 | 1.5331 | 47.5069 | 0.5762 | 0.0103 | 0.1132 | 5.9100 | 99.65 | † |
| **FRB 492** | 0.2058 | 43.7600 | 1.6467 | 46.9512 | 0.7925 | 0.0000 | 0.1235 | 6.0900 | 99.57 | † |
| **FRB 983** | 0.1044 | 46.1600 | 1.1797 | 44.9427 | 0.4593 | 0.0626 | 0.1148 | 6.5100 | 99.53 | † |
| **FRB 999** | 0.1263 | 45.2600 | 0.9897 | 45.3576 | 0.7160 | 0.1158 | 0.1263 | 6.8500 | 99.54 | † |
| **FRB 1007** | 0.0855 | 46.7500 | 0.8548 | 45.4415 | 0.5663 | 0.0748 | 0.1068 | 5.9500 | 99.83 | † |
| **FRB 1008** | 0.1386 | 44.8000 | 1.2157 | 45.5400 | 0.7571 | 0.1706 | 0.1173 | 6.2100 | 98.95 | † |
| **FRB 1009** | 0.1701 | 43.1800 | 1.7114 | 45.9848 | 1.0205 | 0.0744 | 0.1382 | 7.2400 | 99.52 | † |
| **PHN 4257** | 0.0840 | 44.3700 | 1.4285 | 46.8029 | 0.5462 | 0.0840 | 0.1155 | 6.1900 | 99.62 | † |
| **PHN 4259** | 0.0826 | 43.6800 | 1.6840 | 47.3579 | 0.7852 | 0.0103 | 0.1136 | 5.9400 | 99.65 | † |
| **PHN 4265** | 0.0828 | 43.1300 | 1.5731 | 48.4564 | 0.6934 | 0.0103 | 0.1138 | 5.5900 | 99.65 | † |
| **PHN 4274** | 0.0633 | 45.3800 | 0.9603 | 46.8624 | 0.4221 | 0.0106 | 0.1055 | 5.8600 | 99.66 | † |
| **FRB 347** | 0.1355 | 44.4700 | 1.7413 | 46.4935 | 0.7612 | 0.0104 | 0.1251 | 5.9000 | 99.64 | † |
| **FRB 348** | 0.1239 | 42.6000 | 1.8480 | 47.3876 | 1.1769 | 0.0103 | 0.1342 | 6.3400 | 99.62 | † |
| **FRB 823** | 0.0922 | 43.3600 | 1.5570 | 46.7105 | 1.1370 | 0.0205 | 0.1434 | 6.5400 | 99.56 | † |
| **LBM 9** | 0.0415 | 40.0500 | 2.5395 | 49.2248 | 1.4097 | 0.0311 | 0.1244 | 6.3300 | 99.75 | † |
| **LBM 11** | 0.1400 | 41.8900 | 1.4400 | 48.5700 | 0.7600 | 0.0300 | 0.1200 | 6.2900 | 99.24 | † |
| **LBM 16** | 0.0400 | 43.2600 | 1.3000 | 47.5000 | 0.9000 | 0.1000 | 0.2300 | 6.3200 | 99.65 | † |
| **MB 3** | 0.0800 | 43.8400 | 0.0800 | 46.3500 | 0.9200 | 0.0500 | 0.1100 | 6.3300 | 97.76 | † |
| **MB 4** | 0.0100 | 46.8000 | 1.3900 | 43.5100 | 0.7200 | 0.0600 | 0.1100 | 6.6800 | 99.28 | † |
| **MB 7** | 0.1000 | 44.0000 | 1.4300 | 46.5200 | 0.9500 | 0.0300 | 0.1000 | 6.0500 | 99.18 | † |
| **MB 12** | 0.1400 | 42.9500 | 1.4700 | 47.3900 | 1.0300 | 0.0400 | 0.1100 | 6.1600 | 99.29 | † |
| **MB 13** | 0.1000 | 43.3900 | 1.5600 | 47.4800 | 0.7400 | 0.0200 | 0.1000 | 5.9500 | 99.34 | † |
| **AJE 62** | 0.0500 | 42.6700 | 1.5100 | 48.0700 | 0.8000 | 0.0300 | 0.1100 | 6.0500 | 99.29 | † |
| **EJB 4** | 0.1300 | 42.4300 | 1.5100 | 47.1000 | 1.2800 | 0.0300 | 0.1200 | 6.6500 | 99.25 | † |
| **EJB 48** | 0.0600 | 45.5300 | 1.1300 | 45.5800 | 0.6400 | 0.0400 | 0.1000 | 6.2600 | 99.34 | † |
| **BD 2384** | 0.0300 | 44.3900 | 1.6700 | 45.4000 | 0.7200 | | 0.1200 | 6.8700 | 99.20 | † |
| **PHN 2762** | 0.0300 | 44.2300 | 1.3900 | 47.0500 | 0.6000 | 0.0100 | 0.1000 | 5.9600 | 99.37 | † |
| **FRB1350** | 0.0800 | 42.6700 | 1.6800 | 46.5400 | 1.4300 | 0.0100 | 0.1100 | 6.8400 | 99.36 | † |
| **FRB 932** | 0.1042 | 45.2400 | 1.7410 | 46.2763 | 0.6359 | 0.0208 | 0.0938 | 5.5400 | 99.65 | □ |
| **FRB 978** | 0.1579 | 45.6200 | 1.2947 | 45.6522 | 0.8000 | 0.0842 | 0.1263 | 5.8000 | 99.54 | □ |
| **FRB 1013** | 0.1266 | 45.5200 | 1.0230 | 45.0837 | 0.7488 | 0.1476 | 0.1266 | 6.7200 | 99.50 | □ |
| **PHN 4254** | 0.0316 | 45.8200 | 1.0443 | 46.7180 | 0.3375 | 0.0316 | 0.1055 | 5.5100 | 99.60 | □ |
| **PHN 5596** | 0.0758 | 47.4300 | 0.7361 | 43.7519 | 0.3247 | 0.0866 | 0.1082 | 7.0900 | 99.60 | □ |

Cont.

## Appendix D (I) Kaapvaal

Major element oxides Kaapvaal cratonic peridotite xenolith suite

| Sample | $Na_2O$ | MgO | $Al_2O_3$ | $SiO_2$ | CaO | $TiO_2$ | MnO | FeO* | Total | Ref |
|---|---|---|---|---|---|---|---|---|---|---|
| **FRB 1402** | 0.0858 | 46.5600 | 0.9544 | 44.9019 | 0.3110 | 0.0322 | 0.0858 | 6.7100 | 99.64 | □ |
| **FRB 1404** | 0.1050 | 44.9000 | 1.4589 | 46.7895 | 0.4723 | 0.0210 | 0.0840 | 5.8200 | 99.65 | □ |
| **FRB 1409** | 0.1151 | 44.7000 | 1.6421 | 46.8376 | 0.6171 | 0.0209 | 0.0837 | 5.6200 | 99.64 | □ |
| **FRB 1422** | 0.0845 | 45.9400 | 1.1718 | 46.0074 | 0.3695 | 0.0211 | 0.0845 | 5.9900 | 99.67 | □ |
| **FRB 1447** | 0.0743 | 46.1100 | 1.1988 | 45.7228 | 0.3395 | 0.0106 | 0.0849 | 6.1100 | 99.65 | □ |
| **FRB 451** | 0.0500 | 46.0200 | 1.0900 | 45.6500 | 0.2600 | 0.0000 | 0.1200 | 6.0200 | 99.21 | Δ |
| **FRB914** | 0.0700 | 42.9500 | 1.3500 | 47.3900 | 0.8600 | 0.0400 | 0.1300 | 6.3900 | 99.18 | Δ |
| **FRB919** | 0.0400 | 46.1300 | 1.2000 | 44.7300 | 0.5200 | 0.0100 | 0.1100 | 6.5000 | 99.24 | Δ |
| **PHN4258** | 0.0300 | 46.9200 | 0.7700 | 45.2200 | 0.1500 | 0.0400 | 0.1000 | 6.0500 | 99.28 | Δ |
| **PHN4531** | 0.0900 | 45.7900 | 1.1800 | 45.4800 | 0.4000 | 0.0100 | 0.1200 | 6.1100 | 99.18 | Δ |
| **PHN5236** | 0.0400 | 43.6200 | 2.4600 | 46.1800 | 0.8700 | 0.0000 | 0.1100 | 5.9700 | 99.25 | Δ |
| **PHN5244** | 0.1900 | 46.5700 | 1.0600 | 43.7200 | 0.4900 | 0.0300 | 0.1200 | 6.9600 | 99.14 | Δ |
| **PHN5245** | 0.0500 | 45.9300 | 1.1000 | 44.9100 | 0.4000 | 0.0100 | 0.1000 | 6.7800 | 99.28 | Δ |
| **PHN5248** | 0.0100 | 49.1500 | 0.5100 | 43.3700 | 0.0900 | 0.0000 | 0.0700 | 6.1500 | 99.35 | Δ |
| **PHN5254** | 0.0800 | 44.1200 | 1.4100 | 44.8100 | 1.5900 | 0.0500 | 0.1200 | 6.9800 | 99.16 | Δ |
| **PHN5266** | 0.0500 | 44.3600 | 1.4600 | 46.1400 | 0.8600 | 0.0100 | 0.1200 | 6.2200 | 99.22 | Δ |
| **FRB1419** | 0.0500 | 45.9700 | 0.9900 | 45.4600 | 0.4600 | 0.0100 | 0.0800 | 6.3100 | 99.33 | Δ |
| **FRB1425** | 0.0700 | 43.1800 | 1.6500 | 47.5200 | 0.7900 | 0.0100 | 0.0900 | 5.9400 | 99.25 | Δ |
| **FRB1429** | 0.0700 | 44.6400 | 1.2500 | 46.8900 | 0.5500 | 0.0000 | 0.0900 | 5.8000 | 99.29 | Δ |
| **FRB1431** | 0.0600 | 44.4900 | 1.1300 | 46.9200 | 0.5600 | 0.0100 | 0.0900 | 6.0200 | 99.28 | Δ |
| **FRB1434** | 0.0500 | 44.6600 | 1.2100 | 46.8700 | 0.4900 | 0.0100 | 0.0900 | 5.9200 | 99.30 | Δ |
| **FRB1435** | 0.0500 | 47.4300 | 0.7600 | 44.4800 | 0.2800 | 0.0100 | 0.0800 | 6.2400 | 99.33 | Δ |
| **FRB1450** | 0.0700 | 45.5800 | 1.1000 | 45.7300 | 0.5500 | 0.0100 | 0.0800 | 6.2000 | 99.32 | Δ |
| **FRB1353** | 0.0300 | 45.4500 | 0.8100 | 45.8600 | 0.3300 | 0.0100 | 0.1000 | 6.6700 | 99.26 | Δ |
| **FRB1374** | 0.0700 | 46.8100 | 0.9800 | 43.9500 | 0.6300 | 0.0400 | 0.0900 | 6.6600 | 99.23 | Δ |
| **FRB1382** | 0.0900 | 42.8600 | 1.8900 | 45.5000 | 2.1500 | 0.0600 | 0.1100 | 6.6300 | 99.29 | Δ |
| **FRB-1007** | | 47.0269 | 0.8477 | 45.0559 | 0.5616 | 0.0742 | 0.1060 | 5.9887 | 99.66 | ‡ |
| **FRB-1008** | | 45.0808 | 1.2024 | 45.8191 | 0.7489 | 0.1688 | 0.1160 | 6.2522 | 99.39 | ‡ |
| **FRB-999** | | 45.5455 | 0.9874 | 45.2514 | 0.7143 | 0.1155 | 0.1260 | 6.8923 | 99.63 | ‡ |
| **FRB-1009** | | 42.5603 | 1.6709 | 44.8953 | 0.9963 | 0.0726 | 0.1349 | 7.1375 | 97.47 | ‡ |
| **FRB-135** | | 44.2497 | 1.5333 | 47.5119 | 0.5763 | 0.0000 | 0.1132 | 5.9436 | 99.93 | ‡ |
| **FRB-492** | | 44.0342 | 1.6431 | 46.8480 | 0.7907 | 0.0000 | 0.1232 | 6.1295 | 99.57 | ‡ |
| **FRB-983** | | 46.4517 | 1.1769 | 44.8374 | 0.4583 | 0.0521 | 0.1146 | 6.5550 | 99.65 | ‡ |

cont.,

## Appendix D (I) Kaapvaal

Major element oxides Kaapvaal cratonic peridotite xenolith suite

| Sample | $Na_2O$ | MgO | $Al_2O_3$ | $SiO_2$ | CaO | $TiO_2$ | MnO | FeO* | Total | Ref |
|---|---|---|---|---|---|---|---|---|---|---|
| **PHN-4254** | | 46.1594 | 1.0440 | 46.7078 | 0.3375 | 0.0316 | 0.1055 | 5.5509 | 99.94 | ‡ |
| **PHN-4257** | | 44.6566 | 1.4273 | 46.7661 | 0.5457 | 0.0840 | 0.1154 | 6.2368 | 99.83 | ‡ |
| **PHN-4258** | | 47.2482 | 0.7792 | 45.5318 | 0.1474 | 0.0421 | 0.1053 | 6.0933 | 99.95 | ‡ |
| **PHN-4259** | | 43.9456 | 1.6827 | 47.3213 | 0.7846 | 0.0619 | 0.1136 | 5.9768 | 99.89 | ‡ |
| **PHN-4265** | | 43.4266 | 1.5731 | 48.4565 | 0.6934 | 0.0000 | 0.1138 | 5.6330 | 99.90 | ‡ |
| **PHN-4274** | | 45.6691 | 0.9602 | 46.8615 | 0.4221 | 0.0000 | 0.1055 | 5.8972 | 99.92 | ‡ |
| **FRB 932** | | 45.5068 | 1.7394 | 46.2359 | 0.6354 | 0.0208 | 0.0937 | 5.5701 | 99.80 | ○ |
| **FRB 978** | | 45.9331 | 1.2920 | 45.5550 | 0.7983 | 0.0840 | 0.1260 | 5.8334 | 99.62 | ○ |
| **FRB 1013** | | 45.8328 | 1.0201 | 44.9599 | 0.7467 | 0.1578 | 0.1262 | 6.7568 | 99.60 | ○ |
| **FRB 1402** | | 46.8244 | 0.9536 | 44.8636 | 0.3107 | 0.0321 | 0.0857 | 6.7476 | 99.82 | ○ |
| **FRB 1404** | | 45.1688 | 1.4577 | 46.7523 | 0.4719 | 0.0210 | 0.0839 | 5.8556 | 99.81 | ○ |
| **FRB 1409** | | 44.9835 | 1.6409 | 46.8021 | 0.6166 | 0.0209 | 0.0836 | 5.6538 | 99.80 | ○ |
| **FRB 1422** | | 46.1961 | 1.1710 | 45.9746 | 0.3692 | 0.0211 | 0.0844 | 6.0253 | 99.84 | ○ |
| **FRB 1447** | | 46.4007 | 1.1985 | 45.7113 | 0.3394 | 0.0000 | 0.0848 | 6.1487 | 99.88 | ○ |
| **PHN 4254** | | 46.1594 | 1.0440 | 46.7078 | 0.3375 | 0.0316 | 0.1055 | 5.5509 | 99.94 | ○ |
| **PHN 5596** | | 47.7384 | 0.7356 | 43.7250 | 0.3245 | 0.0865 | 0.1082 | 7.1412 | 99.86 | ○ |
| **FRB 914** | | 43.2695 | 1.3606 | 47.7356 | 0.8621 | 0.0415 | 0.1350 | 6.4294 | 99.83 | ♦ |
| **FRB919** | | 46.4719 | 1.2092 | 45.0646 | 0.5212 | 0.0136 | 0.1147 | 6.5111 | 99.91 | ♦ |
| **FRB1353** | | 45.7869 | 0.8142 | 46.2047 | 0.3321 | 0.0075 | 0.0964 | 6.7196 | 99.96 | ♦ |
| **FRB1374** | | 47.1409 | 0.9863 | 44.2555 | 0.6295 | 0.0420 | 0.0944 | 6.7045 | 99.85 | ♦ |
| **FRB1382** | | 43.1400 | 1.9037 | 45.8031 | 2.1638 | 0.0624 | 0.1144 | 6.6774 | 99.86 | ♦ |
| **PHN5236** | | 42.1767 | 2.3783 | 44.6453 | 0.8429 | 0.0010 | 0.1104 | 5.7611 | 95.92 | ♦ |
| **PHN5244** | | 46.8201 | 1.0608 | 43.9601 | 0.4888 | 0.0312 | 0.1248 | 6.9943 | 99.48 | ♦ |
| **PHN5245** | | 45.9020 | 1.1018 | 44.8858 | 0.3958 | 0.0053 | 0.0963 | 7.5380 | 99.93 | ♦ |
| **PHN5248** | | 49.4734 | 0.5110 | 43.6562 | 0.0870 | 0.0000 | 0.0761 | 6.1777 | 99.98 | ♦ |
| **PHN5254** | | 44.4430 | 1.4232 | 45.1441 | 1.6011 | 0.0523 | 0.1256 | 7.0224 | 99.81 | ♦ |
| **PHN5266** | | 44.6736 | 1.4690 | 46.4759 | 0.8647 | 0.0052 | 0.1250 | 6.2511 | 99.86 | ♦ |
| **PHN4531** | | 46.1401 | 1.1847 | 45.8361 | 0.3984 | 0.0063 | 0.1258 | 6.1408 | 99.83 | ♦ |
| **FRB1419** | | 46.2648 | 0.9979 | 45.7553 | 0.4671 | 0.0106 | 0.0849 | 6.3557 | 99.94 | ♦ |
| **FRB1425** | | 43.4733 | 1.6586 | 47.8470 | 0.7923 | 0.0106 | 0.0951 | 5.9751 | 99.85 | ♦ |
| **FRB1429** | | 44.9268 | 1.2573 | 47.2004 | 0.5553 | 0.0031 | 0.0943 | 5.8370 | 99.87 | ♦ |
| **FRB1431** | | 46.4879 | 1.1049 | 45.7922 | 0.5422 | 0.0102 | 0.0921 | 5.8682 | 99.90 | ♦ |

cont..

## Appendix D (I) Kaapvaal

Major element oxides Kaapvaal cratonic peridotite xenolith suite

| Sample | $Na_2O$ | MgO | $Al_2O_3$ | $SiO_2$ | CaO | $TiO_2$ | MnO | FeO* | Total | Ref |
|---|---|---|---|---|---|---|---|---|---|---|
| **FRB1434** | | 44.9672 | 1.2159 | 47.1893 | 0.4926 | 0.0052 | 0.0943 | 5.9620 | 99.93 | ♦ |
| **FRB1435** | | 47.7253 | 0.7680 | 44.7492 | 0.2773 | 0.0107 | 0.0853 | 6.2881 | 99.90 | ♦ |
| **FRB1450** | | 45.8558 | 1.1087 | 46.0127 | 0.5544 | 0.0105 | 0.0837 | 6.2278 | 99.85 | ♦ |
| **FRB451** | | 46.3383 | 1.1020 | 45.9675 | 0.2649 | 0.0032 | 0.1166 | 6.0592 | 99.85 | ♦ |
| **PHN4258** | | 47.2460 | 0.7792 | 45.5297 | 0.1474 | 0.0421 | 0.1053 | 6.0924 | 99.94 | ♦ |
| **PHN5232** | | 45.1505 | 1.1882 | 45.7759 | 0.8651 | 0.0208 | 0.1251 | 6.6451 | 99.77 | ♦ |
| **PHN5246** | | 44.2702 | 1.3937 | 46.1074 | 0.9819 | 0.0317 | 0.1373 | 6.7295 | 99.65 | ♦ |
| **Average** | 0.0834 | 45.0493 | 1.2872 | 46.0445 | 0.6654 | 0.0350 | 0.1081 | 6.2625 | 99.50 | |

† Pearson et al, 1995.Low T

□ Boyd et al, 1993

Δ Pearson et al., 1995. spinel peridotite

‡ Boyd and Mertzman, 1987 garnet peridotite

○ Boyd et al, 1993 garnet harzburgite

♦ Boyd et al, 1999 Kaapvaal root, spinel peridotite

## Appendix D (II) Canadian

Major element oxides Canadian cratonic peridotite suite

| Sample | $Na_2O$ | MgO | $Al_2O_3$ | $SiO_2$ | CaO | $TiO_2$ | MnO | FeO* | Cr2O3 | NiO | Ref |
|---|---|---|---|---|---|---|---|---|---|---|---|
| **9-12** | | 46.82 | 0.34 | 42.64 | 0.35 | 0.05 | 0.10 | 6.37 | 0.33 | 0.31 | † |
| **9-13** | | 45.33 | 0.53 | 44.47 | 0.54 | 0.02 | 0.10 | 6.19 | 0.32 | 0.26 | † |
| **10-8** | | 44.07 | 1.13 | 44.88 | 0.76 | 0.02 | 0.11 | 6.77 | 0.42 | 0.29 | † |
| **10-12B** | | 45.46 | 0.65 | 45.24 | 0.63 | 0.05 | 0.10 | 6.00 | 0.35 | 0.28 | † |
| **11-18** | | 47.72 | 0.41 | 43.82 | 0.25 | 0.02 | 0.10 | 6.08 | 0.20 | 0.31 | † |
| **23-9** | | 44.62 | 0.67 | 45.63 | 0.28 | 0.02 | 0.10 | 5.87 | 0.38 | 0.29 | † |
| **39-4** | | 44.46 | 1.18 | 44.98 | 0.56 | 0.02 | 0.10 | 6.19 | 0.39 | 0.29 | † |
| **39-23** | | 46.43 | 1.28 | 42.08 | 0.92 | 0.04 | 0.10 | 6.68 | 0.53 | 0.31 | † |
| **41-2** | | 42.58 | 1.20 | 48.67 | 0.41 | 0.01 | 0.10 | 5.16 | 0.45 | 0.24 | † |
| **44-12** | | 42.87 | 1.05 | 41.41 | 0.25 | 0.02 | 0.08 | 6.45 | 0.41 | 0.31 | † |
| **10-456'** | | 42.30 | 0.95 | 44.30 | 1.75 | 0.05 | 0.12 | 7.12 | 0.41 | 0.27 | † |
| **40-16** | | 43.91 | 0.74 | 46.37 | 0.36 | 0.03 | 0.10 | 5.87 | 0.51 | 0.28 | † |
| **53-10** | | 41.98 | 0.64 | 38.80 | 0.74 | 0.06 | 0.09 | 8.02 | 0.41 | 0.37 | † |
| **10-11** | | 45.69 | 1.21 | 43.56 | 0.95 | 0.05 | 0.11 | 6.71 | 0.38 | 0.28 | † |
| **10-12A** | | 44.16 | 1.25 | 44.46 | 0.90 | 0.04 | 0.11 | 6.60 | 0.39 | 0.28 | † |
| **21-1** | | 43.58 | 0.66 | 45.89 | 0.54 | 0.03 | 0.12 | 6.64 | 0.43 | 0.28 | † |
| **22-4** | | 42.85 | 1.41 | 45.10 | 1.21 | 0.04 | 0.12 | 7.01 | 0.48 | 0.27 | † |
| **28-15** | | 41.85 | 1.49 | 44.18 | 0.84 | 0.10 | 0.12 | 7.11 | 0.41 | 0.28 | † |
| **41-4** | | 44.67 | 0.72 | 43.87 | 0.67 | 0.04 | 0.12 | 7.11 | 0.37 | 0.31 | † |
| **21-3** | | 42.59 | 1.53 | 42.05 | 1.50 | 0.15 | 0.12 | 7.89 | 0.30 | 0.29 | † |
| **8-7** | | 45.58 | 0.64 | 46.00 | 0.60 | 0.02 | 0.10 | 5.78 | 0.28 | 0.26 | † |
| **5-3** | | 39.86 | 1.88 | 39.19 | 1.45 | 0.06 | 0.10 | 8.42 | 0.40 | 0.32 | † |
| **10-9** | | 44.33 | 0.82 | 42.71 | 1.07 | 0.07 | 0.13 | 7.93 | 0.43 | 0.32 | † |
| **11-22** | | 41.31 | 1.61 | 44.35 | 1.78 | 0.08 | 0.14 | 7.28 | 0.85 | 0.26 | † |
| **13-2** | | 44.15 | 0.47 | 41.77 | 0.79 | 0.05 | 0.12 | 7.90 | 0.29 | 0.30 | † |
| **21-2** | | 45.67 | 0.81 | 41.76 | 0.47 | 0.08 | 0.12 | 8.09 | 0.43 | 0.32 | † |
| **23-1** | | 44.82 | 0.82 | 42.65 | 0.65 | 0.05 | 0.12 | 7.71 | 0.48 | 0.32 | † |
| **26-9** | | 39.11 | 2.53 | 41.61 | 3.13 | 0.18 | 0.15 | 9.31 | 0.40 | 0.23 | † |
| **39-3** | | 43.46 | 1.34 | 41.25 | 1.46 | 0.12 | 0.12 | 7.23 | 0.44 | 0.31 | † |
| **39-10** | | 44.70 | 0.94 | 42.30 | 0.59 | 0.04 | 0.12 | 8.29 | 0.40 | 0.30 | † |
| **40-9** | | 45.50 | 0.73 | 42.61 | 0.58 | 0.06 | 0.13 | 8.36 | 0.33 | 0.31 | † |
| **NK1-5** | | 41.54 | 1.95 | 42.33 | 1.44 | 0.07 | 0.12 | 7.75 | 0.85 | 0.30 | ¤ |
| **NK2-3** | | 41.82 | 2.90 | 42.40 | 1.98 | 0.09 | 0.13 | 7.20 | 1.04 | 0.31 | ¤ |

cont..

## Appendix D (II) Canadian

Major element oxides Canadian cratonic peridotite suite

| Sample | $Na_2O$ | MgO | $Al_2O_3$ | $SiO_2$ | CaO | $TiO_2$ | MnO | FeO* | Cr2O3 | NiO | Ref |
|---|---|---|---|---|---|---|---|---|---|---|---|
| **NK2-10** | | 45.54 | 1.25 | 41.55 | 1.22 | 0.03 | 0.11 | 7.43 | 0.53 | 0.32 | ¤ |
| **NK3-20** | | 37.62 | 3.22 | 43.33 | 3.22 | 0.10 | 0.13 | 7.60 | 0.67 | 0.28 | ¤ |
| **NK3-25** | | 39.52 | 4.29 | 41.48 | 2.13 | 0.21 | 0.13 | 7.42 | 1.09 | 0.25 | ¤ |
| **NK1-2** | | 44.51 | 1.31 | 41.83 | 1.11 | 0.03 | 0.11 | 7.40 | 0.52 | 0.32 | ¤ |
| **NK1-3** | | 44.29 | 1.34 | 41.05 | 0.82 | 0.03 | 0.11 | 7.46 | 0.60 | 0.33 | ¤ |
| **NK1-6** | | 43.60 | 1.26 | 40.54 | 0.41 | 0.02 | 0.10 | 7.13 | 0.68 | 0.33 | ¤ |
| **NK1-7** | | 43.72 | 1.58 | 41.40 | 0.72 | 0.03 | 0.10 | 7.09 | 0.70 | 0.31 | ¤ |
| **NK1-17** | | 45.35 | 0.81 | 41.18 | 0.49 | 0.01 | 0.11 | 7.04 | 0.68 | 0.31 | ¤ |
| **NK1-18** | | 44.93 | 0.79 | 42.94 | 0.54 | 0.03 | 0.10 | 6.97 | 0.51 | 0.35 | ¤ |

† Kopylova & Russell, 2000, Slave, Jericho ¤ Schmidberger & Francis, 1999

## Appendix D (III) Tanzanian

Major element oxides Tanzanian cratonic peridotite suite

| Sample | $Na_2O$ | MgO | $Al_2O_3$ | $SiO_2$ | CaO | $TiO_2$ | MnO | FeO* | Ref |
|---|---|---|---|---|---|---|---|---|---|
| **LB1 ave** | | 48.09 | 0.40 | 44.52 | 0.25 | 0.08 | 0.12 | 6.48 | † |
| **LB6 ave** | | 48.57 | 0.67 | 42.21 | 0.57 | 0.14 | 0.13 | 7.52 | † |
| **LB7 ave** | | 49.18 | 0.57 | 41.87 | 0.28 | 0.13 | 0.14 | 7.69 | † |
| **LB8 ave** | | 48.66 | 0.35 | 43.98 | 0.19 | 0.07 | 0.12 | 6.57 | † |
| **LB 9 ave** | | 49.05 | 0.37 | 43.39 | 0.22 | 0.06 | 0.12 | 6.72 | † |
| **LB 11 ave** | | 47.33 | 0.86 | 43.97 | 0.31 | 0.04 | 0.13 | 7.33 | † |
| **LB 16 ave** | | 47.36 | 0.61 | 43.87 | 0.41 | 0.14 | 0.13 | 7.38 | † |
| **LB21 ave** | | 50.22 | 0.31 | 41.90 | 0.54 | 0.11 | 0.12 | 6.70 | † |
| **LB 22 ave** | | 46.96 | 0.69 | 44.06 | 0.40 | 0.08 | 0.13 | 7.61 | † |
| **LB 23 ave** | | 48.19 | 0.55 | 43.23 | 0.42 | 0.03 | 0.13 | 7.35 | † |
| **LB 29 ave** | | 47.48 | 0.90 | 43.78 | 0.31 | 0.07 | 0.13 | 7.25 | † |
| **LB 31 ave** | | 45.95 | 1.04 | 44.36 | 0.98 | 0.04 | 0.14 | 7.41 | † |
| **LB 36 ave** | | 46.42 | 0.90 | 44.58 | 0.63 | 0.07 | 0.13 | 7.11 | † |
| **LB 39 ave** | | 44.91 | 0.87 | 45.11 | 0.73 | 0.16 | 0.14 | 7.88 | † |
| **LB 55 ave** | | 47.28 | 0.78 | 44.09 | 0.42 | 0.09 | 0.13 | 6.96 | † |
| **LB61 ave** | | 48.66 | 0.51 | 43.10 | 0.24 | 0.11 | 0.13 | 7.14 | † |
| **LB33 ave** | | 47.60 | 0.62 | 42.96 | 0.71 | 0.35 | 0.13 | 7.48 | † |
| **LB26 ave** | | 48.44 | 0.47 | 43.26 | 0.18 | 0.15 | 0.14 | 7.29 | † |
| **LB 17 ave** | | 45.79 | 0.57 | 45.16 | 0.43 | 0.25 | 0.14 | 7.56 | † |
| **LB 18 ave** | | 48.04 | 0.43 | 42.36 | 0.39 | 0.11 | 0.13 | 8.46 | † |
| **LB 19R ave** | | 46.56 | 0.84 | 42.97 | 0.47 | 0.09 | 0.15 | 8.66 | † |
| **LB 14 ave** | | 49.91 | 0.33 | 42.14 | 0.04 | 0.08 | 0.12 | 7.30 | † |
| **KAT 1 WSU** | | 45.97 | 0.65 | 45.54 | 0.39 | 0.11 | 0.11 | 7.04 | † |
| **KAT 17 WSU** | | 43.28 | 0.41 | 44.80 | 0.64 | 0.06 | 0.13 | 10.55 | † |
| **LB2 AVERAGE** | | 46.86 | 1.20 | 44.36 | 0.51 | 0.07 | 0.13 | 6.72 | † |
| **LB4 AVERAGE** | | 44.21 | 1.57 | 45.20 | 1.09 | 0.03 | 0.13 | 7.65 | † |
| **LB12 ave** | | 42.90 | 2.02 | 44.47 | 1.82 | 0.05 | 0.15 | 8.50 | † |
| **LB24 ave** | | 46.68 | 1.24 | 44.15 | 0.62 | 0.06 | 0.13 | 7.07 | † |
| **LB34 ave** | | 46.86 | 0.70 | 42.06 | 0.44 | 0.19 | 0.14 | 9.50 | † |
| **LB45 ave** | | 39.67 | 3.99 | 44.40 | 2.81 | 0.21 | 0.16 | 8.55 | † |
| **LB50-1** | | 44.93 | 1.39 | 44.52 | 0.99 | 0.05 | 0.14 | 7.93 | † |
| **LB50-2** | | 44.95 | 1.34 | 44.64 | 0.97 | 0.05 | 0.14 | 7.88 | † |
| **LB53 ave** | | 44.90 | 1.77 | 43.54 | 1.37 | 0.13 | 0.14 | 8.11 | † |
| **89-661** | | 48.41 | 0.70 | 42.68 | 0.95 | 0.08 | 0.09 | 6.82 | □ |

cont..

# Appendix D

## Cratonic Data
## Major Elements

## Appendix D (III) Tanzanian

Major element oxides Tanzanian cratonic peridotite suite

| Sample | $Na_2O$ | MgO | $Al_2O_3$ | $SiO_2$ | CaO | $TiO_2$ | MnO | FeO* | Ref |
|---|---|---|---|---|---|---|---|---|---|
| **89-662** | | 49.64 | 0.17 | 41.21 | 0.09 | 0.05 | 0.11 | 8.57 | □ |
| **89-663** | | 47.28 | 0.69 | 41.94 | 0.36 | 0.10 | 0.11 | 9.13 | □ |
| **89-664** | | 47.92 | 0.19 | 42.19 | 0.31 | 0.15 | 0.12 | 8.92 | □ |
| **89-669** | | 45.09 | 0.57 | 42.11 | 1.81 | 0.10 | 0.12 | 9.76 | □ |
| **89-671** | | 46.71 | 0.42 | 40.55 | 0.09 | 0.13 | 0.14 | 11.62 | □ |
| **89-672** | | 49.42 | 0.19 | 41.91 | 0.95 | 0.06 | 0.08 | 7.22 | □ |
| **89-674** | | 45.57 | 0.86 | 43.59 | 1.06 | 0.11 | 0.12 | 8.44 | □ |
| **89-675** | | 46.15 | 0.92 | 45.56 | 0.62 | 0.05 | 0.10 | 6.37 | □ |
| **89-676** | | 33.97 | 0.67 | 46.20 | 7.71 | 0.14 | 0.16 | 10.83 | □ |
| **89-678** | | 48.86 | 0.26 | 42.03 | 0.30 | 0.07 | 0.11 | 8.19 | □ |
| **89-680** | | 46.33 | 1.23 | 44.67 | 0.82 | 0.03 | 0.10 | 6.67 | □ |
| **89-719** | | 47.78 | 1.09 | 43.47 | 0.55 | 0.02 | 0.09 | 6.84 | □ |
| **TZ 2-16** | | 48.68 | 1.28 | 43.85 | 0.21 | 0.03 | 0.07 | 5.74 | □ |
| **BD730** | | 42.96 | 2.49 | 45.24 | 1.48 | 0.08 | 0.09 | 7.33 | □ |
| **89-772** | | 46.01 | 0.11 | 40.56 | 0.66 | 0.00 | 0.15 | 12.46 | Δ |
| **89-773** | | 49.24 | 0.39 | 44.12 | 0.11 | 0.01 | 0.08 | 5.98 | Δ |
| **89-774** | | 51.94 | 0.10 | 41.35 | 0.16 | 0.00 | 0.08 | 6.27 | Δ |
| **89-776** | | 51.57 | 0.09 | 41.73 | 0.58 | 0.02 | 0.09 | 5.86 | Δ |
| **89-777** | | 48.17 | 0.17 | 41.33 | 1.36 | 0.05 | 0.16 | 8.51 | Δ |
| **89-778** | | 49.56 | 0.22 | 40.93 | 0.28 | 0.05 | 0.11 | 8.83 | Δ |
| **89-780** | | 51.00 | 0.12 | 41.49 | 0.48 | 0.03 | 0.10 | 6.72 | Δ |

† Lee & Rudnick (Unpublished)

□ Rudnick et al, 1993

Δ Rudnick et al, 1993

## Appendix D (IV) Siberian

Major element oxides Siberian cratonic peridotite suite

| Sample | $Na_2O$ | MgO | $Al_2O_3$ | $SiO_2$ | CaO | $TiO_2$ | MnO | FeO* | Total | Ref |
|---|---|---|---|---|---|---|---|---|---|---|
| **UV 191/89** | | 49.30 | 0.28 | 42.72 | 0.33 | 0.01 | 0.11 | 7.20 | 99.94 | † |
| **UV 563/89** | | 45.98 | 1.07 | 45.08 | 0.33 | 0.02 | 0.10 | 7.30 | 99.90 | † |
| **UV 564/89** | | 44.59 | 1.09 | 44.94 | 1.69 | 0.04 | 0.13 | 7.27 | 99.74 | † |
| **UV 565/89** | | 45.39 | 1.08 | 44.56 | 1.40 | 0.03 | 0.10 | 7.21 | 99.77 | † |
| **UV 111/91** | | 47.50 | 0.45 | 45.00 | 0.39 | 0.00 | 0.10 | 6.44 | 99.88 | † |
| **UV 65/92** | | 46.81 | 1.32 | 44.37 | 0.54 | 0.01 | 0.12 | 6.58 | 99.76 | † |
| **UV 34/93** | | 43.82 | 1.38 | 47.54 | 0.78 | 0.04 | 0.10 | 6.12 | 99.77 | † |
| **UV 105/93** | | 45.70 | 0.59 | 46.05 | 0.56 | 0.02 | 0.23 | 6.58 | 99.73 | † |
| **UV 215/93** | | 43.98 | 1.33 | 46.72 | 0.90 | 0.02 | 0.12 | 6.70 | 99.77 | † |
| **Uv 274/89** | | 48.24 | 0.61 | 42.23 | 1.03 | 0.09 | 0.10 | 7.51 | 99.81 | † |
| **Uv 285/89** | | 48.13 | 0.56 | 42.46 | 0.99 | 0.09 | 0.10 | 7.50 | 99.83 | † |
| **Uv 293/89** | | 47.02 | 0.76 | 43.27 | 1.26 | 0.06 | 0.11 | 7.33 | 99.81 | † |
| **Uv 306/89** | | 45.66 | 1.21 | 44.22 | 0.67 | 0.02 | 0.12 | 7.92 | 99.82 | † |
| **Uv 417/89** | | 39.33 | 3.69 | 44.88 | 2.94 | 0.19 | 0.19 | 8.33 | 99.55 | † |
| **Uv 485/89** | | 47.45 | 0.86 | 43.08 | 0.96 | 0.06 | 0.11 | 7.34 | 99.87 | † |
| **Uv 25/91** | | 45.96 | 1.30 | 44.15 | 0.72 | 0.01 | 0.12 | 7.60 | 99.86 | † |
| **Uv 100/91** | | 42.05 | 3.65 | 45.76 | 1.48 | 0.01 | 0.18 | 6.68 | 99.80 | † |
| **Uv 51/93** | | 45.43 | 0.37 | 45.47 | 0.35 | 0.07 | 0.13 | 7.87 | 99.69 | † |
| **Uv 76/93** | | 43.93 | 1.05 | 46.49 | 0.54 | 0.07 | 0.13 | 7.47 | 99.67 | † |
| **Uv 178/93** | | 45.55 | 0.70 | 44.28 | 1.04 | 0.02 | 0.25 | 7.93 | 99.78 | † |
| **Uv 219/93** | | 45.17 | 1.01 | 44.64 | 1.04 | 0.04 | 0.25 | 7.64 | 99.80 | † |
| **52/76** | | 46.27 | 0.51 | 44.06 | 0.66 | 0.12 | 0.10 | 8.20 | 99.92 | † |
| **74/89** | | 44.05 | 1.27 | 44.99 | 1.19 | 0.11 | 0.10 | 8.07 | 99.77 | † |
| **107/89** | | 46.20 | 0.53 | 44.31 | 0.64 | 0.05 | 0.14 | 7.99 | 99.85 | † |
| **115/89** | | 44.42 | 1.47 | 44.89 | 1.06 | 0.10 | 0.13 | 7.80 | 99.88 | † |
| **228/89** | | 44.10 | 0.72 | 45.72 | 0.84 | 0.13 | 0.10 | 8.23 | 99.83 | † |
| **239/89** | | 44.93 | 0.68 | 44.59 | 1.22 | 0.12 | 0.14 | 8.11 | 99.78 | † |
| **246/89** | | 42.66 | 1.59 | 45.58 | 1.14 | 0.17 | 0.10 | 8.64 | 99.88 | † |
| **267/89** | | 41.01 | 2.70 | 44.98 | 2.55 | 0.20 | 0.14 | 8.17 | 99.76 | † |
| **424/89** | | 45.28 | 0.85 | 44.56 | 1.02 | 0.10 | 0.14 | 7.91 | 99.87 | † |
| **61/91** | | 44.88 | 0.75 | 44.90 | 1.69 | 0.11 | 0.12 | 7.37 | 99.83 | † |
| **121/91** | | 46.19 | 0.72 | 44.53 | 1.09 | 0.11 | 0.12 | 7.06 | 99.83 | † |
| **51/92** | | 43.05 | 1.17 | 44.55 | 1.64 | 0.18 | 0.13 | 9.03 | 99.76 | † |

cont..

## Appendix D (IV) Siberian

Major element oxides Siberian cratonic peridotite suite

| Sample | $Na_2O$ | MgO | $Al_2O_3$ | $SiO_2$ | CaO | $TiO_2$ | MnO | FeO* | Total | Ref |
|---|---|---|---|---|---|---|---|---|---|---|
| **70/92** | | 46.59 | 0.54 | 44.08 | 0.90 | 0.09 | 0.14 | 7.48 | 99.82 | † |
| **74/92** | | 41.07 | 1.06 | 44.13 | 2.57 | 0.16 | 0.14 | 10.48 | 99.61 | † |
| **76/92** | | 45.38 | 0.62 | 44.41 | 0.97 | 0.02 | 0.14 | 8.02 | 99.55 | † |
| **80/92** | | 44.91 | 0.63 | 44.62 | 0.77 | 0.15 | 0.11 | 8.59 | 99.79 | † |
| **32842** | | 43.02 | 1.75 | 45.57 | 1.50 | 0.11 | 0.11 | 7.74 | 99.80 | † |
| **128/93** | | 43.63 | 1.37 | 44.49 | 1.38 | 0.09 | 0.23 | 8.50 | 99.68 | † |
| **166/93** | | 44.21 | 0.96 | 45.02 | 1.31 | 0.08 | 0.15 | 8.04 | 99.78 | † |
| **813** | | 45.93 | 0.77 | 44.02 | 0.88 | 0.13 | 0.13 | 7.96 | 99.82 | † |

† Boyd et al, 1997

## Appendix D (V) East Greenland

Major element oxides E. Greenland cratonic peridotite suite

| Sample | $Na_2O$ | MgO | $Al_2O_3$ | $SiO_2$ | CaO | $TiO_2$ | MnO | FeO* | Cr2O3 | NiO | Ref |
|---|---|---|---|---|---|---|---|---|---|---|---|
| **1-7a** | | 47.06 | 1.15 | 43.80 | 0.10 | 0.01 | 0.18 | 6.75 | 0.92 | 0.31 | † |
| **36171** | | 49.41 | 0.27 | 43.94 | 0.08 | 0.00 | 0.19 | 6.02 | 0.06 | 0.33 | † |
| **1-15A** | | 49.25 | 0.85 | 41.77 | 0.73 | 0.02 | 0.20 | 5.91 | 1.23 | 0.35 | † |
| **1-15B** | | 48.42 | 0.50 | 43.42 | 0.21 | 0.01 | 0.19 | 6.99 | 0.24 | 0.33 | † |
| **1-16A** | | 49.66 | 0.29 | 42.97 | 0.13 | 0.00 | 0.19 | 6.52 | 0.21 | 0.34 | † |
| **1-16B** | | 47.39 | 0.67 | 44.40 | 0.24 | 0.01 | 0.18 | 6.81 | 0.28 | 0.31 | † |
| **1-16C** | | 48.62 | 0.91 | 42.65 | 0.12 | 0.01 | 0.19 | 6.64 | 0.85 | 0.33 | † |
| **1-17B** | | 49.13 | 0.46 | 42.91 | 0.18 | 0.01 | 0.19 | 6.72 | 0.39 | 0.34 | † |
| **36178** | | 47.55 | 0.50 | 44.93 | 0.11 | 0.01 | 0.18 | 6.49 | 0.23 | 0.31 | † |
| **36179** | | 48.68 | 1.50 | 41.69 | 0.08 | 0.01 | 0.20 | 6.92 | 0.89 | 0.34 | † |
| **36180** | | 46.94 | 1.51 | 43.44 | 0.26 | 0.01 | 0.19 | 6.66 | 0.97 | 0.31 | † |
| **1-21A** | | 49.22 | 0.57 | 43.19 | 0.07 | 0.00 | 0.19 | 6.27 | 0.46 | 0.33 | † |
| **1-21B** | | 46.92 | 0.71 | 44.76 | 0.27 | 0.01 | 0.18 | 6.59 | 0.55 | 0.30 | † |
| **1-22A** | | 49.84 | 0.75 | 42.69 | 0.06 | 0.01 | 0.19 | 5.62 | 0.81 | 0.34 | † |
| **1-22b** | | 49.74 | 0.24 | 43.67 | 0.07 | 0.00 | 0.19 | 6.01 | 0.06 | 0.34 | † |
| **36201** | | 47.23 | 0.91 | 44.36 | 0.22 | 0.01 | 0.18 | 6.43 | 0.63 | 0.31 | † |
| **36202** | | 49.24 | 0.43 | 43.54 | 0.08 | 0.00 | 0.19 | 6.21 | 0.29 | 0.33 | † |
| **2-12a** | | 48.10 | 1.23 | 42.79 | 0.08 | 0.01 | 0.19 | 6.43 | 1.14 | 0.32 | † |
| **2-12b** | | 48.71 | 1.02 | 42.03 | 0.06 | 0.01 | 0.19 | 6.69 | 1.26 | 0.34 | † |
| **2-15A** | | 49.56 | 0.38 | 42.47 | 0.05 | 0.00 | 0.19 | 6.92 | 0.40 | 0.35 | † |
| **2-15B** | | 49.15 | 0.92 | 41.85 | 0.06 | 0.01 | 0.20 | 6.63 | 1.17 | 0.34 | † |
| **2-16A** | | 50.22 | 1.07 | 39.57 | 0.02 | 0.01 | 0.21 | 6.70 | 2.17 | 0.37 | † |
| **2-16B** | | 49.23 | 0.40 | 43.47 | 0.07 | 0.00 | 0.19 | 6.22 | 0.40 | 0.33 | † |
| **36210** | | 48.30 | 1.28 | 42.27 | 0.09 | 0.01 | 0.19 | 7.07 | 0.76 | 0.33 | † |
| **36212** | | 48.41 | 0.91 | 39.13 | 0.02 | 0.01 | 0.21 | 9.00 | 2.28 | 0.37 | † |
| **36213** | | 51.26 | 0.24 | 40.73 | 0.02 | 0.00 | 0.20 | 6.47 | 1.05 | 0.37 | † |
| **2-24a** | | 47.63 | 0.80 | 43.74 | 0.40 | 0.01 | 0.18 | 6.93 | 0.27 | 0.32 | † |
| **2-24Aa** | | 47.55 | 1.29 | 43.40 | 0.34 | 0.01 | 0.19 | 6.71 | 0.48 | 0.32 | † |
| **2-24Ab** | | 44.98 | 0.54 | 46.05 | 0.41 | 0.01 | 0.17 | 7.72 | 0.11 | 0.28 | † |
| **2-24b** | | 50.05 | 0.38 | 43.09 | 0.06 | 0.00 | 0.19 | 5.83 | 0.36 | 0.34 | † |
| **36216** | | 46.12 | 1.43 | 44.18 | 0.61 | 0.02 | 0.18 | 6.49 | 0.93 | 0.30 | † |
| **36217** | | 49.49 | 0.53 | 42.38 | 0.08 | 0.00 | 0.19 | 6.88 | 0.42 | 0.35 | † |
| **36219** | | 44.64 | 0.76 | 43.33 | 0.37 | 0.01 | 0.18 | 9.61 | 1.07 | 0.31 | † |

cont..

## Appendix D (V) East Greenland

Major element oxides E. Greenland cratonic peridotite suite

| Sample | $Na_2O$ | MgO | $Al_2O_3$ | $SiO_2$ | CaO | $TiO_2$ | MnO | FeO* | Cr2O3 | NiO | Ref |
|---|---|---|---|---|---|---|---|---|---|---|---|
| **10990** | | 42.86 | 3.00 | 43.32 | 2.00 | 0.04 | 0.18 | 6.77 | 1.71 | 0.28 | † |
| **2-31a** | | 49.88 | 0.47 | 42.02 | 0.11 | 0.00 | 0.20 | 6.93 | 0.35 | 0.36 | † |
| **2-32a** | | 48.36 | 0.43 | 44.21 | 0.09 | 0.00 | 0.18 | 6.49 | 0.21 | 0.32 | † |
| **12086** | | 50.86 | 0.30 | 41.59 | 0.03 | 0.00 | 0.20 | 6.38 | 0.61 | 0.36 | † |
| **4-24a** | | 48.73 | 1.24 | 42.56 | 0.07 | 0.01 | 0.19 | 6.34 | 0.83 | 0.33 | † |
| **4-24b** | | 50.26 | 0.55 | 39.98 | 0.02 | 0.01 | 0.21 | 7.18 | 1.77 | 0.37 | † |
| **4-25a** | | 49.94 | 1.21 | 41.18 | 0.06 | 0.01 | 0.20 | 6.50 | 0.86 | 0.35 | † |
| **4-26a** | | 48.81 | 0.55 | 43.12 | 0.14 | 0.00 | 0.19 | 6.94 | 0.23 | 0.34 | † |
| **4-26b** | | 47.12 | 1.05 | 43.81 | 0.35 | 0.01 | 0.18 | 6.73 | 0.72 | 0.31 | † |
| **36277** | | 44.87 | 1.38 | 44.61 | 0.95 | 0.02 | 0.18 | 7.54 | 0.39 | 0.29 | † |
| **36279** | | 47.53 | 0.95 | 43.77 | 0.14 | 0.01 | 0.18 | 6.87 | 0.51 | 0.32 | † |
| **429285a** | | 48.27 | 0.45 | 44.52 | 0.10 | 0.00 | 0.18 | 6.24 | 0.22 | 0.32 | † |
| **42928.5** | | 47.23 | 1.30 | 43.41 | 0.10 | 0.01 | 0.19 | 6.00 | 1.73 | 0.31 | † |

† Bernstein et al, 1998

# Appendix E

## Non-cratonic Data
## Non-European
## Major Elements

## Appendix D (VI) W. Australia

Major element oxides W. Australia cratonic peridotite suite

| Sample | $Na_2O$ | MgO | $Al_2O_3$ | $SiO_2$ | CaO | $TiO_2$ | MnO | FeO* | Ref |
|---|---|---|---|---|---|---|---|---|---|
| **N23** | | 46.48 | 0.75 | 44.96 | 0.80 | 0.04 | 0.07 | 6.64 | † |
| **N25** | | 44.81 | 1.06 | 47.32 | 0.24 | 0.06 | 0.07 | 6.15 | † |
| **N40** | | 47.68 | 0.57 | 44.00 | 0.56 | 0.07 | 0.08 | 6.73 | † |
| **N48** | | 43.99 | 1.10 | 46.52 | 0.97 | 0.03 | 0.06 | 6.94 | † |

† Jaques et al, 1990

## Appendix E (I) African

Non-cratonic major element oxides African peridotite xenolith siute

| Sample | $Na_2O$ | MgO | $Al_2O_3$ | $SiO_2$ | CaO | $TiO_2$ | MnO | FeO* | Total | Ref |
|---|---|---|---|---|---|---|---|---|---|---|
| **Africa, East African Rift, Ethiopia** | | | | | | | | | | |
| **ET69** | | 40.79 | 2.65 | 45.65 | 2.71 | 0.03 | 0.12 | 7.89 | 99.84 | ∞ |
| **ET46** | | 42.15 | 2.10 | 44.99 | 2.52 | 0.03 | 0.13 | 7.80 | 99.73 | ∞ |
| **ET84** | | 47.00 | 0.85 | 44.01 | 0.50 | 0.02 | 0.11 | 7.44 | 99.92 | ∞ |
| **ET57** | | 45.70 | 1.08 | 44.28 | 0.95 | 0.01 | 0.12 | 7.78 | 99.92 | ∞ |
| **ET27** | | 46.65 | 0.78 | 43.62 | 0.49 | 0.04 | 0.13 | 8.21 | 99.92 | ∞ |
| **ET35** | | 46.00 | 0.73 | 44.27 | 0.82 | 0.02 | 0.12 | 8.00 | 99.96 | ∞ |
| **ET74** | | 36.74 | 2.74 | 46.73 | 6.40 | 0.12 | 0.09 | 6.79 | 99.60 | ∞ |
| **ET75** | | 37.62 | 4.00 | 45.21 | 4.29 | 0.17 | 0.13 | 8.27 | 99.68 | ∞ |
| **ET48** | | 39.31 | 3.25 | 45.31 | 3.11 | 0.12 | 0.14 | 8.52 | 99.76 | ∞ |
| **ET80** | | 39.17 | 3.33 | 44.98 | 3.48 | 0.11 | 0.13 | 8.57 | 99.77 | ∞ |
| **ET36** | | 44.10 | 1.75 | 43.74 | 1.44 | 0.07 | 0.12 | 8.66 | 99.88 | ∞ |
| **ET42** | | 45.82 | 1.29 | 43.41 | 1.21 | 0.05 | 0.13 | 8.02 | 99.93 | ∞ |
| **Africa** | | | | | | | | | | |
| **Ka196** | | 38.04 | 2.23 | 43.45 | 3.94 | 0.38 | 0.17 | 11.48 | 99.70 | ≠ |
| **Ka197** | | 39.76 | 2.52 | 46.33 | 2.78 | 0.09 | 0.14 | 8.11 | 99.74 | ≠ |
| **Ka198** | | 39.77 | 2.44 | 45.95 | 2.71 | 0.14 | 0.14 | 8.61 | 99.76 | ≠ |
| **Ka199** | | 38.26 | 3.14 | 46.90 | 3.07 | 0.15 | 0.13 | 7.99 | 99.65 | ≠ |
| **Ka200** | | 41.21 | 2.00 | 45.81 | 2.43 | 0.05 | 0.14 | 8.20 | 99.84 | ≠ |
| **Ka201** | | 45.42 | 1.57 | 42.79 | 1.56 | 0.05 | 0.14 | 8.32 | 99.84 | ≠ |
| **Ka202** | | 42.04 | 2.02 | 45.09 | 1.48 | 0.15 | 0.16 | 8.74 | 99.68 | ≠ |
| **Ka203** | | 45.36 | 1.22 | 44.64 | 0.99 | 0.09 | 0.12 | 7.43 | 99.85 | ≠ |
| **Ka204** | | 40.02 | 3.66 | 44.50 | 2.83 | 0.15 | 0.14 | 8.30 | 99.59 | ≠ |
| **Ka205** | | 45.47 | 1.20 | 45.07 | 0.79 | 0.06 | 0.11 | 7.13 | 99.84 | ≠ |
| **Ka206** | | 38.97 | 3.06 | 45.74 | 3.33 | 0.16 | 0.13 | 8.20 | 99.59 | ≠ |
| **Ka207** | | 41.72 | 2.14 | 45.14 | 2.80 | 0.11 | 0.12 | 7.75 | 99.77 | ≠ |
| **Ka208** | | 44.62 | 1.12 | 44.49 | 1.20 | 0.08 | 0.13 | 8.24 | 99.88 | ≠ |
| **Algeria, Hoggar** | | | | | | | | | | |
| **Ka209** | | 41.51 | 2.34 | 44.41 | 1.84 | 0.23 | 0.15 | 9.20 | 99.69 | Φ |
| **Ka210** | | 40.46 | 2.54 | 46.24 | 2.65 | 0.07 | 0.13 | 7.60 | 99.70 | Φ |
| **Ka211** | | 39.87 | 3.33 | 44.52 | 2.86 | 0.10 | 0.14 | 8.81 | 99.64 | Φ |
| **Ka212** | | 39.87 | 3.46 | 44.67 | 2.98 | 0.11 | 0.13 | 8.55 | 99.77 | Φ |

cont..

## Appendix E (I) African

Non-cratonic major element oxides African peridotite xenolith siute

| Sample | $Na_2O$ | MgO | $Al_2O_3$ | $SiO_2$ | CaO | $TiO_2$ | MnO | FeO* | Total | Ref |
|---|---|---|---|---|---|---|---|---|---|---|
| **Algeria, Hoggar cont..** | | | | | | | | | | |
| **Ka213** | | 35.62 | 3.84 | 46.41 | 3.29 | 0.17 | 0.16 | 10.20 | 99.70 | Φ |
| **Ka214** | | 38.40 | 3.93 | 46.13 | 2.53 | 0.11 | 0.14 | 8.57 | 99.81 | Φ |
| **Ka215** | | 34.92 | 4.55 | 47.79 | 3.79 | 0.14 | 0.15 | 8.37 | 99.71 | Φ |
| **Ka216** | | 40.97 | 2.03 | 46.73 | 2.24 | 0.07 | 0.13 | 7.65 | 99.84 | Φ |
| **Ka217** | | 41.09 | 2.23 | 45.80 | 2.32 | 0.06 | 0.14 | 8.19 | 99.84 | Φ |
| **Ka218** | | 40.89 | 2.25 | 45.89 | 2.43 | 0.07 | 0.14 | 8.17 | 99.84 | Φ |

∞ Bedini et al, 1997, East African Rift. ≠ Dautria & Girod, 1987, Africa Φ Dupuy et al, 1986, Algeria, Hoggar Oxides in wt.%

## Appendix E (II) Australian

Non-cratonic major element oxides Australian peridotite xenolith sute

| Sample | $Na_2O$ | MgO | $Al_2O_3$ | $SiO_2$ | CaO | $TiO_2$ | MnO | FeO* | Total | Ref |
|---|---|---|---|---|---|---|---|---|---|---|
| **SE Australia** | | | | | | | | | | |
| **FG 2604** | | 47.67 | 1.08 | 43.27 | 0.58 | 0.02 | 0.13 | 7.13 | 99.89 | † |
| **FG 2669** | | 46.22 | 0.86 | 44.39 | 0.76 | 0.00 | 0.13 | 7.47 | 99.84 | † |
| **FG 2640** | | 43.87 | 1.02 | 43.77 | 0.97 | 0.03 | 0.15 | 10.04 | 99.85 | † |
| **FG 2728** | | 43.43 | 2.13 | 44.42 | 2.31 | 0.01 | 0.13 | 7.39 | 99.81 | † |
| **FG 2700** | | 42.74 | 1.45 | 44.18 | 2.87 | 0.00 | 0.11 | 8.30 | 99.66 | † |
| **FG 2642** | | 40.86 | 3.00 | 45.52 | 2.52 | 0.06 | 0.13 | 7.71 | 99.80 | † |
| **VIC 2730** | | 43.50 | 1.43 | 45.89 | 0.87 | 0.03 | 0.11 | 8.02 | 99.86 | □ |
| **VIC 2736** | | 43.08 | 1.44 | 46.55 | 0.88 | 0.03 | 0.12 | 7.85 | 99.95 | □ |
| **VIC 2769** | | 41.93 | 2.02 | 44.99 | 1.85 | 0.07 | 0.13 | 8.77 | 99.76 | □ |
| **VIC 84-402** | | 43.80 | 1.32 | 45.07 | 0.86 | 0.04 | 0.13 | 8.69 | 99.91 | □ |
| **VIC 84-413** | | 35.58 | 2.91 | 45.06 | 2.62 | 0.84 | 0.16 | 10.79 | 97.96 | □ |
| **VIC 84-438** | | 39.12 | 2.56 | 43.23 | 3.74 | 0.35 | 0.15 | 9.38 | 98.54 | □ |
| **VIC 85-168** | | 41.92 | 1.48 | 44.41 | 1.13 | 0.12 | 0.15 | 10.51 | 99.73 | □ |
| **70965** | | 41.29 | 0.99 | 44.28 | 4.33 | 0.08 | 0.15 | 8.28 | 99.40 | Δ |
| **70969** | | 44.87 | 0.49 | 42.11 | 2.27 | 0.04 | 0.16 | 9.53 | 99.47 | Δ |
| **70972** | | 44.31 | 0.69 | 43.28 | 3.60 | 0.02 | 0.13 | 7.47 | 99.50 | Δ |
| **70987** | | 43.43 | 1.02 | 43.61 | 2.03 | 0.15 | 0.15 | 9.19 | 99.59 | Δ |
| **70997** | | 42.07 | 0.92 | 42.68 | 3.82 | 0.10 | 0.16 | 9.89 | 99.64 | Δ |
| **71000** | | 42.25 | 1.22 | 42.94 | 3.79 | 0.06 | 0.15 | 8.68 | 99.09 | Δ |
| **71001** | | 42.92 | 0.93 | 41.56 | 2.74 | 0.10 | 0.18 | 10.06 | 98.50 | Δ |
| **71004** | | 43.20 | 1.46 | 42.40 | 3.40 | 0.20 | 0.14 | 8.72 | 99.51 | Δ |
| **71007** | | 43.10 | 1.12 | 43.80 | 2.39 | 0.06 | 0.14 | 8.89 | 99.51 | Δ |
| **7108** | | 41.71 | 1.09 | 42.11 | 3.17 | 0.05 | 0.16 | 10.78 | 99.08 | Δ |
| **2631** | | 43.65 | 0.94 | 43.29 | 2.75 | 0.07 | 0.15 | 8.34 | 99.19 | Δ |
| **E. Australia** | | | | | | | | | | |
| **BM 20** | | 43.34 | 1.74 | 44.43 | 1.25 | 0.11 | 0.13 | 8.86 | 99.86 | ‡ |
| **GN 14** | | 40.46 | 3.14 | 45.27 | 2.44 | 0.06 | 0.13 | 8.51 | 100.00 | ‡ |
| **GN 13** | | 44.55 | 1.04 | 44.97 | 1.21 | 0.02 | 0.12 | 7.99 | 99.90 | ‡ |
| **GN 24** | | 39.01 | 2.45 | 43.32 | 3.47 | 0.26 | 0.18 | 11.09 | 99.79 | ‡ |
| **GN 5** | | 45.61 | 0.62 | 42.91 | 1.58 | 0.06 | 0.14 | 8.57 | 99.49 | ‡ |
| **BM 18** | | 40.95 | 0.80 | 44.19 | 0.80 | 0.06 | 0.17 | 12.86 | 99.82 | ‡ |

cont..

## Appendix E (II) Australian

Non-cratonic major element oxides Australian peridotite xenolith sute

| Sample | $Na_2O$ | MgO | $Al_2O_3$ | $SiO_2$ | CaO | $TiO_2$ | MnO | FeO* | Total | Ref |
|---|---|---|---|---|---|---|---|---|---|---|
| **GN 8** | | 41.30 | 1.99 | 44.81 | 1.97 | 0.03 | 0.14 | 9.05 | 99.30 | ‡ |
| **GN 4** | | 39.37 | 2.84 | 44.95 | 2.69 | 0.03 | 0.14 | 9.09 | 99.11 | ‡ |
| **GN 11** | | 41.06 | 1.67 | 45.08 | 3.09 | 0.08 | 0.14 | 8.06 | 99.18 | ‡ |
| **GN 16** | | 38.70 | 3.38 | 44.98 | 3.07 | 0.07 | 0.14 | 8.84 | 99.18 | ‡ |
| **GN 20** | | 39.82 | 2.50 | 45.32 | 2.63 | 0.04 | 0.14 | 8.78 | 99.23 | ‡ |
| **GN 12** | | 39.28 | 2.67 | 45.16 | 3.09 | 0.05 | 0.14 | 8.70 | 99.10 | ‡ |
| **GN 2** | | 38.49 | 2.12 | 44.13 | 2.37 | 0.04 | 0.17 | 11.88 | 99.20 | ‡ |
| **GN 6** | | 45.27 | 0.53 | 43.54 | 1.72 | 0.02 | 0.14 | 8.55 | 99.77 | ‡ |
| **GN3** | | 38.90 | 2.91 | 43.65 | 4.19 | 0.16 | 0.14 | 9.08 | 99.04 | ‡ |
| **Australia, Queensland** | | | | | | | | | | |
| **Ka180** | | 39.06 | 3.17 | 45.44 | 2.55 | 0.11 | 0.17 | 9.09 | 99.60 | ○ |
| **Ka181** | | 38.71 | 3.37 | 45.07 | 3.29 | 0.10 | 0.15 | 8.91 | 99.61 | ○ |

† Frey & Green, 1974
□ McDonough, unpublished
Δ Yaxley et al, 1991
‡ Stoltz & Davies, 1988, E. Australia
○ Griffin et al, 1987, Australia, Queensland

Oxides in wt.%

## Appendix E (III) Mongolian

Non-cratonic major element oxides Mongolian peridotite xenolith siute

| Sample | $Na_2O$ | MgO | $Al_2O_3$ | $SiO_2$ | CaO | $TiO_2$ | MnO | FeO* | Total | Ref |
|---|---|---|---|---|---|---|---|---|---|---|
| **Mongolia** | | | | | | | | | | |
| **Mo101** | | 37.48 | 4.48 | 45.03 | 4.17 | 0.19 | 0.13 | 7.70 | 99.18 | ♦ |
| **Mo102** | | 42.43 | 2.62 | 44.29 | 2.39 | 0.07 | 0.13 | 7.53 | 99.45 | ♦ |
| **Mo103** | | 43.28 | 2.34 | 44.21 | 1.80 | 0.05 | 0.13 | 7.57 | 99.38 | ♦ |
| **Mo104** | | 41.63 | 3.03 | 44.56 | 2.25 | 0.11 | 0.13 | 7.81 | 99.53 | ♦ |
| **Mo105** | | 35.94 | 5.29 | 45.97 | 4.36 | 0.21 | 0.13 | 7.33 | 99.23 | ♦ |
| **Mo-z/1** | | 37.15 | 4.29 | 42.75 | 6.83 | 0.18 | 0.13 | 7.92 | 99.24 | ♦ |
| **MHP 79/1** | | 39.15 | 4.23 | 44.57 | 2.97 | 0.15 | 0.13 | 8.07 | 99.27 | ♦ |
| **MHP 79/2** | | 38.21 | 4.40 | 45.31 | 3.26 | 0.17 | 0.13 | 7.83 | 99.32 | ♦ |
| **MHP 79/3** | | 41.86 | 3.24 | 43.96 | 2.28 | 0.10 | 0.13 | 7.88 | 99.45 | ♦ |
| **MHP 79/4** | | 42.20 | 3.13 | 44.15 | 2.04 | 0.10 | 0.13 | 7.76 | 99.52 | ♦ |
| **Mo 4230/16** | | 37.53 | 4.57 | 44.73 | 3.93 | 0.23 | 0.13 | 8.25 | 99.37 | ♦ |
| **Mo 22** | | 40.20 | 3.56 | 44.24 | 2.78 | 0.13 | 0.14 | 8.27 | 99.32 | ♦ |

♦ Press et al, 1986, Mongolia

Oxides in wt.%

## Appendix E (IV) China

Non-cratonic major element oxides China peridotite xenolith siute

| Sample | $Na_2O$ | MgO | $Al_2O_3$ | $SiO_2$ | CaO | $TiO_2$ | MnO | FeO* | Total | Ref |
|---|---|---|---|---|---|---|---|---|---|---|
| **S.E. China** | | | | | | | | | | |
| **M33** | | 34.16 | 5.43 | 46.28 | 5.40 | 0.31 | 0.13 | 7.80 | 99.50 | ◊ |
| **M38** | | 37.44 | 3.98 | 46.19 | 3.44 | 0.18 | 0.12 | 8.46 | 99.81 | ◊ |
| **M31** | | 38.64 | 3.61 | 45.37 | 3.29 | 0.19 | 0.14 | 8.46 | 99.71 | ◊ |
| **M6** | | 39.11 | 3.72 | 45.21 | 2.98 | 0.14 | 0.13 | 8.43 | 99.72 | ◊ |
| **M44** | | 42.55 | 2.44 | 44.47 | 1.91 | 0.09 | 0.12 | 8.26 | 99.85 | ◊ |
| **M24** | | 43.15 | 1.65 | 45.20 | 1.79 | 0.03 | 0.12 | 7.98 | 99.93 | ◊ |
| **NS28** | | 41.56 | 2.24 | 45.47 | 1.92 | 0.07 | 0.13 | 8.33 | 99.73 | ◊ |
| **M40** | | 47.38 | 0.88 | 42.95 | 0.58 | 0.06 | 0.12 | 7.97 | 99.94 | ◊ |
| **M25** | | 44.24 | 0.90 | 45.66 | 0.83 | 0.03 | 0.11 | 8.12 | 99.90 | ◊ |
| **NS25** | | 39.25 | 1.34 | 42.37 | 3.80 | 0.21 | 0.20 | 12.41 | 99.59 | ◊ |
| **China, Hannuoba** | | | | | | | | | | |
| **Ka174** | | 40.74 | 2.70 | 45.13 | 2.21 | 0.06 | 0.14 | 8.84 | 99.82 | ♣ |
| **Ka175** | | 42.36 | 2.28 | 43.70 | 1.84 | 0.06 | 0.14 | 9.46 | 99.85 | ♣ |
| **Ka176** | | 40.28 | 2.73 | 45.69 | 2.54 | 0.09 | 0.13 | 8.36 | 99.81 | ♣ |
| **Ka177** | | 42.55 | 1.93 | 45.28 | 1.56 | 0.07 | 0.13 | 8.36 | 99.87 | ♣ |
| **Ka178** | | 42.01 | 1.71 | 45.73 | 1.94 | 0.05 | 0.13 | 8.30 | 99.88 | ♣ |
| **Ka179** | | 44.33 | 1.28 | 44.38 | 1.24 | 0.02 | 0.13 | 8.54 | 99.93 | ♣ |

◊ Qi et al, 1995, S.E. China

♣ Song & Frey, 1989. China, Hannuoba

Oxides in wt.%

## Appendix E (V) Beni Bousera

Non-cratonic major element oxides Beni Bousera, Morocco peridotite xenolith suite

| Sample | $Na_2O$ | MgO | $Al_2O_3$ | $SiO_2$ | CaO | $TiO_2$ | MnO | FeO* | Total | Ref |
|---|---|---|---|---|---|---|---|---|---|---|
| **GP13** | 0.3 | 39.79 | 3.45 | 44.91 | 3.01 | 0.14 | 0.15 | 8.19 | 99.94 | † |
| **GP91** | 0 | 46.35 | 0.72 | 43.91 | 0.56 | 0.02 | 0.14 | 8.27 | 99.97 | † |
| **GP132** | 0.47 | 46.11 | 1.28 | 42.99 | 0.82 | 0.03 | 0.14 | 8.13 | 99.97 | † |
| **GP189** | 0.1 | 43.63 | 2.04 | 44.29 | 1.88 | 0.04 | 0.14 | 7.86 | 99.98 | † |
| **GP191** | 0.31 | 41.11 | 3.09 | 44.13 | 2.8 | 0.11 | 0.15 | 8.29 | 99.99 | † |
| **GP220** | 0.58 | 44.68 | 1.61 | 43.91 | 1.44 | 0.02 | 0.14 | 7.6 | 99.98 | † |
| **GP178** | 0.15 | 46.99 | 0.91 | 42.78 | 0.83 | 0.05 | 0.13 | 8.13 | 99.97 | † |
| **GP222** | 0.31 | 41.17 | 2.89 | 44.89 | 2.43 | 0.12 | 0.15 | 8.05 | 100.01 | † |
| **GP240** | 0.51 | 40.73 | 3.13 | 44.73 | 2.16 | 0.11 | 0.14 | 8.01 | 99.52 | † |

† Pearson et al, 2004

Oxides in Wt. %

## Appendix E (VI) Vitim

Non-cratonic major element oxides Vitim, Siberia peridotite xenolith suite

| Sample | $Na_2O$ | MgO | $Al_2O_3$ | $SiO_2$ | CaO | $TiO_2$ | MnO | FeO* | Total | Ref |
|---|---|---|---|---|---|---|---|---|---|---|
| **314-72** | 0.17 | 40.11 | 2.62 | 44.56 | 2.03 | 0.11 | 0.13 | 8.36 | 98.09 | † |
| **314-74** | 0.2 | 41.8 | 2.84 | 44.2 | 2.35 | 0.1 | | 7.91 | 99.40 | † |
| **314-6** | 0.11 | 43.75 | 1.53 | 44.45 | 1.4 | 0.06 | | 7.53 | 98.83 | † |
| **314-58** | 0.3 | 39.6 | 3.93 | 44.3 | 3.28 | 0.15 | | 8.16 | 99.72 | † |
| **314-59** | 0.33 | 39.9 | 3.4 | 44.4 | 3.54 | 0.12 | | 7.84 | 99.53 | † |
| **313-6** | 0.3 | 38.95 | 3.88 | 43.95 | 3.04 | 0.15 | | 8.3 | 98.57 | † |
| **313-54** | 0.36 | 38.7 | 4.1 | 44.6 | 3.42 | 0.16 | | 7.9 | 99.24 | † |
| **313-102** | 0.33 | 36.66 | 4.65 | 45.25 | 3.37 | 0.13 | 0.15 | 8.17 | 98.71 | † |
| **313-104** | 0.36 | 38.08 | 3.7 | 44.92 | 3.45 | 0.16 | 0.14 | 8.24 | 99.05 | † |
| **314-5a** | 0.11 | 43.7 | 1.43 | 42.9 | 0.5 | 0.08 | | 10.01 | 98.73 | † |
| **313-05** | 0.24 | 39.15 | 3.41 | 44.45 | 2.83 | 0.12 | | 7.92 | 98.12 | † |

† Pearson et al, 2004

Oxides in Wt. %

# Appendix F

## Non-cratonic Data
## European
## Major Elements

## Appendix F (I) Hungarian

Non-cratonic major element oxides Hungarian peridotite xenolith suite

| Sample | $Na_2O$ | MgO | $Al_2O_3$ | $SiO_2$ | CaO | $TiO_2$ | MnO | FeO* | Total | Ref |
|---|---|---|---|---|---|---|---|---|---|---|
| **Hungary** | | | | | | | | | | |
| **Bo-1022** | | 45.87 | 1.32 | 44.39 | 0.64 | 0.02 | 0.12 | 7.62 | 99.98 | † |
| **Szg-1001** | | 39.84 | 3.98 | 44.43 | 3.09 | 0.15 | 0.15 | 8.08 | 99.72 | † |
| **Szg-1087** | | 32.54 | 3.83 | 52.02 | 4.86 | 0.05 | 0.12 | 6.39 | 99.81 | † |
| **Szt-1002** | | 39.31 | 3.53 | 45.58 | 3.34 | 0.08 | 0.14 | 7.82 | 99.81 | † |
| **Szt-1006** | | 41.23 | 2.96 | 44.08 | 2.57 | 0.16 | 0.13 | 8.61 | 99.74 | † |
| **Szg-1009** | | 40.60 | 3.50 | 44.74 | 2.69 | 0.10 | 0.13 | 8.06 | 99.82 | † |
| **Szt 1016** | | 45.47 | 0.95 | 45.06 | 0.65 | 0.02 | 0.12 | 7.72 | 99.99 | † |
| **Szt 1033** | | 41.50 | 2.12 | 45.66 | 1.85 | 0.08 | 0.14 | 8.59 | 99.95 | † |
| **Szt 1034** | | 44.68 | 1.31 | 44.46 | 1.15 | 0.04 | 0.13 | 8.11 | 99.88 | † |
| **Szt 1106** | | 38.72 | 3.65 | 44.15 | 4.59 | 0.16 | 0.14 | 8.28 | 99.69 | † |
| **Szt 1108** | | 39.68 | 3.51 | 45.09 | 3.00 | 0.14 | 0.13 | 8.22 | 99.79 | † |
| **Szt 1116** | | 44.84 | 1.26 | 44.12 | 1.06 | 0.04 | 0.13 | 8.43 | 99.88 | † |
| **Szt-1120** | | 38.82 | 3.94 | 45.71 | 2.97 | 0.12 | 0.14 | 8.17 | 99.87 | † |
| **G-1055** | | 40.31 | 3.19 | 44.12 | 3.17 | 0.14 | 0.13 | 8.70 | 99.77 | † |
| **G-1067** | | 41.79 | 2.05 | 45.73 | 1.96 | 0.04 | 0.12 | 8.28 | 99.97 | † |
| **G-1071** | | 40.24 | 3.05 | 44.60 | 3.15 | 0.11 | 0.12 | 8.59 | 99.86 | † |

† Embey-Isztin et al, 1989, Hugary

Oxides in Wt. %

## Appendix F (II) Romanian

Non-cratonic major element oxides Romanian peridotite xenolith suite

| Sample | $Na_2O$ | MgO | $Al_2O_3$ | $SiO_2$ | CaO | $TiO_2$ | MnO | FeO* | Total | Ref |
|---|---|---|---|---|---|---|---|---|---|---|
| **Romania** | | | | | | | | | | |
| **BG01** | | 45.87 | 0.92 | 43.62 | 1.49 | 0.03 | 0.12 | 7.92 | 99.97 | □ |
| **BG02** | | 39.88 | 3.06 | 44.59 | 3.24 | 0.12 | 0.13 | 8.68 | 99.71 | □ |
| **BG04** | | 42.89 | 2.04 | 44.34 | 1.74 | 0.10 | 0.12 | 8.26 | 99.49 | □ |
| **BG07** | | 39.10 | 3.65 | 45.33 | 3.03 | 0.15 | 0.12 | 8.40 | 99.78 | □ |
| **BG09** | | 40.39 | 3.06 | 45.15 | 2.63 | 0.12 | 0.13 | 8.18 | 99.67 | □ |
| **BG10** | | 41.92 | 2.84 | 44.33 | 2.54 | 0.10 | 0.12 | 7.95 | 99.80 | □ |
| **BG15** | | 40.61 | 3.23 | 45.11 | 2.84 | 0.12 | 0.12 | 7.86 | 99.90 | □ |
| **BG16** | | 43.51 | 2.30 | 44.14 | 1.83 | 0.08 | 0.12 | 7.91 | 99.90 | □ |
| **BG18** | | 41.06 | 2.78 | 44.39 | 2.72 | 0.12 | 0.13 | 8.27 | 99.47 | □ |
| **BGt.3** | | 39.61 | 3.82 | 45.19 | 3.21 | 0.15 | 0.13 | 7.69 | 99.80 | □ |
| **Bgt.6** | | 37.72 | 4.29 | 45.39 | 4.06 | 0.18 | 0.13 | 7.99 | 99.76 | □ |
| **Bgt.7** | | 39.42 | 3.73 | 44.99 | 3.16 | 0.15 | 0.13 | 8.26 | 99.86 | □ |
| **Bgt.13** | | 38.99 | 3.90 | 45.13 | 3.25 | 0.17 | 0.13 | 8.20 | 99.76 | □ |
| **Bgt.17** | | 36.45 | 4.24 | 46.95 | 3.45 | 0.21 | 0.13 | 8.39 | 99.81 | □ |
| **Bgt.18** | | 41.58 | 2.51 | 44.54 | 2.07 | 0.09 | 0.13 | 8.99 | 99.91 | □ |
| **Bgt.19** | | 42.16 | 2.67 | 44.33 | 2.30 | 0.09 | 0.13 | 8.20 | 99.89 | □ |
| **Bgt.21** | | 42.27 | 2.43 | 44.70 | 2.15 | 0.08 | 0.12 | 8.14 | 99.90 | □ |
| **Bgt.22** | | 42.32 | 2.52 | 44.36 | 2.14 | 0.08 | 0.12 | 8.32 | 99.86 | □ |
| **BC-01** | | 38.49 | 2.98 | 44.21 | 2.82 | 0.10 | 0.19 | 10.97 | 99.76 | □ |
| **BC-02** | | 40.46 | 3.42 | 44.33 | 2.93 | 0.12 | 0.15 | 8.28 | 99.69 | □ |
| **BC-09** | | 43.13 | 2.00 | 44.39 | 2.04 | 0.05 | 0.13 | 8.21 | 99.95 | □ |
| **LGR.9** | | 41.13 | 3.22 | 44.31 | 2.76 | 0.10 | 0.13 | 8.08 | 99.74 | □ |

□ Vaselli et al, 1995, Romania

Oxides in Wt. %

## Appendix F (III) Italian

Non-cratonic major element oxides Itallian peridotite xenolith suite

| Sample | $Na_2O$ | MgO | $Al_2O_3$ | $SiO_2$ | CaO | $TiO_2$ | MnO | FeO* | Total | Ref |
|---|---|---|---|---|---|---|---|---|---|---|
| **Italy** | | | | | | | | | | |
| **Ka182** | | 38.78 | 3.68 | 44.83 | 3.36 | 0.14 | 0.17 | 8.61 | 99.58 | Δ |
| **Ka183** | | 39.71 | 3.85 | 42.98 | 3.78 | 0.24 | 0.17 | 8.84 | 99.57 | Δ |
| **Ka184** | | 40.39 | 3.13 | 42.89 | 3.58 | 0.12 | 0.18 | 9.38 | 99.67 | Δ |
| **Ka185** | | 38.75 | 4.27 | 43.46 | 1.10 | 0.30 | 0.26 | 11.43 | 99.57 | Δ |
| **Ka186** | | 39.62 | 2.84 | 43.81 | 3.44 | 0.18 | 0.18 | 9.64 | 99.71 | Δ |
| **Ka187** | | 39.80 | 2.88 | 44.35 | 2.15 | 0.28 | 0.19 | 10.14 | 99.79 | Δ |
| **Ka188** | | 43.29 | 1.77 | 39.89 | 0.82 | 0.25 | 0.23 | 13.28 | 99.54 | Δ |
| **Ka189** | | 41.96 | 2.60 | 42.88 | 2.01 | 0.16 | 0.19 | 9.64 | 99.43 | Δ |
| **Ka190** | | 37.79 | 3.92 | 44.81 | 3.56 | 0.17 | 0.17 | 8.98 | 99.40 | Δ |
| **Ka191** | | 42.27 | 3.26 | 43.19 | 1.48 | 0.12 | 0.17 | 8.66 | 99.16 | Δ |
| **Ka192** | | 39.11 | 3.29 | 42.16 | 3.71 | 0.36 | 0.20 | 10.63 | 99.46 | Δ |
| **Ka193** | | 41.89 | 1.80 | 41.25 | 1.72 | 0.27 | 0.22 | 12.57 | 99.72 | Δ |
| **Ka194** | | 39.65 | 3.67 | 45.27 | 3.23 | 0.13 | 0.15 | 7.59 | 99.67 | Δ |
| **Ka195** | | 38.75 | 5.79 | 43.43 | 3.59 | 0.19 | 0.16 | 7.76 | 99.67 | Δ |
| **Ka225** | | 49.67 | 0.30 | 41.30 | 0.25 | 0.01 | 0.12 | 8.28 | 99.94 | ‡ |
| **Ka226** | | 45.97 | 0.67 | 45.22 | 0.45 | 0.01 | 0.12 | 7.50 | 99.93 | ‡ |
| **Ka227** | | 45.67 | 1.01 | 43.66 | 1.50 | 0.05 | 0.12 | 7.78 | 99.79 | ‡ |
| **Ka228** | | 46.63 | 1.08 | 42.98 | 0.51 | 0.03 | 0.13 | 8.54 | 99.90 | ‡ |
| **Ka229** | | 45.53 | 1.13 | 44.49 | 0.87 | 0.04 | 0.13 | 7.67 | 99.86 | ‡ |
| **Ka230** | | 44.58 | 1.31 | 41.92 | 3.24 | 0.07 | 0.14 | 8.44 | 99.70 | ‡ |
| **Ka231** | | 44.62 | 1.33 | 44.45 | 0.95 | 0.02 | 0.15 | 8.33 | 99.85 | ‡ |
| **Ka232** | | 45.29 | 1.56 | 43.96 | 1.18 | 0.01 | 0.12 | 7.80 | 99.93 | ‡ |
| **Ka233** | | 41.68 | 1.99 | 45.81 | 2.24 | 0.02 | 0.13 | 7.92 | 99.80 | ‡ |
| **Ka234** | | 41.78 | 2.05 | 46.30 | 1.44 | 0.04 | 0.14 | 8.05 | 99.81 | ‡ |
| **Ka235** | | 41.36 | 2.52 | 45.63 | 2.12 | 0.05 | 0.13 | 7.94 | 99.75 | ‡ |
| **Ka236** | | 39.38 | 2.84 | 46.71 | 2.58 | 0.11 | 0.14 | 8.04 | 99.80 | ‡ |

Δ Morten, Italy ‡ Dupuy et al, 1987 Oxides in Wt. %

## Appendix F (IV) British

Non-cratonic major element oxides British peridotite xenolith suite

| Sample | $Na_2O$ | MgO | $Al_2O_3$ | $SiO_2$ | CaO | $TiO_2$ | MnO | FeO* | Total | Ref |
|---|---|---|---|---|---|---|---|---|---|---|
| **British Isles** | | | | | | | | | | |
| **Ka219** | | 42.69 | 2.13 | 44.75 | 2.38 | 0.07 | 0.12 | 7.75 | 99.90 | ○ |
| **Ka220** | | 39.28 | 2.55 | 45.60 | 3.72 | 0.21 | 0.12 | 7.80 | 99.27 | ○ |
| **Ka221** | | 41.36 | 2.49 | 44.82 | 2.72 | 0.20 | 0.06 | 8.10 | 99.76 | ○ |
| **Ka222** | | 41.97 | 2.12 | 44.53 | 2.52 | 0.07 | 0.14 | 7.95 | 99.30 | ○ |

○ Hunter & Upton, British Isles

Oxides in Wt. %

# Appendix G

## Other Peridotite Suites
## Platinum Group Element Data

## Appendix G (I) Kaapvaal xenolith suite Pearson et al, 1995.

| | Measured | | | | | | Chondrite normalised | | | | | |
|---|---|---|---|---|---|---|---|---|---|---|---|---|
| **Samp No.** | **Os (ppb)** | **Ir (ppb)** | **Ru (ppb)** | **Pt (ppb)** | **Pd (ppb)** | **Re (ppb)** | **Os (ppb)** | **Ir (ppb)** | **Ru (ppb)** | **Pt (ppb)** | **Pd (ppb)** | **Re (ppb)** |
| **FRB1431** | 1.7610 | 2.04 | 2.93 | 315 | 0.299 | 0.0110 | | | | | | |
| **FRB1382** | 3.7911 | 2.89 | 4.64 | 5.94 | 4.65 | 0.1288 | | | | | | |
| **Low-T Spinel** | | | | | | | | | | | | |
| **FRB979#** | 0.8040 | | | | | 0.1330 | 0.0017 | | | | | 0.0035 |
| **FRB1001#** | 3.5700 | | | | | 0.1160 | 0.0073 | | | | | 0.0031 |
| **PHN2600** | 0.6250 | | | | | 0.0350 | 0.0013 | | | | | 0.0009 |
| **PHN5266** | 3.2500 | | | | | 0.1180 | 0.0067 | | | | | 0.0031 |
| **PHN5254** | 6.1300 | | | | | 0.1060 | 0.0126 | | | | | 0.0028 |
| **PHN5275** | 8.2300 | | | | | 0.1030 | 0.0169 | | | | | 0.0027 |
| **Low-T Garnet** | | | | | | | | | | | | |
| ***F556** | 1.7300 | | | | | 0.0340 | 0.0036 | | | | | 0.0009 |
| ***F865** | 1.3800 | | | | | 0.0860 | 0.0028 | | | | | 0.0023 |
| ***F866** | 2.6600 | | | | | 0.0810 | 0.0055 | | | | | 0.0021 |
| **FRB921** | 2.6600 | | | | | 0.0530 | 0.0055 | | | | | 0.0014 |
| **FRB1350** | 3.3900 | | | | | 0.0260 | 0.0070 | | | | | 0.0007 |
| **PHN1569** | 2.6100 | | | | | 0.0790 | 0.0054 | | | | | 0.0021 |
| ***BD2125** | 0.0190 | | | | | 0.0410 | 0.0000 | | | | | 0.0011 |
| **PHN2302** | 1.5100 | | | | | 0.0150 | 0.0031 | | | | | 0.0004 |
| **PHN2823** | 9.2000 | | | | | 0.0730 | 0.0189 | | | | | 0.0019 |
| **PHN2825** | 1.4100 | | | | | 0.0950 | 0.0029 | | | | | 0.0025 |
| **PHN5273** | 3.1700 | | | | | 0.0320 | 0.0065 | | | | | 0.0008 |
| **PHN5595** | 4.2400 | | | | | 0.1350 | 0.0087 | | | | | 0.0036 |
| **High-T Garnet** | | | | | | | | | | | | |
| **FRB909** | 1.6900 | | | | | 0.0510 | 0.0035 | | | | | 0.0013 |
| **PHN1596** | 5.9400 | | | | | 0.0740 | 0.0122 | | | | | 0.0019 |
| **PHN1611** | 1.2600 | | | | | 0.2850 | 0.0026 | | | | | 0.0075 |
| **PHN5239** | 1.5400 | | | | | 0.1000 | 0.0032 | | | | | 0.0026 |
| **PHN5267** | 5.3300 | | | | | 0.0600 | 0.0110 | | | | | 0.0016 |
| **K7-318** | 2.4500 | | | | | 1.0300 | 0.005041 | | | | | 0.0271 |

* = diamond bearing samples

## Appendix G (II) Beni Bousera xenolith suite, Pearson et al, 2004

| | Measured | | | | | | Chondrite normalised | | | | | |
|---|---|---|---|---|---|---|---|---|---|---|---|---|
| Samp No. | Os (ppb) | Ir (ppb) | Ru (ppb) | Pt (ppb) | Pd (ppb) | Re (ppb) | Os (ppb) | Ir (ppb) | Ru (ppb) | Pt (ppb) | Pd (ppb) | Re (ppb) |
| **GP13** | 3.5780 | 3.2800 | 6.7100 | 6.6500 | 5.8500 | 0.3300 | 0.0074 | 0.0071 | 0.0094 | 0.0067 | 0.0105 | 0.0087 |
| **GP91** | 17.5220 | 4.7000 | 7.4000 | 7.0300 | 6.5800 | 0.0890 | 0.0361 | 0.0102 | 0.0104 | 0.0071 | 0.0118 | 0.0023 |
| **GP132** | 4.5300 | 4.1500 | 7.4600 | 9.7200 | 2.0700 | 0.0760 | 0.0093 | 0.0090 | 0.0104 | 0.0098 | 0.0037 | 0.0020 |
| **GP189** | 3.4400 | 3.2300 | 6.4900 | 6.7700 | 5.4000 | 0.1680 | 0.0071 | 0.0070 | 0.0091 | 0.0068 | 0.0097 | 0.0044 |
| **GP191** | 3.6300 | 3.2700 | 6.3600 | 6.7000 | 6.4800 | 0.2680 | 0.0075 | 0.0071 | 0.0089 | 0.0067 | 0.0117 | 0.0071 |
| **GP220** | 0.9195 | 3.3600 | 0.4030 | 4.3900 | 4.4600 | 0.0280 | 0.0019 | 0.0073 | 0.0006 | 0.0044 | 0.0080 | 0.0007 |
| **GP178** | 3.2800 | | | | | 0.1910 | 0.0067 | | | | | 0.0050 |
| **GP222** | 3.4100 | | | | | 0.2010 | 0.0070 | | | | | 0.0053 |
| **GP240** | 3.7900 | | | | | 0.2520 | 0.0078 | | | | | 0.0066 |

## Appendix G (III) Vitim, Pearson et al, 2004

| | Measured | | | | | | Chondrite normalised | | | | | |
|---|---|---|---|---|---|---|---|---|---|---|---|---|
| **Samp No.** | **Os (ppb)** | **Ir (ppb)** | **Ru (ppb)** | **Pt (ppb)** | **Pd (ppb)** | **Re (ppb)** | **Os (ppb)** | **Ir (ppb)** | **Ru (ppb)** | **Pt (ppb)** | **Pd (ppb)** | **Re (ppb)** |
| **314-72** | 0.8310 | 3.0100 | 4.7700 | 3.7200 | 2.0500 | 0.0390 | 0.0017 | 0.0066 | 0.0067 | 0.0037 | 0.0037 | 0.0010 |
| **314-74** | 0.4120 | 2.5300 | 4.3300 | 3.5200 | 2.1900 | 0.0700 | 0.0008 | 0.0055 | 0.0061 | 0.0035 | 0.0039 | 0.0018 |
| **314-6** | 0.4130 | 2.4300 | 6.2400 | 4.9500 | 2.1900 | 0.0250 | 0.0008 | 0.0053 | 0.0087 | 0.0050 | 0.0039 | 0.0007 |
| **314-58** | 0.9790 | 3.2600 | 6.4100 | 3.3000 | 2.4800 | 0.0530 | 0.0020 | 0.0071 | 0.0090 | 0.0033 | 0.0045 | 0.0014 |
| **314-59** | 0.4580 | 2.4600 | 4.1300 | 3.5900 | 2.3600 | 0.0670 | 0.0009 | 0.0054 | 0.0058 | 0.0036 | 0.0042 | 0.0018 |
| **313-6** | 0.7910 | 2.5500 | 4.8500 | 3.2100 | 1.6300 | 0.0250 | 0.0016 | 0.0056 | 0.0068 | 0.0032 | 0.0029 | 0.0007 |
| **313-54** | 0.8890 | 2.5800 | 6.9300 | 3.6100 | 2.0900 | 0.0240 | 0.0018 | 0.0056 | 0.0097 | 0.0036 | 0.0038 | 0.0006 |
| **313-102** | 0.5540 | 1.7000 | 3.4800 | 3.0200 | 1.9600 | 0.0690 | 0.0011 | 0.0037 | 0.0049 | 0.0030 | 0.0035 | 0.0018 |
| **313-104** | 0.7580 | 2.3900 | 4.8100 | 4.2300 | 2.5500 | 0.0260 | 0.0016 | 0.0052 | 0.0067 | 0.0043 | 0.0046 | 0.0007 |
| **314-5a** | 1.9000 | 3.8700 | 7.0500 | 2.8000 | 0.6340 | 0.0220 | 0.0039 | 0.0084 | 0.0099 | 0.0028 | 0.0011 | 0.0006 |
| **314-5b** | 0.4300 | 3.8800 | 7.0800 | 3.3200 | 0.8700 | 0.0220 | 0.0009 | 0.0085 | 0.0099 | 0.0033 | 0.0016 | 0.0006 |
| **313-05** | 0.9400 | 2.1700 | 4.0800 | 3.0600 | 1.7500 | 0.0160 | 0.0019 | 0.0047 | 0.0057 | 0.0031 | 0.0031 | 0.0004 |
| **314-71** | 0.5240 | 2.3900 | 3.9100 | 1.3400 | 1.3000 | 0.0400 | 0.0011 | 0.0052 | 0.0055 | 0.0013 | 0.0023 | 0.0011 |
| **86-1** | 0.7190 | | | | | 0.0430 | 0.0015 | | | | | 0.0011 |
| **313-37** | 0.8980 | | | | | 0.0270 | 0.0018 | | | | | 0.0007 |
| **313-240** | 0.6880 | | | | | 0.0260 | 0.0014 | | | | | 0.0007 |
| **314-580** | 0.9980 | | | | | 0.0360 | 0.0021 | | | | | 0.0009 |
| **314-56** | 0.9230 | | | | | 0.0240 | 0.0019 | | | | | 0.0006 |

## Appendix G (IV) Slave & Namibia

| | Measured | | | | | | Chondrite normalised | | | | | |
|---|---|---|---|---|---|---|---|---|---|---|---|---|
| **Samp No.** | **Os (ppb)** | **Ir (ppb)** | **Ru (ppb)** | **Pt (ppb)** | **Pd (ppb)** | **Re (ppb)** | **Os (ppb)** | **Ir (ppb)** | **Ru (ppb)** | **Pt (ppb)** | **Pd (ppb)** | **Re (ppb)** |
| **Slave** | | | | | | | | | | | | |
| **8 to 7** | 2.4700 | 2.0300 | 3.4700 | 0.2530 | 0.0490 | 0.0060 | 0.0051 | 0.0044 | 0.0049 | 0.0003 | 0.0001 | 0.0002 |
| **10 to 12A** | 3.1000 | 2.5300 | 4.1600 | 0.3380 | 0.0730 | 0.0360 | 0.0064 | 0.0055 | 0.0058 | 0.0003 | 0.0001 | 0.0009 |
| **40 to 21** | 2.4300 | 2.5200 | 5.4700 | 2.2600 | 0.8560 | 0.0337 | 0.0050 | 0.0055 | 0.0077 | 0.0023 | 0.0015 | 0.0009 |
| **Namibia** | | | | | | | | | | | | |
| **FRB1181** | 5.1100 | 4.9600 | 10.0200 | 5.9000 | 1.5600 | 0.0580 | 0.0105 | 0.0108 | 0.0140 | 0.0059 | 0.0028 | 0.0015 |
| **FRB1650** | 2.4900 | 3.2500 | 9.7900 | 3.1400 | 0.9200 | 0.0490 | 0.0051 | 0.0071 | 0.0137 | 0.0032 | 0.0017 | 0.0013 |
| **FRB1652** | 2.4700 | 2.5400 | 9.3800 | 3.5400 | 1.1800 | 0.0290 | 0.0051 | 0.0055 | 0.0131 | 0.0036 | 0.0021 | 0.0008 |
| **PHN5304** | 5.0100 | 4.5600 | 7.6900 | 2.9400 | 1.2100 | 0.3190 | 0.0103 | 0.0099 | 0.0108 | 0.0030 | 0.0022 | 0.0084 |
| **PHN5315** | 4.7500 | 3.6000 | 9.0800 | 4.8500 | 3.4300 | 0.1430 | 0.0098 | 0.0078 | 0.0127 | 0.0049 | 0.0062 | 0.0038 |
| **JJG2514** | 3.2300 | 2.8100 | 4.3700 | 2.7800 | 0.6400 | 0.1360 | 0.0066 | 0.0061 | 0.0061 | 0.0028 | 0.0012 | 0.0036 |

Slave = Kopylova & Russel, 2000
Namibia = Pearson et al., 2004

## Appendix G (V) Lesotho, Pearson et al, 2004

| | Measured | | | | | | Chondrite normalised | | | | | |
|---|---|---|---|---|---|---|---|---|---|---|---|---|
| Samp No. | Os (ppb) | Ir (ppb) | Ru (ppb) | Pt (ppb) | Pd (ppb) | Re (ppb) | Os (ppb) | Ir (ppb) | Ru (ppb) | Pt (ppb) | Pd (ppb) | Re (ppb) |
| **LET2** | 5.7100 | 5.2600 | 8.1700 | 3.7600 | 0.7320 | 0.3300 | 0.0117 | 0.0115 | 0.0114 | 0.0038 | 0.0013 | 0.0087 |
| **LET6** | 3.1800 | 1.7200 | 1.4200 | 0.1820 | 0.0350 | 0.1370 | 0.0065 | 0.0037 | 0.0020 | 0.0002 | 0.0001 | 0.0036 |
| **LET8** | 1.6000 | 1.8900 | 2.1600 | 0.2880 | 0.9300 | 0.2510 | 0.0033 | 0.0041 | 0.0030 | 0.0003 | 0.0017 | 0.0066 |
| **LET12** | 3.1600 | 2.6500 | 4.4400 | 0.5350 | 0.0740 | 0.1530 | 0.0065 | 0.0058 | 0.0062 | 0.0005 | 0.0001 | 0.0040 |
| **LET13** | 3.3100 | 3.3700 | 4.7000 | 0.8860 | 0.0220 | 0.0410 | 0.0068 | 0.0073 | 0.0066 | 0.0009 | 0.0000 | 0.0011 |
| **LET14** | 4.7000 | 4.6900 | 6.1900 | 1.5000 | 0.3780 | 0.0890 | 0.0097 | 0.0102 | 0.0087 | 0.0015 | 0.0007 | 0.0023 |
| **LET25** | 1.9800 | 2.2200 | 3.6500 | 2.1200 | 0.1210 | 0.1500 | 0.0041 | 0.0048 | 0.0051 | 0.0021 | 0.0002 | 0.0039 |
| **LET27** | 6.2500 | 5.4400 | 8.1200 | 3.9200 | 0.1020 | 0.3670 | 0.0129 | 0.0119 | 0.0114 | 0.0039 | 0.0002 | 0.0097 |
| **LET28** | 3.8800 | 3.3300 | 5.4100 | 2.4000 | 0.0280 | 0.0960 | 0.0080 | 0.0073 | 0.0076 | 0.0024 | 0.0001 | 0.0025 |
| **LET29** | 3.4400 | 1.7100 | 2.4500 | 1.4100 | 0.2110 | 0.2600 | 0.0071 | 0.0037 | 0.0034 | 0.0014 | 0.0004 | 0.0068 |
| **LET30** | 2.3700 | 2.3300 | 2.3800 | 0.2250 | 0.1110 | 0.2170 | 0.0049 | 0.0051 | 0.0033 | 0.0002 | 0.0002 | 0.0057 |
| **LET31** | 5.8200 | 4.1200 | 7.7400 | 2.6900 | 0.5180 | 0.2010 | 0.0120 | 0.0090 | 0.0108 | 0.0027 | 0.0009 | 0.0053 |
| **LET38** | 13.7000 | 8.5400 | 15.5200 | 9.6300 | 0.0390 | 0.0900 | 0.0282 | 0.0186 | 0.0217 | 0.0097 | 0.0001 | 0.0024 |
| **LET47** | 4.3500 | 4.2700 | 6.3900 | 3.3200 | 0.0280 | 0.1900 | 0.0090 | 0.0093 | 0.0089 | 0.0033 | 0.0001 | 0.0050 |
| **LET48** | 1.9900 | 2.2700 | 9.7300 | 3.1600 | 1.7600 | 0.2300 | 0.0041 | 0.0049 | 0.0136 | 0.0032 | 0.0032 | 0.0061 |
| **LET49** | 3.8600 | 3.8100 | 7.4400 | 6.7500 | 5.9200 | 0.1100 | 0.0079 | 0.0083 | 0.0104 | 0.0068 | 0.0106 | 0.0029 |
| **LET58** | 5.2200 | 4.1700 | 5.7100 | 4.2900 | 0.8510 | 0.3300 | 0.0107 | 0.0091 | 0.0080 | 0.0043 | 0.0015 | 0.0087 |
| **LET63** | 4.1300 | 3.6800 | 6.8800 | 3.7000 | 1.7580 | 0.0900 | 0.0085 | 0.0080 | 0.0096 | 0.0037 | 0.0032 | 0.0024 |
| **LET64** | 6.4200 | 6.4100 | 10.0000 | 7.4800 | 0.2410 | 0.6000 | 0.0132 | 0.0140 | 0.0140 | 0.0075 | 0.0004 | 0.0158 |

## Appendix G (VI) Somerset Island, Irvine et al, 2003

| | Measured | | | | | | Chondrite normalised | | | | | |
|---|---|---|---|---|---|---|---|---|---|---|---|---|
| Samp No. | Os (ppb) | Ir (ppb) | Ru (ppb) | Pt (ppb) | Pd (ppb) | Re (ppb) | Os (ppb) | Ir (ppb) | Ru (ppb) | Pt (ppb) | Pd (ppb) | Re (ppb) |
| **Batty Bay** | | | | | | | | | | | | |
| K11A14 | 2.3900 | 2.2000 | 4.4300 | 1.9800 | 1.4200 | 0.0300 | 0.0049 | 0.0048 | 0.0062 | 0.0020 | 0.0026 | 0.0008 |
| K11A15 | 2.3500 | 2.5000 | 5.4000 | 1.1100 | 6.8900 | 0.0200 | 0.0048 | 0.0054 | 0.0076 | 0.0011 | 0.0124 | 0.0005 |
| K11A16 | 3.2500 | 3.6600 | 6.6400 | 4.2100 | 1.4000 | 0.0500 | 0.0067 | 0.0080 | 0.0093 | 0.0042 | 0.0025 | 0.0013 |
| K11A17 | 2.5800 | 2.7500 | 6.0200 | 1.2500 | 0.9600 | 0.0200 | 0.0053 | 0.0060 | 0.0084 | 0.0013 | 0.0017 | 0.0005 |
| K11A18 | 0.6200 | 0.6400 | 1.2300 | 0.0900 | 0.4100 | 0.0100 | 0.0013 | 0.0014 | 0.0017 | 0.0001 | 0.0007 | 0.0003 |
| K12A1 | 3.6000 | 2.5600 | 4.5300 | 2.8200 | 1.4400 | 0.0500 | 0.0074 | 0.0056 | 0.0063 | 0.0028 | 0.0026 | 0.0013 |
| K13A1 | 4.4900 | 4.4200 | 9.8100 | 7.5400 | 1.7700 | 0.1300 | 0.0092 | 0.0096 | 0.0137 | 0.0076 | 0.0032 | 0.0034 |
| K13A3 | 4.2000 | 3.9700 | 7.1900 | 2.0800 | 0.5800 | 0.0300 | 0.0086 | 0.0086 | 0.0101 | 0.0021 | 0.0010 | 0.0008 |
| K13A4 | 2.2500 | 3.3200 | 6.1900 | 5.2400 | 3.9500 | 0.0400 | 0.0046 | 0.0072 | 0.0087 | 0.0053 | 0.0071 | 0.0011 |
| K13A5 | 3.7300 | 4.6600 | 8.6700 | 2.8100 | 1.7200 | 0.2200 | 0.0077 | 0.0102 | 0.0121 | 0.0028 | 0.0031 | 0.0058 |
| K13B4 | 4.1800 | 4.2500 | 6.1400 | 8.3200 | 0.4600 | 0.0100 | 0.0086 | 0.0093 | 0.0086 | 0.0084 | 0.0008 | 0.0003 |
| K15A4 | 1.8000 | 2.2000 | 7.5200 | 2.9200 | 0.6900 | 1.5000 | 0.0037 | 0.0048 | 0.0105 | 0.0029 | 0.0012 | 0.0395 |
| **Nord** | | | | | | | | | | | | |
| NIC | 3.3800 | 3.3100 | 6.3100 | 2.1900 | 1.2200 | 0.2100 | 0.0070 | 0.0072 | 0.0088 | 0.0022 | 0.0022 | 0.0055 |
| N2B | 1.7400 | 1.8700 | 3.8500 | 1.5900 | 0.9100 | 0.0300 | 0.0036 | 0.0041 | 0.0054 | 0.0016 | 0.0016 | 0.0008 |
| **Nikos** | | | | | | | | | | | | |
| X04 | 3.3100 | 3.1000 | 5.2800 | 3.8600 | 3.3800 | 0.2300 | 0.0068 | 0.0068 | 0.0074 | 0.0039 | 0.0061 | 0.0061 |
| X05 | 3.2300 | 2.9700 | 6.7800 | 1.9300 | 1.3400 | 0.3900 | 0.0066 | 0.0065 | 0.0095 | 0.0019 | 0.0024 | 0.0103 |
| X06 | 2.8700 | 2.6600 | 6.1200 | 2.4000 | 1.6400 | 0.1400 | 0.0059 | 0.0058 | 0.0086 | 0.0024 | 0.0029 | 0.0037 |
| X07 | 5.9500 | 5.9300 | 10.8100 | 5.3500 | 1.5000 | 0.0700 | 0.0122 | 0.0129 | 0.0151 | 0.0054 | 0.0027 | 0.0018 |
| **JP** | | | | | | | | | | | | |
| JP1-X2 | 3.4100 | 3.2100 | 5.6100 | 3.0700 | 2.4300 | 0.1100 | 0.0070 | 0.0070 | 0.0079 | 0.0031 | 0.0044 | 0.0029 |
| JP2-X2 | 3.5800 | 3.1800 | 5.5700 | 2.9000 | 0.1600 | 0.0300 | 0.0074 | 0.0069 | 0.0078 | 0.0029 | 0.0003 | 0.0008 |
| JP3-X | 2.8900 | 2.8200 | 5.1300 | 2.2700 | 1.3700 | 0.0500 | 0.0059 | 0.0061 | 0.0072 | 0.0023 | 0.0025 | 0.0013 |
| JP3-X1 | 2.6500 | 2.6500 | 3.4200 | 1.1200 | 0.2700 | 1.0900 | 0.0055 | 0.0058 | 0.0048 | 0.0011 | 0.0005 | 0.0287 |
| JPN2 | 4.9100 | 4.6100 | 9.1200 | 4.0100 | 2.4800 | 0.0600 | 0.0101 | 0.0100 | 0.0128 | 0.0040 | 0.0045 | 0.0016 |
| JPN3A | 6.7000 | 6.5200 | 12.3800 | 7.5200 | 4.2000 | 0.0800 | 0.0138 | 0.0142 | 0.0173 | 0.0076 | 0.0076 | 0.0021 |
| JPN3B | 5.8100 | 5.7800 | 9.7700 | 5.7800 | 3.8200 | 0.1600 | 0.0120 | 0.0126 | 0.0137 | 0.0058 | 0.0069 | 0.0042 |
| JPN4 | 2.9100 | 2.5900 | 4.7700 | 1.9300 | 1.4300 | 0.0300 | 0.0060 | 0.0056 | 0.0067 | 0.0019 | 0.0026 | 0.0008 |
| JPN9 | 4.2500 | 3.7900 | 6.8700 | 2.8500 | 1.8900 | 0.0900 | 0.0087 | 0.0083 | 0.0096 | 0.0029 | 0.0034 | 0.0024 |
| JPN11 | 2.7700 | 2.9300 | 5.1700 | 1.4700 | 0.0800 | 0.0300 | 0.0057 | 0.0064 | 0.0072 | 0.0015 | 0.0001 | 0.0008 |
| JPS1 | 6.0700 | 5.6300 | 10.8800 | 4.4300 | 1.1800 | 1.6500 | 0.0125 | 0.0123 | 0.0152 | 0.0045 | 0.0021 | 0.0434 |
| JPS4 | 3.4800 | 4.0400 | 7.4000 | 2.4200 | 1.4700 | 0.4500 | 0.0072 | 0.0088 | 0.0104 | 0.0024 | 0.0026 | 0.0118 |
| JPS6A | 4.4300 | 4.1500 | 7.8000 | 3.7100 | 2.2800 | 2.5800 | 0.0091 | 0.0090 | 0.0109 | 0.0037 | 0.0041 | 0.0679 |
| JPS6B | 3.9700 | 3.9000 | 7.4200 | 4.1700 | 2.5900 | 1.9900 | 0.0082 | 0.0085 | 0.0104 | 0.0042 | 0.0047 | 0.0524 |